Playing topological physics with microwave resonators

Fabrice Mortessagne

Waves in Complex Systems team

- Flexible experimental platforms in microwaves or optics
- Random Matrix Theory, effective Hamiltonian formalism, numerical simulations
- Complex geometries : multimode optical fibres, 2D or 3D microwave cavities
- (dis)ordered lattices : coupled μwave resonators, photo-induced/laser-written photonic structures
- Wave chaos
- Light diffusion – Anderson localization
- Quantum fluids of light
- Artificial Dirac materials
- Topological photonics

INPHYNI

Waves in Complex Systems team

- Flexible experimental platforms in microwaves or optics
- Random Matrix Theory, effective Hamiltonian formalism, numerical simulations
- Complex geometries : multimode optical fibres, 2D or 3D microwave cavities
- (dis)ordered lattices : coupled μwave resonators, photo-induced/laser-written photonic structures
- Wave chaos
- Light diffusion – Anderson localization
- Quantum fluids of light
- Artificial Dirac materials
- Topological photonics

INPHYNI

Outline

1. The playground: coupled microwave resonator lattices

   dielectric resonators, TE modes, evanescent coupling, LDOS & eigenstates

2. Initiatory game: topological phase transition in strained graphene

   Berry phase, merging of Dirac points, Zak phase, manipulation of edge states

3. 'Flat games': Lieb lattice & Pseudo-Landau levels

   flat band, sublattice polarization, gigantic pseudo-magnetic field, supersymmetric oscillator

Experimental setup

- Vector Network Analyzer (@ 0-24 GHz)
- coaxial SMA 3.5mm connectors
- ‘kink’ and ‘loop’ antennas: TE polarization
- dielectric resonators sandwiched between metallic plates

Experimental setup

- Vector Network Analyzer (@ 0-24 GHz)
- coaxial SMA 3.5mm connectors
- 'kink' and 'loop' antennas: TE polarization
- dielectric resonators sandwiched between metallic plates

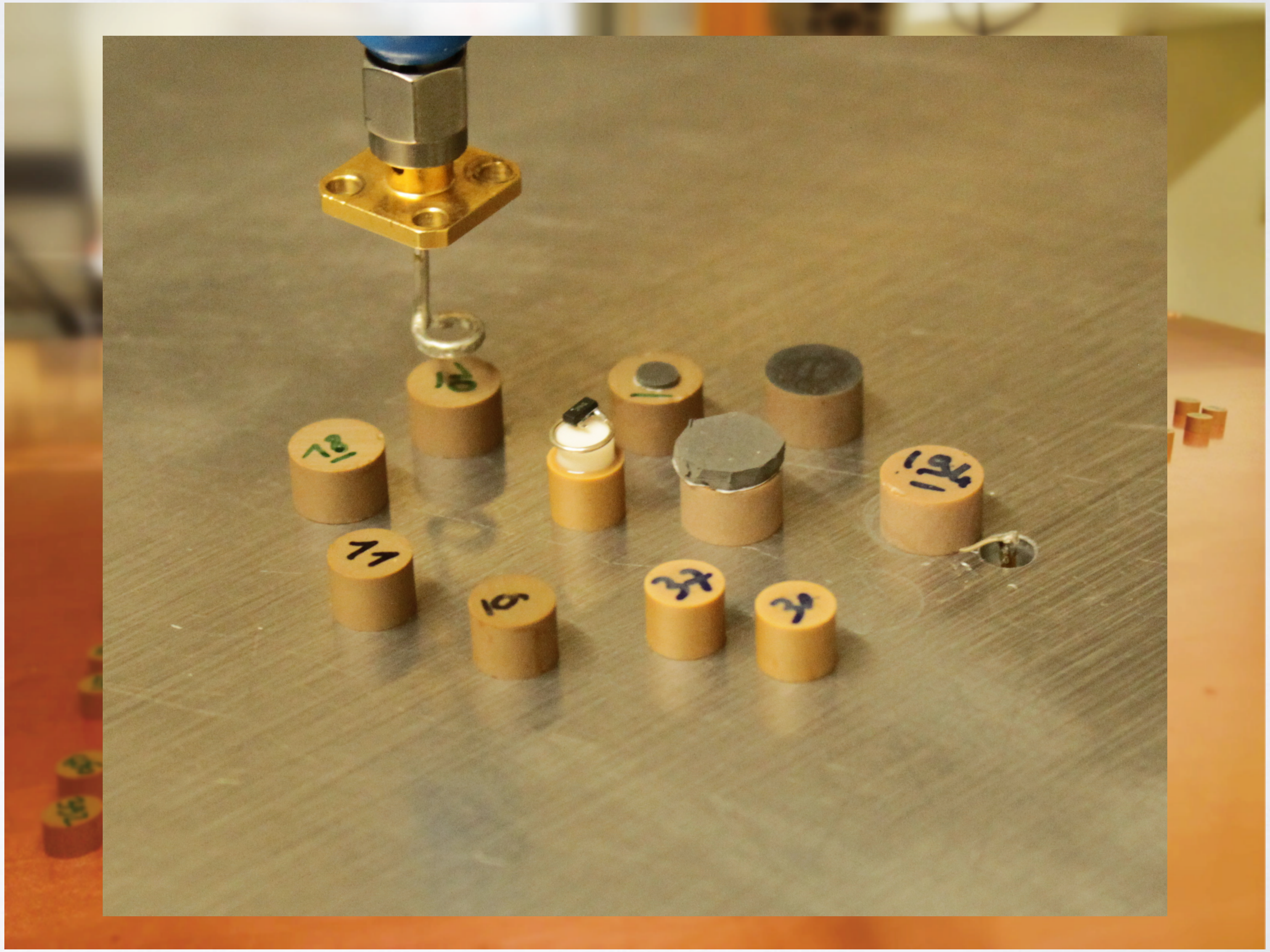

INPHYNI

Experimental setup

- Vector Network Analyzer (@ 0-24 GHz)
- coaxial SMA 3.5mm connectors
- ‘kink’ and ‘loop’ antennas: TE polarization
- dielectric resonators sandwiched between metallic plates

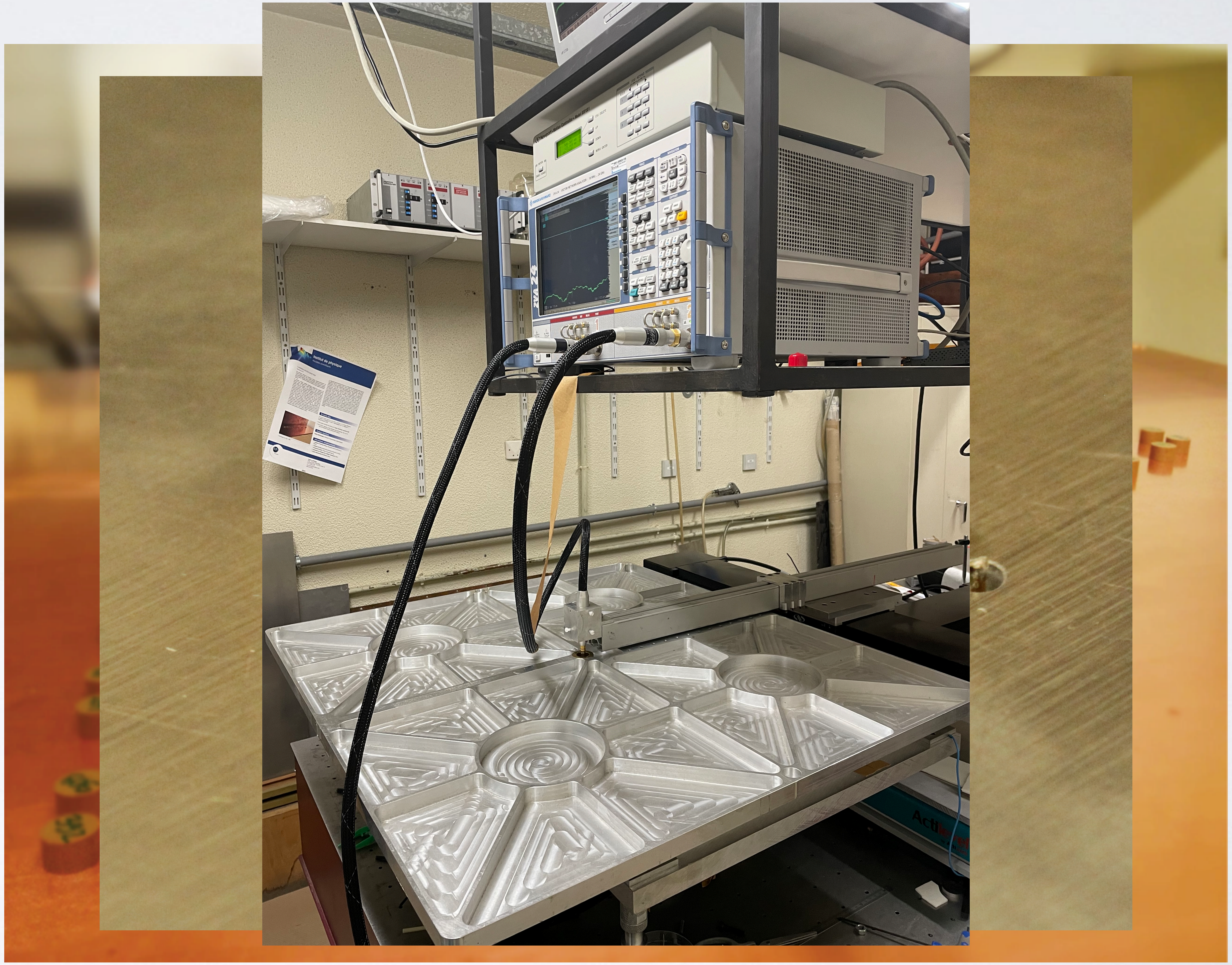

INPHYNI

Microwave resonators

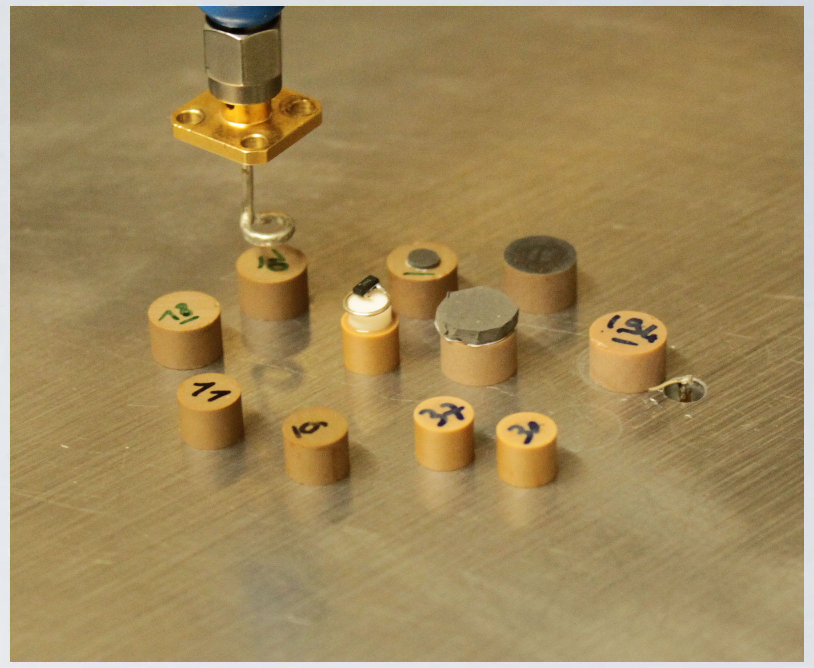

Dielectric ceramic (ZrSnTiO, TiZrNbZnO):

- high permittivity: $\varepsilon = 37 \rightarrow 45$
- low loss: $Q \simeq 3000$

Microwave resonators

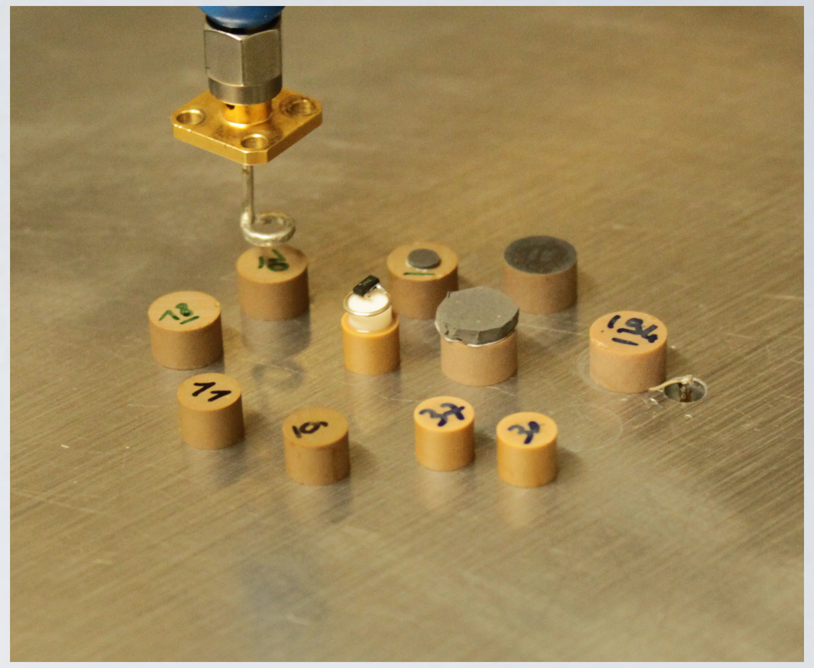

Dielectric ceramic (ZrSnTiO, TiZrNbZnO):

- high permittivity: $\varepsilon = 37 \rightarrow 45$
- low loss: $Q \simeq 3000$

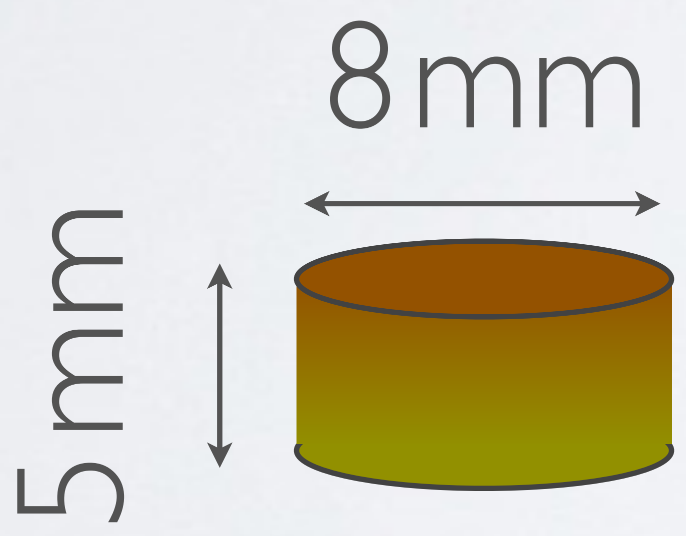

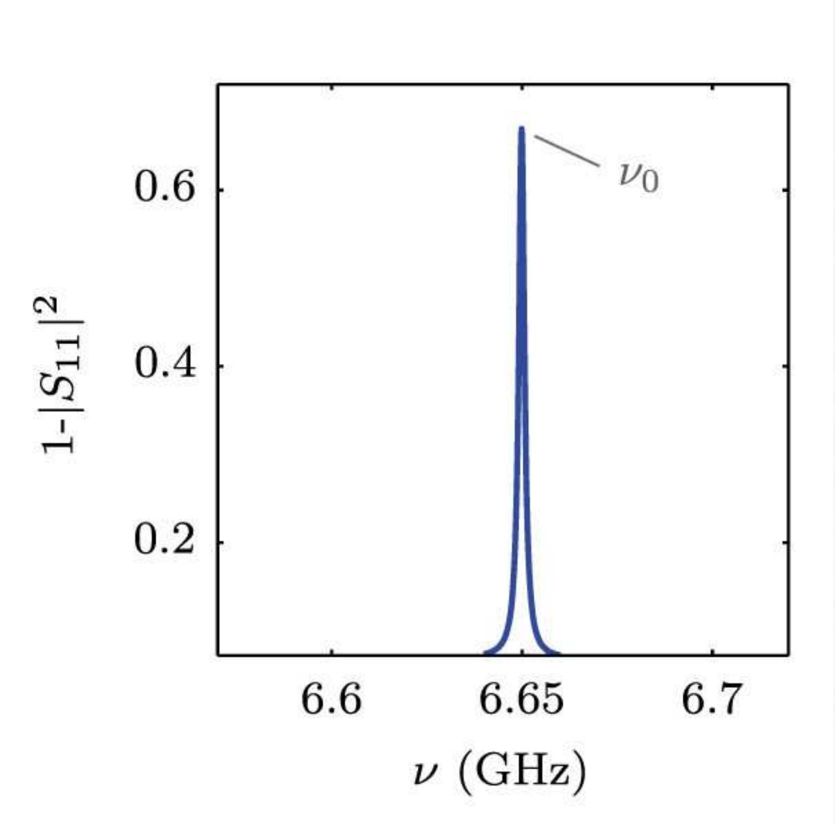

$$S_{11}(\nu) = 1 - i\sigma \frac{|\Psi(\vec{r}_1)|^2}{\nu - \nu_0 + \mathrm{i}\Gamma}$$

Microwave resonators

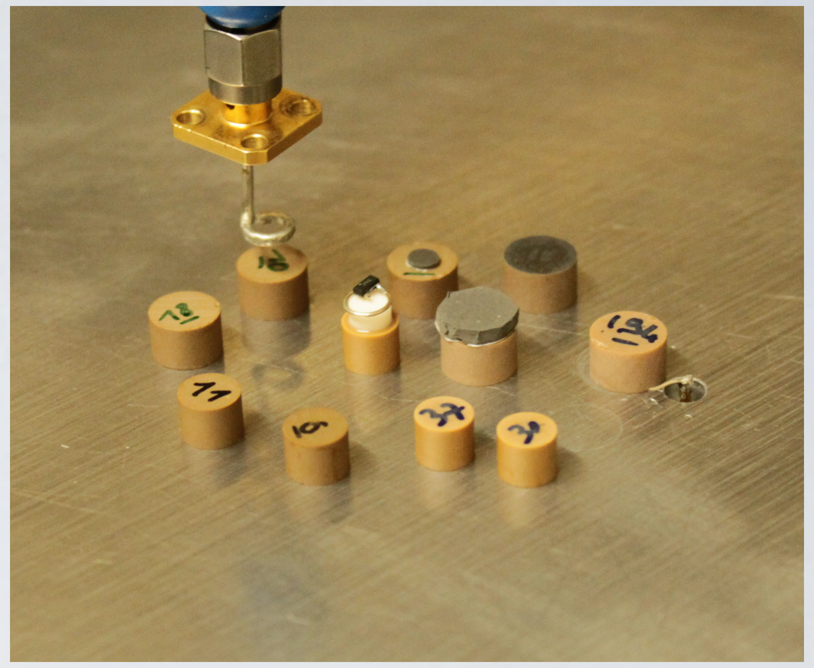

Dielectric ceramic (ZrSnTiO, TiZrNbZnO):

- high permittivity: $\varepsilon = 37 \rightarrow 45$
- low loss: $Q \simeq 3000$

- TE$_1$ Mie resonance
- s-mode @ 6.65 GHz

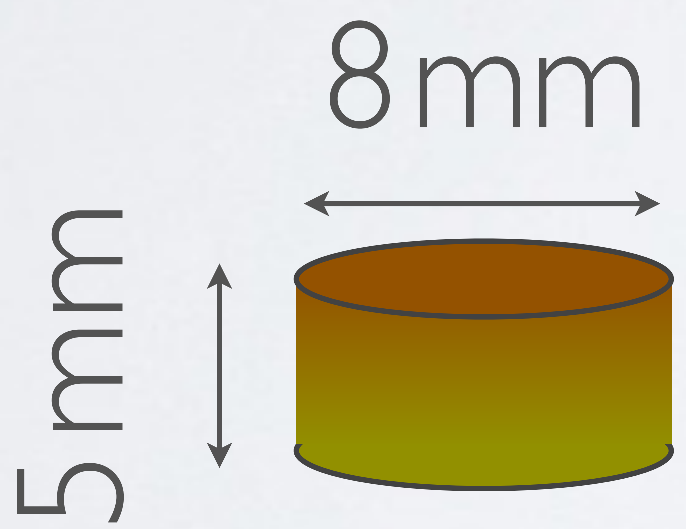

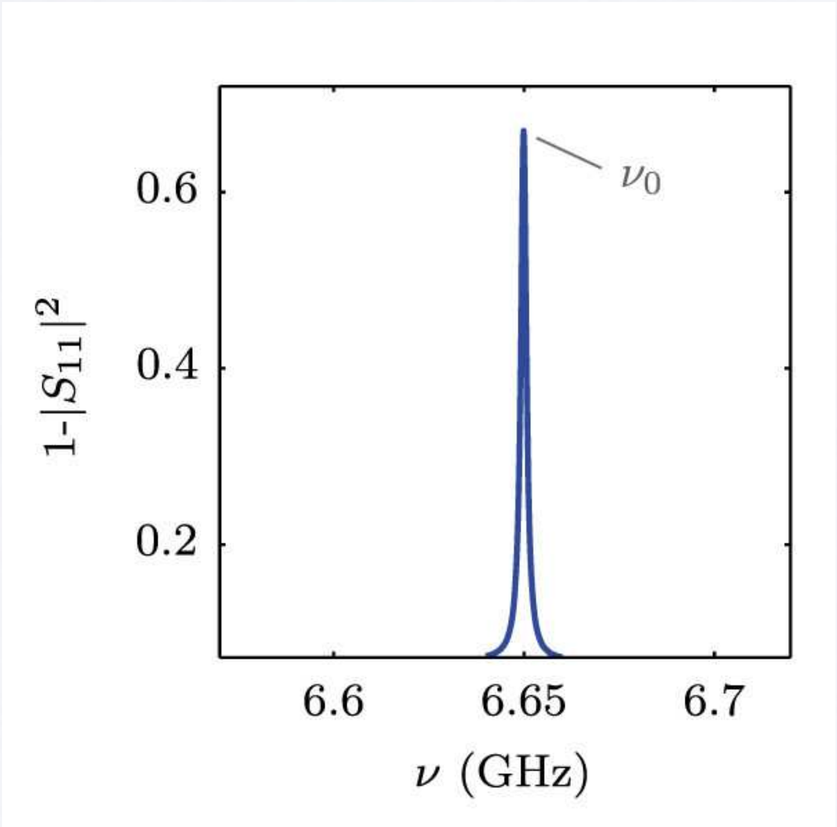

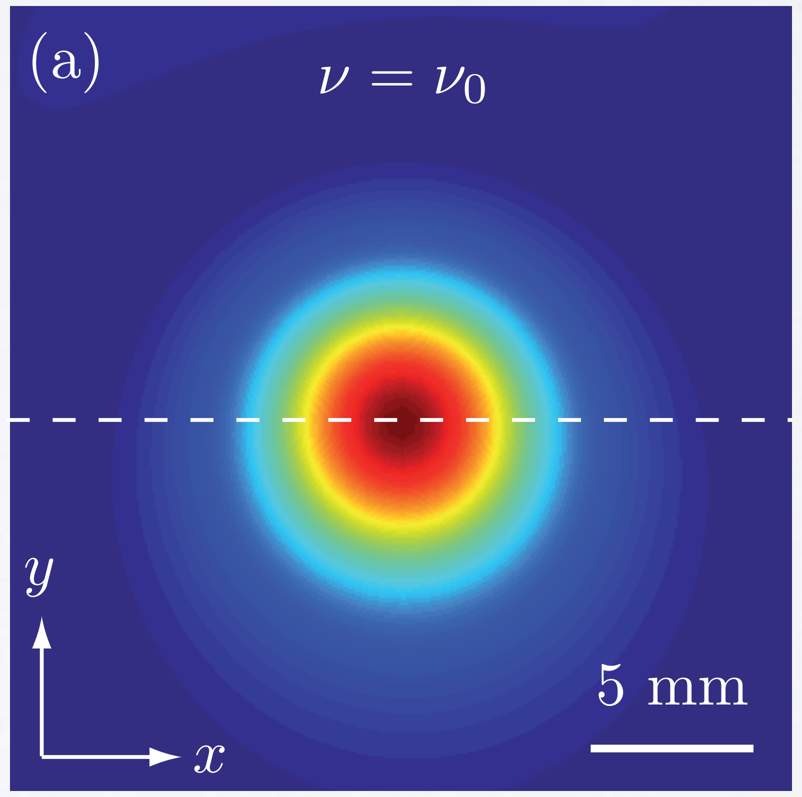

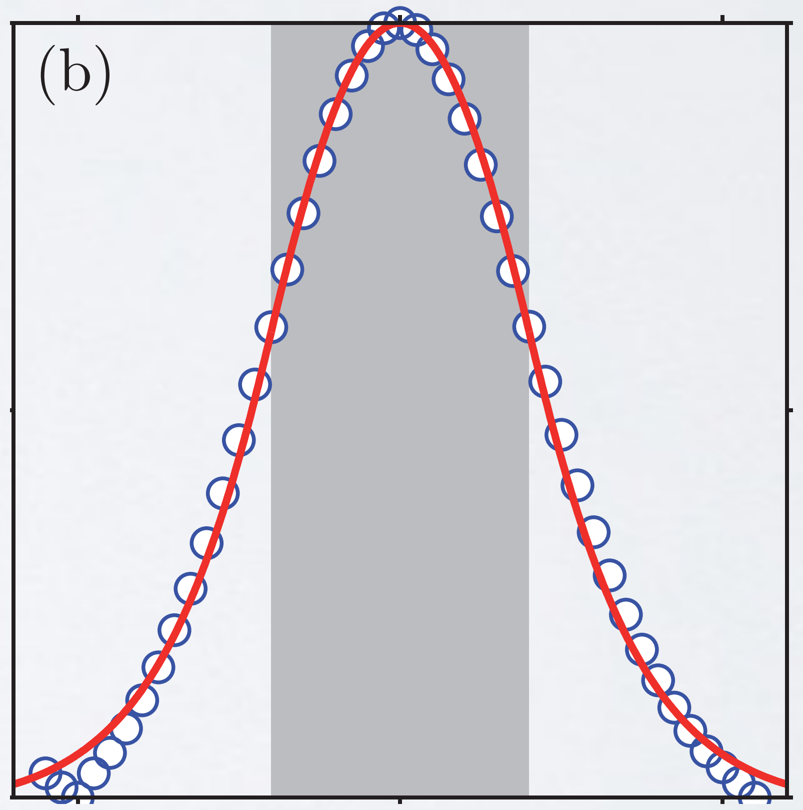

$$S_{11}(\nu) = 1 - i\sigma \frac{|\Psi(\vec{r}_1)|^2}{\nu - \nu_0 + \mathrm{i}\Gamma}$$

$$B_z(\vec{r}, z) = B_0 \sin\left(\frac{\pi}{h} z\right) \times \begin{cases} J_0(\gamma_j \vec{r}) \\ \alpha K_0(\gamma_k \vec{r}) \end{cases}$$

Tight-binding coupling

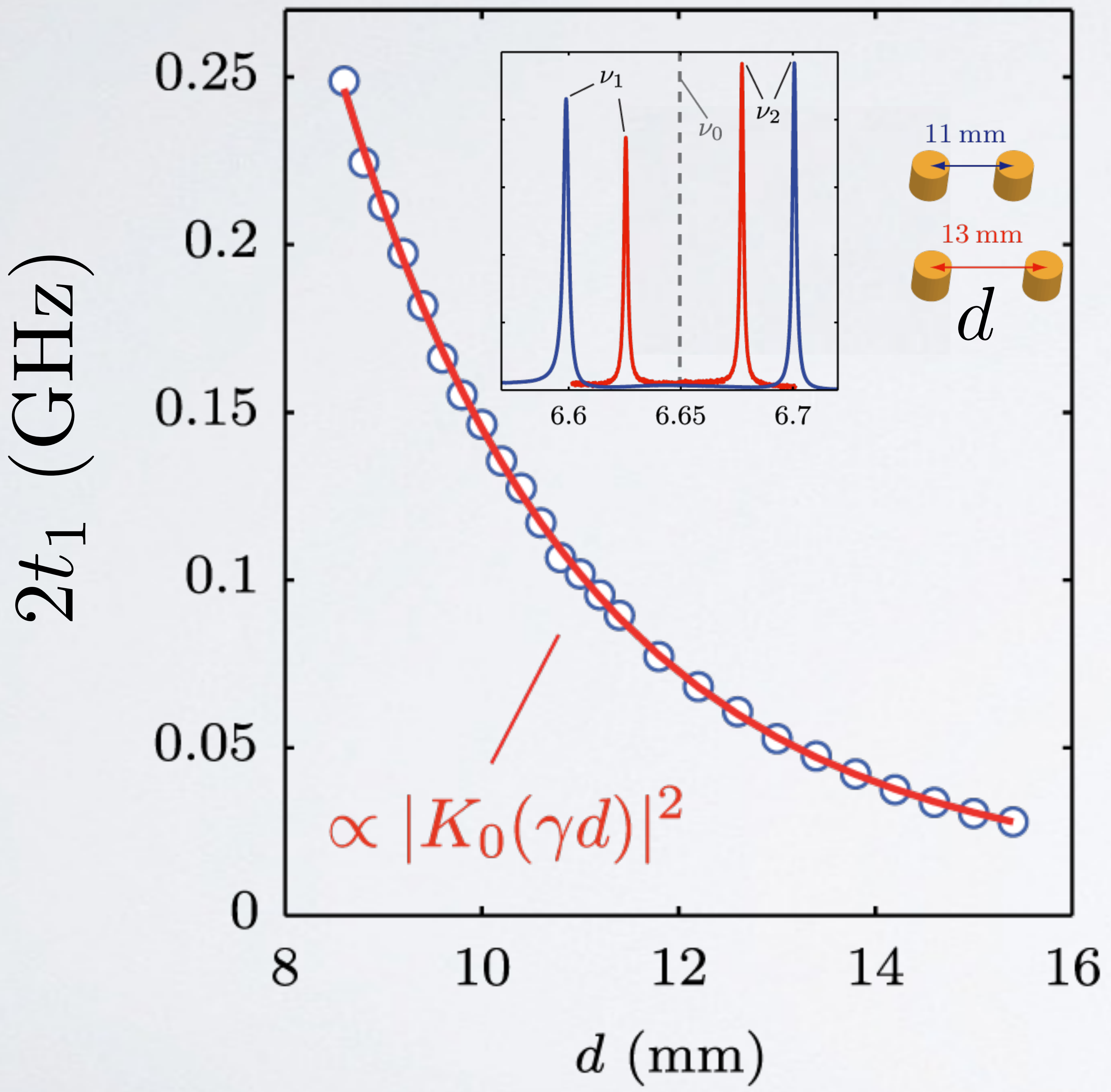

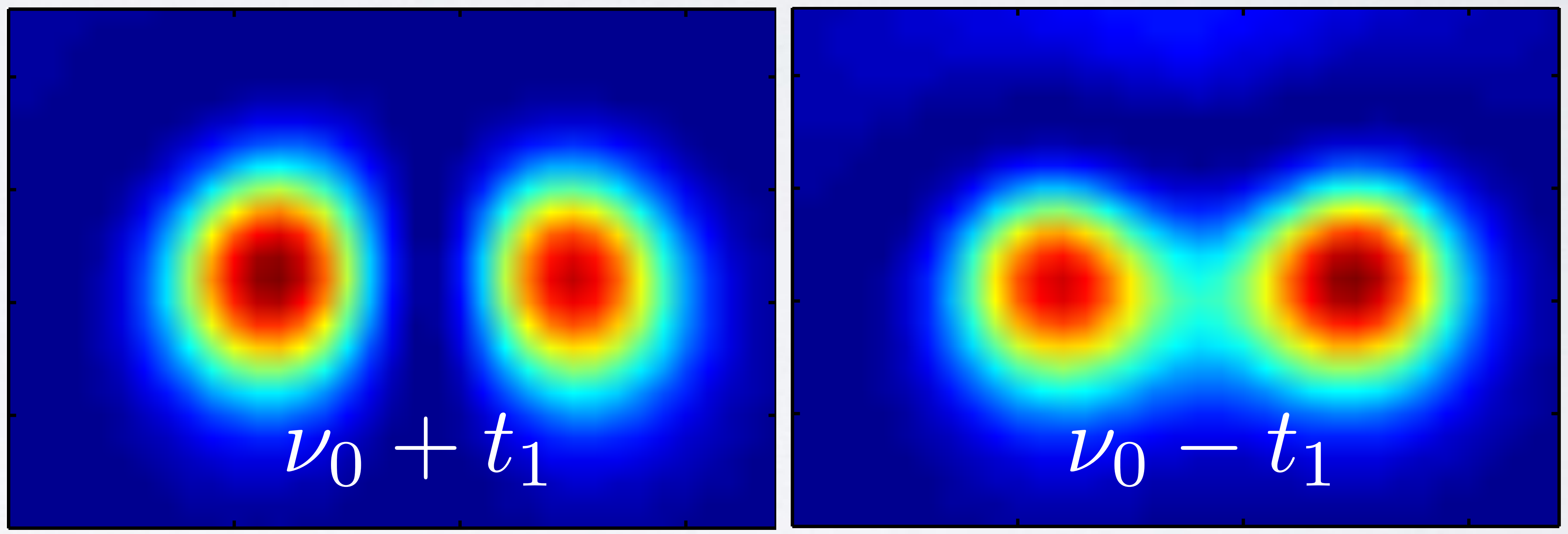

$$H(d) = \begin{pmatrix} \nu_0 & -t_1(d) \\ -t_1(d) & \nu_0 \end{pmatrix}$$

$$t_1(d) \propto -|K_0(d/2\ell)|^2 \quad \ell \simeq 3\,\mathrm{mm}$$

INPHYNI

Tight-binding coupling

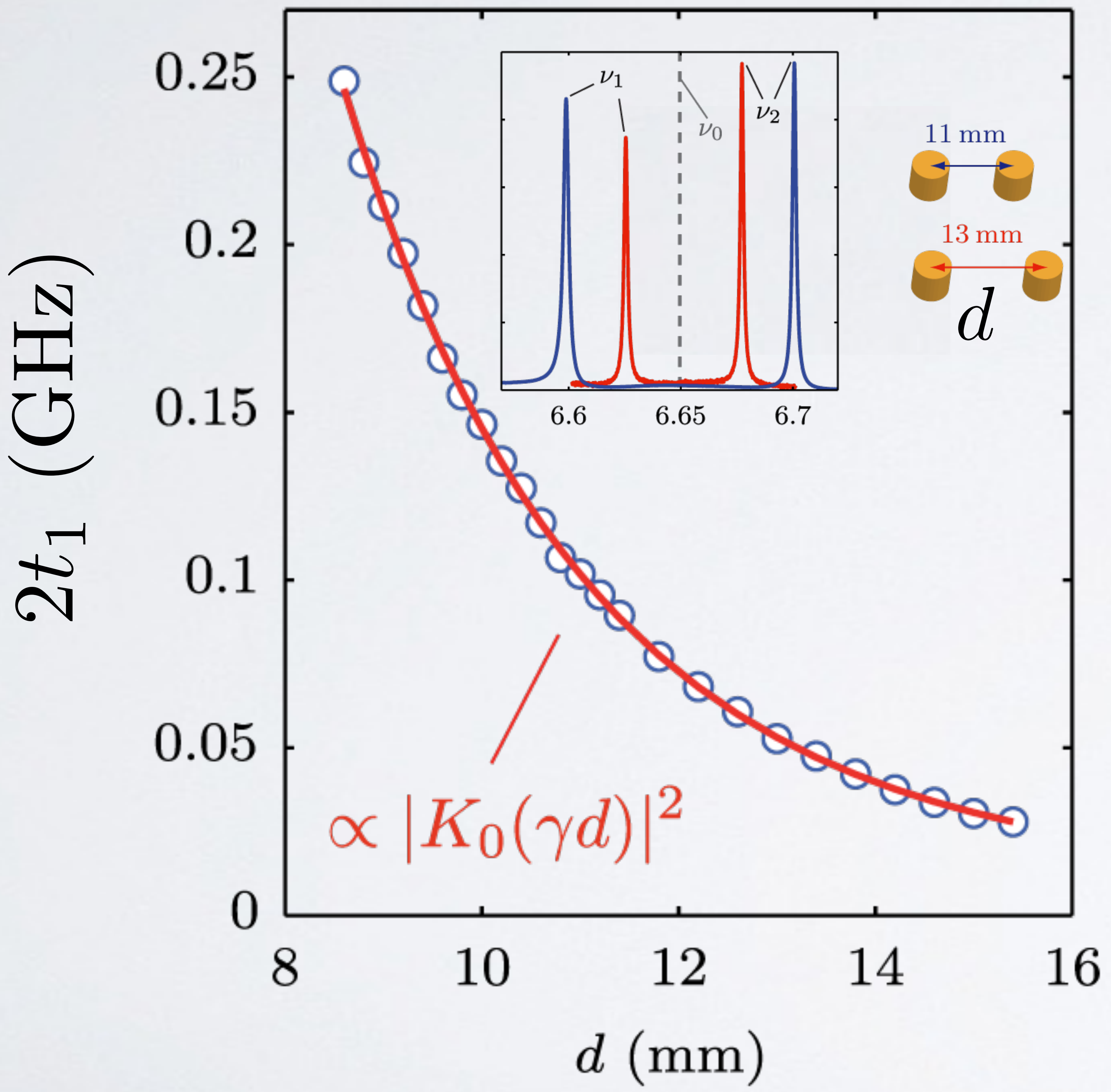

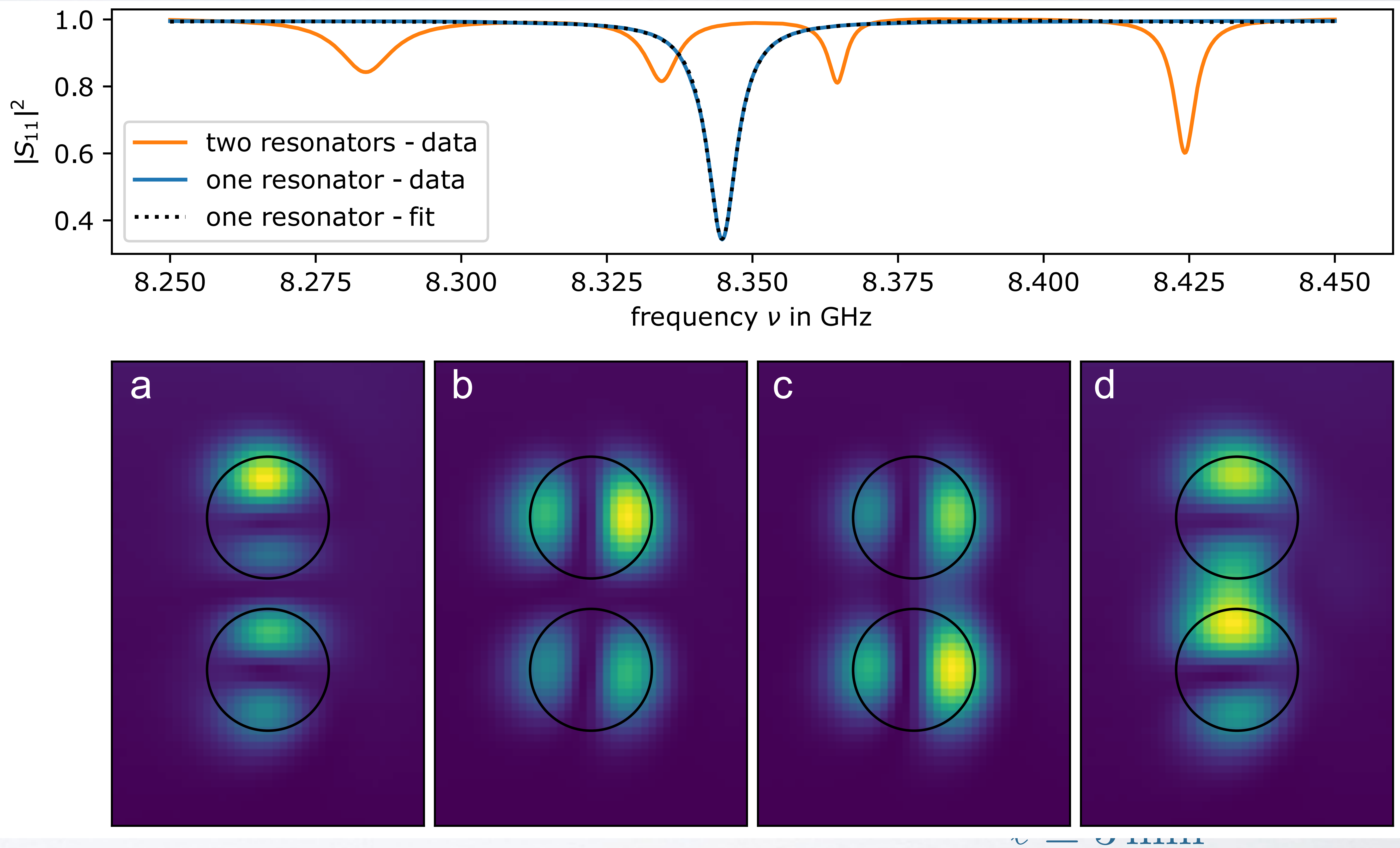

Coupled microwave resonator lattices

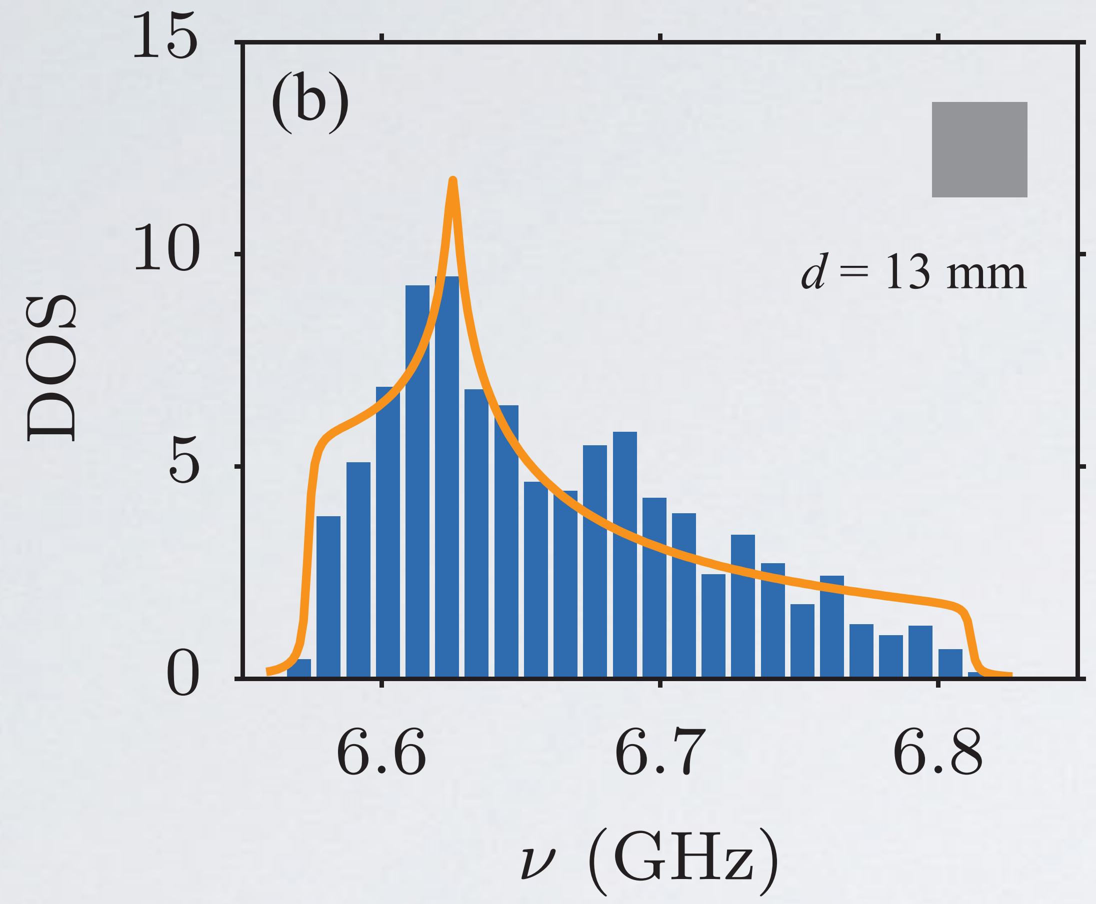

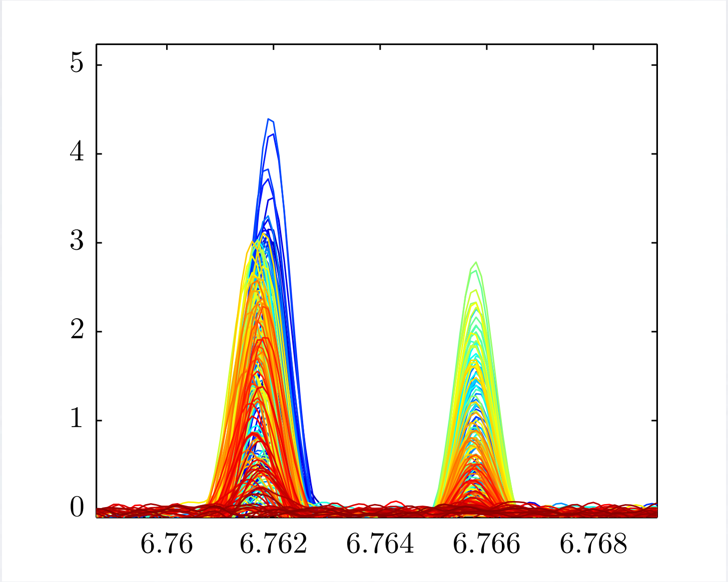

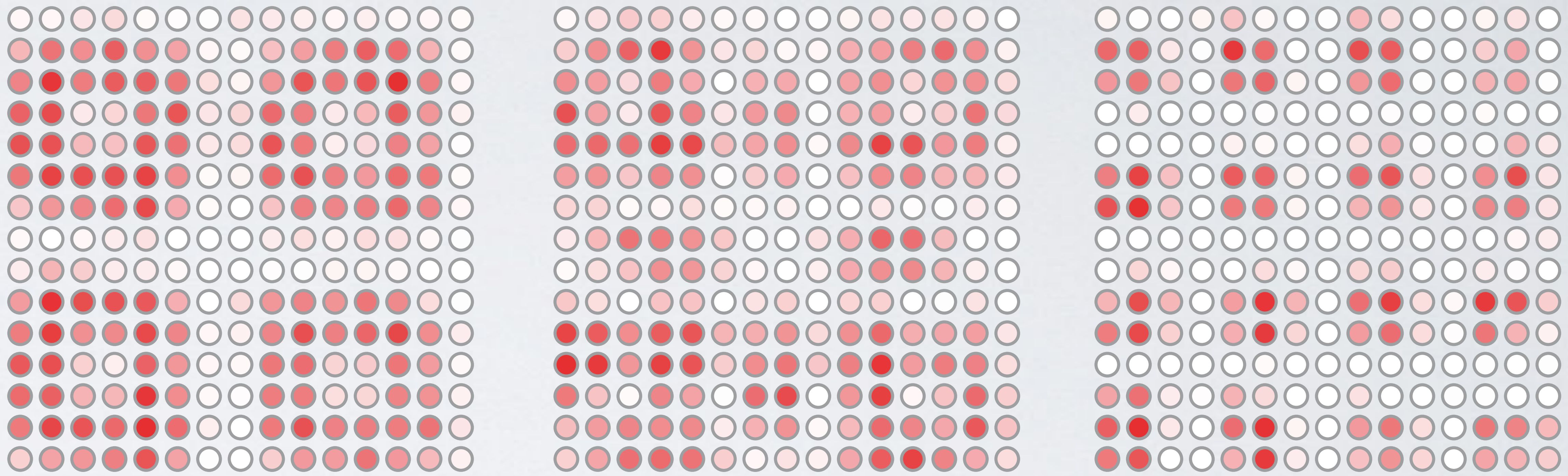

Transmission measurement

$$S_{12}(\nu;\vec{r}_1,\vec{r}_2) = -\mathrm{i}\sqrt{\sigma_1\sigma_2}\sum_{n=1}^{N}\frac{\Psi_n(\vec{r}_1)\Psi_n^*(\vec{r}_2)}{\nu-\nu_n+\mathrm{i}\Gamma_n}$$

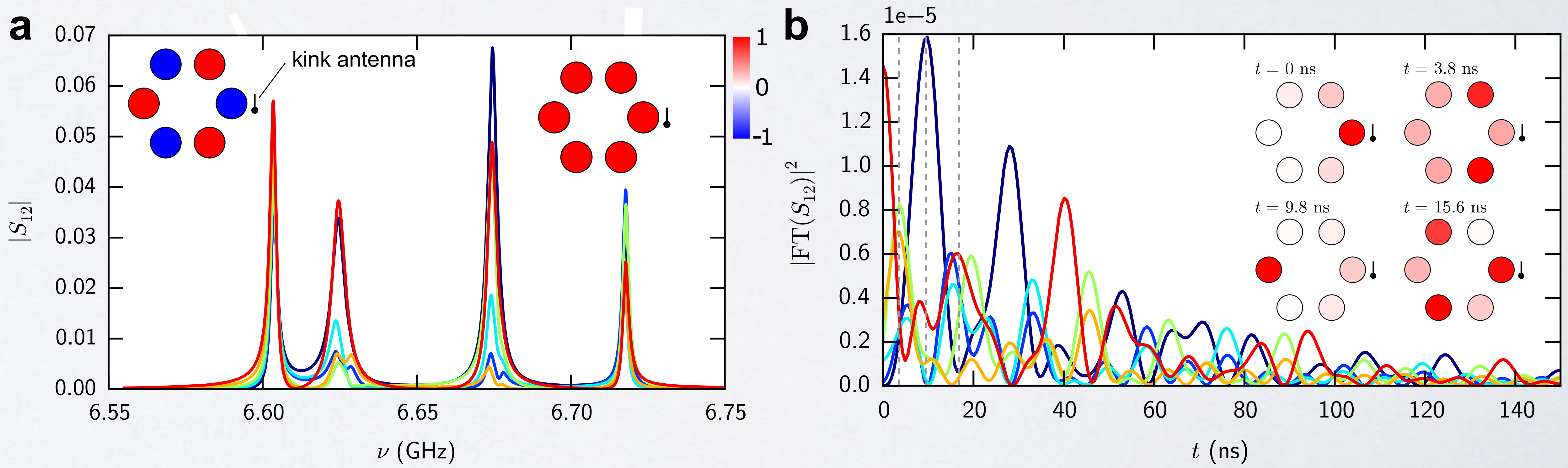

Experimental access to LDoS, DoS, wavefunctions and pulse spreadings

Phys. Rev. B **88**, 115437 (2013); Opt. Mater. Express **11**, 629 (2021)

INPHYNI

Microwave artificial graphene

nature nanotechnology
REVIEW ARTICLE
PUBLISHED ONLINE: 4 SEPTEMBER 2013 | DOI: 10.1038/NNANO.2013.161

Artificial honeycomb lattices for electrons, atoms and photons

Marco Polini[1]*, Francisco Guinea[2], Maciej Lewenstein[3,4], Hari C. Manoharan[5,6] and Vittorio Pellegrini[1,7]


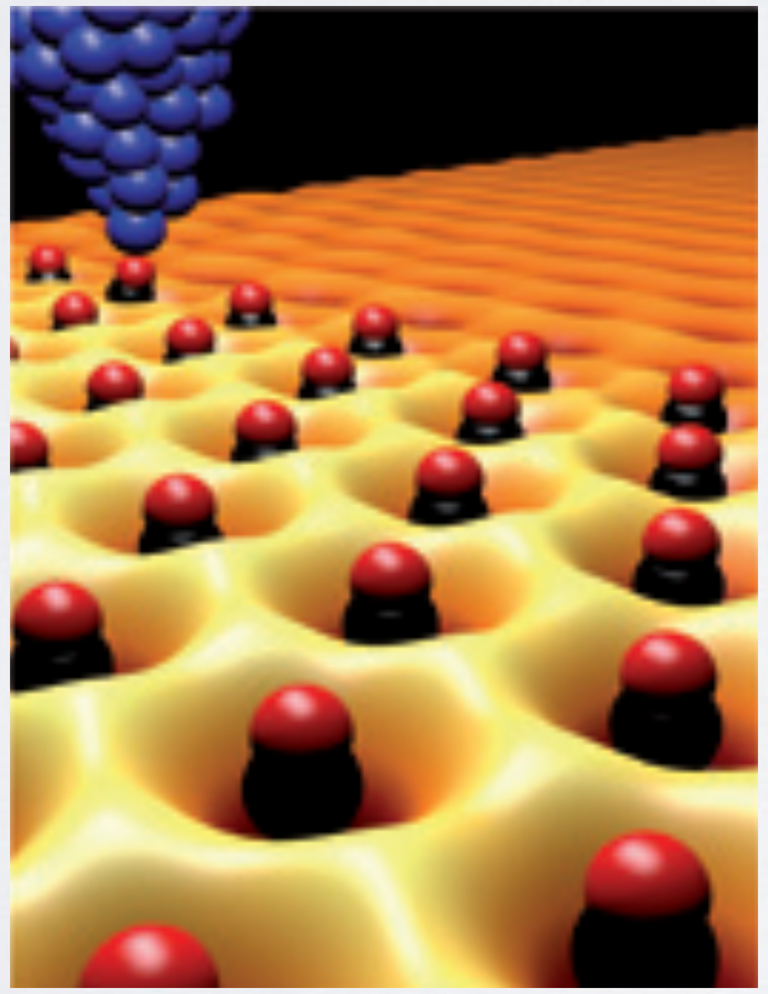
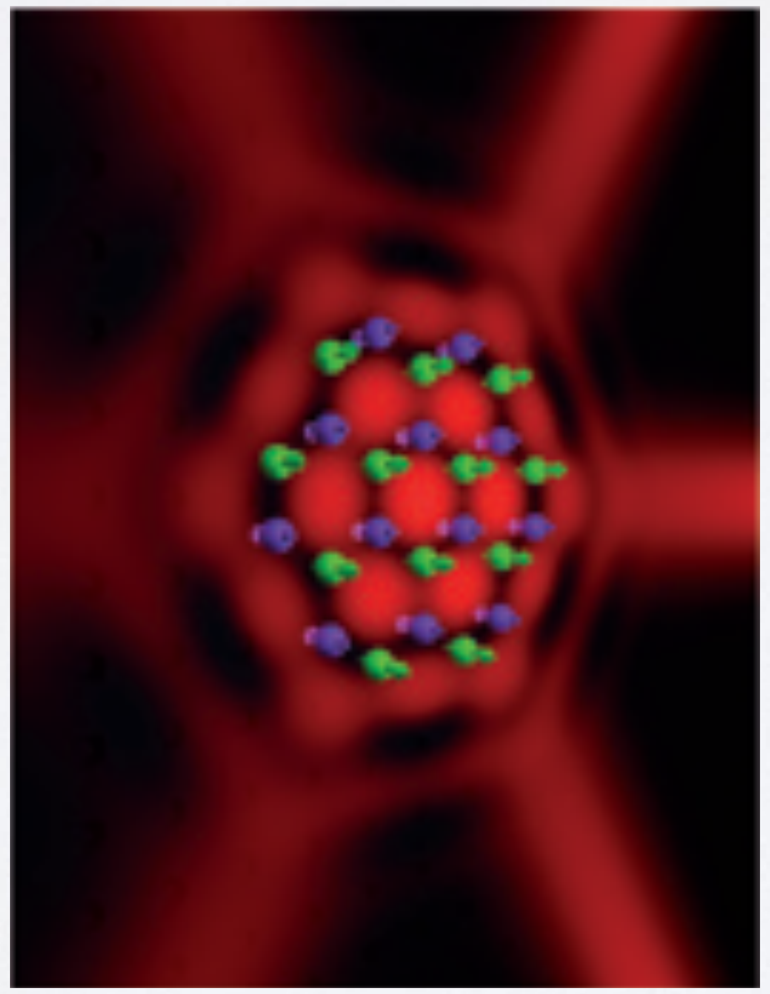
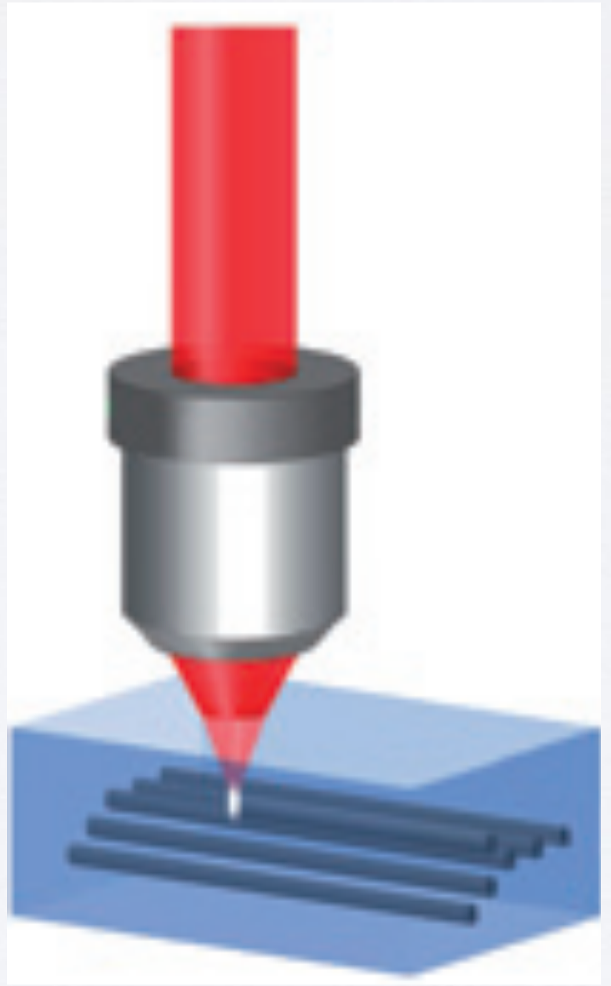

nanopatterned SC micropillar lattice | molecular lattice | optical lattice | refractive index lattice

2DEG | Light/microwave

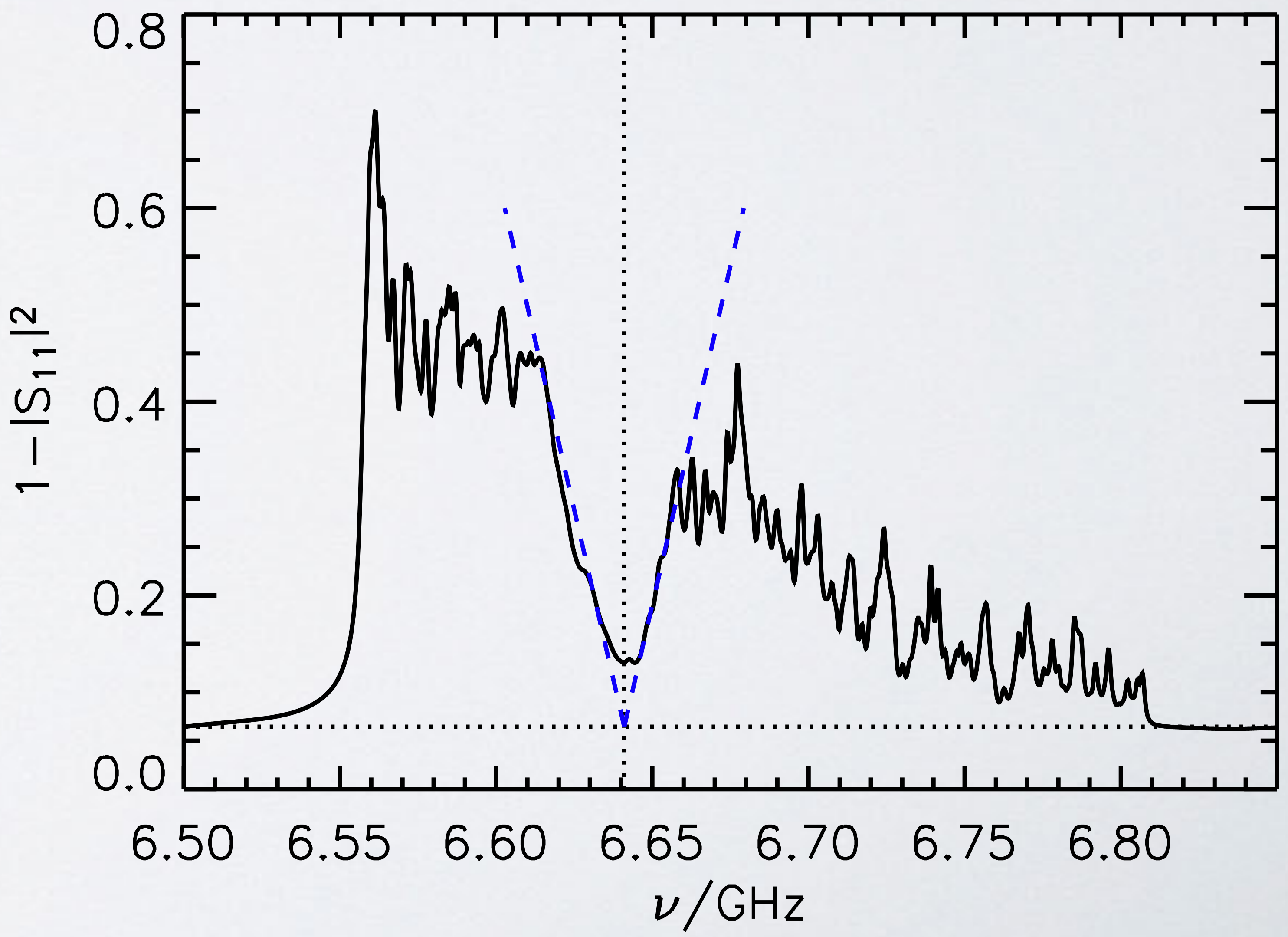

INPHYNI

Outline

1. The playground: coupled microwave resonator lattices

   dielectric resonators, TE modes, evanescent coupling, LDOS & eigenstates

2. Initiatory game: topological phase transition in strained graphene

   Berry phase, merging of Dirac points, Zak phase, manipulation of edge states

3. 'Flat games': Lieb lattice & Pseudo-Landau levels

   flat band, sublattice polarization, gigantic pseudo-magnetic field, supersymmetric oscillator

INPHYNI

Honeycomb lattice

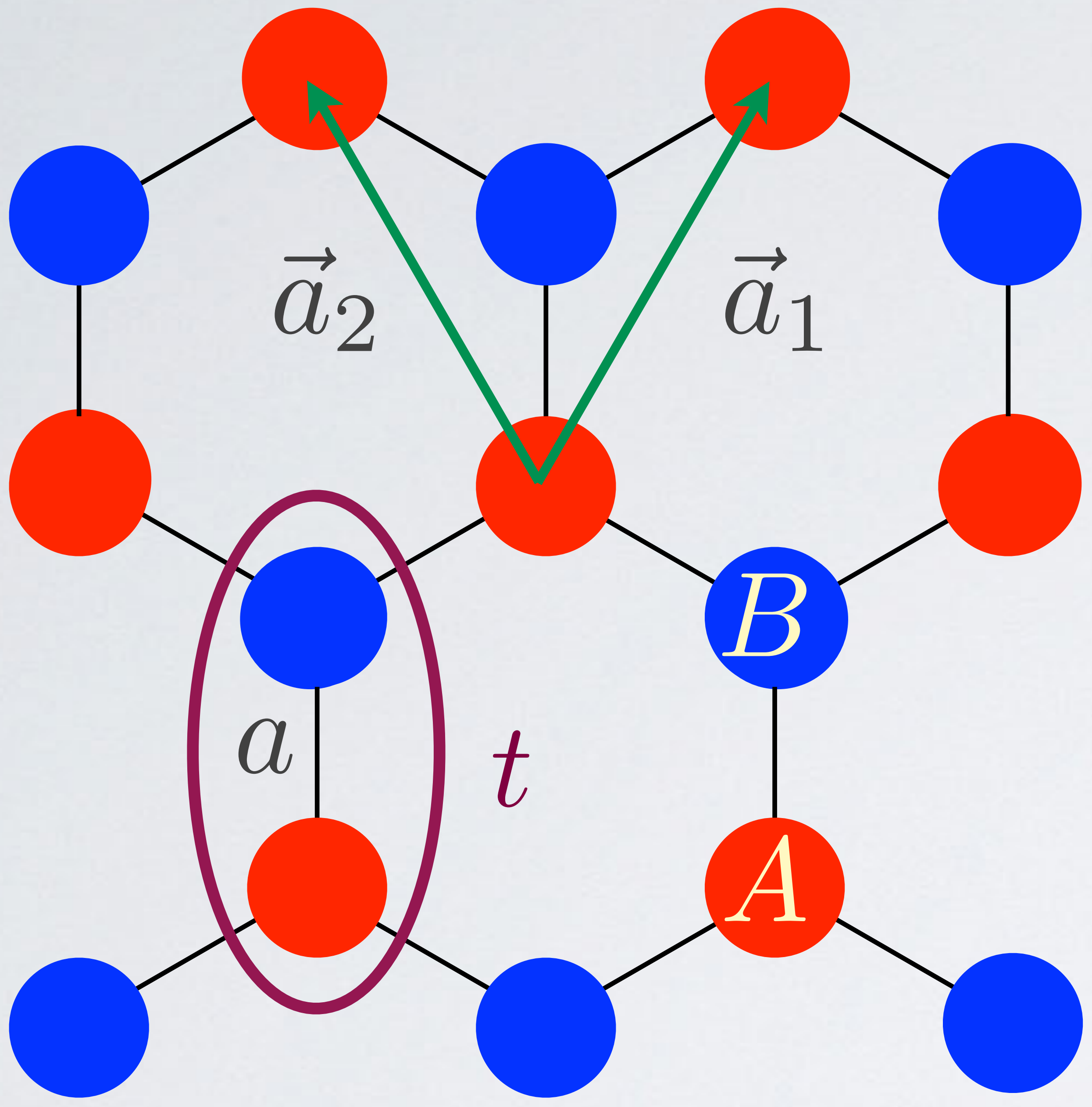

In the Bloch representation:

$$|\psi_k\rangle = \frac{1}{N}\sum_{\text{cells}} \left(\lambda_A|\varphi_j^A\rangle + \lambda_B|\varphi_j^B\rangle\right) e^{i\boldsymbol{k}\cdot\boldsymbol{R}_j}$$

Hamiltonian in k-space

$$\mathcal{H}_{\boldsymbol{k}} = -t\begin{pmatrix} 0 & f^*(\boldsymbol{k}) \\ f(\boldsymbol{k}) & 0 \end{pmatrix}$$

$$f(\mathbf{k}) = 1 + e^{i\mathbf{k}\cdot\mathbf{a}_1} + e^{i\mathbf{k}\cdot\mathbf{a}_2}$$

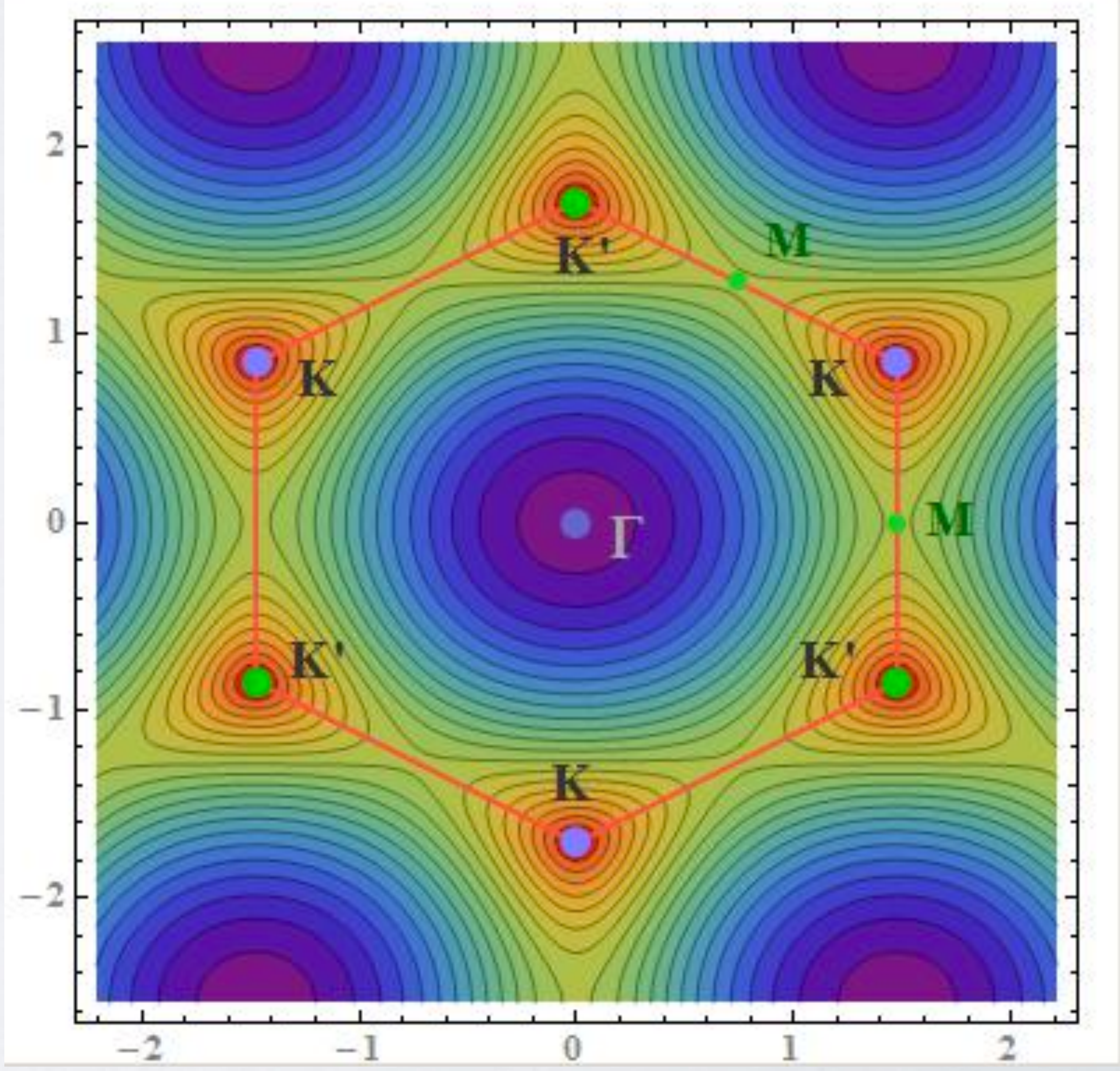

Dispersion relation:

$$\varepsilon(\mathbf{k}) = \pm t\left[3 + 2\cos\mathbf{k}\cdot\mathbf{a}_1 + 2\cos\mathbf{k}\cdot\mathbf{a}_2 + 2\cos\mathbf{k}\cdot(\mathbf{a}_1 - \mathbf{a}_2)\right]^{1/2}$$

INPHYNI

Topology of Dirac points

$$\mathcal{H}_{\boldsymbol{k}} = -t \begin{pmatrix} 0 & f^*(\boldsymbol{k}) \\ f(\boldsymbol{k}) & 0 \end{pmatrix} \qquad f(\mathbf{k}) = \beta + \mathrm{e}^{\mathrm{i}\mathbf{k}\cdot\mathbf{a}_1} + \mathrm{e}^{\mathrm{i}\mathbf{k}\cdot\mathbf{a}_2} \qquad \varepsilon(\boldsymbol{k}) = \pm|f(\boldsymbol{k})|^{1/2}$$

$$\phi_{\boldsymbol{k}} = \arg[f(\boldsymbol{k})]$$

Eigenstates:

$$\psi_{\boldsymbol{k}}^{\pm}(\boldsymbol{r}) = \frac{1}{\sqrt{2}} \begin{pmatrix} \pm 1 \\ \mathrm{e}^{\mathrm{i}\phi_{\boldsymbol{k}}} \end{pmatrix} \mathrm{e}^{\mathrm{i}\boldsymbol{k}\cdot\boldsymbol{r}}$$

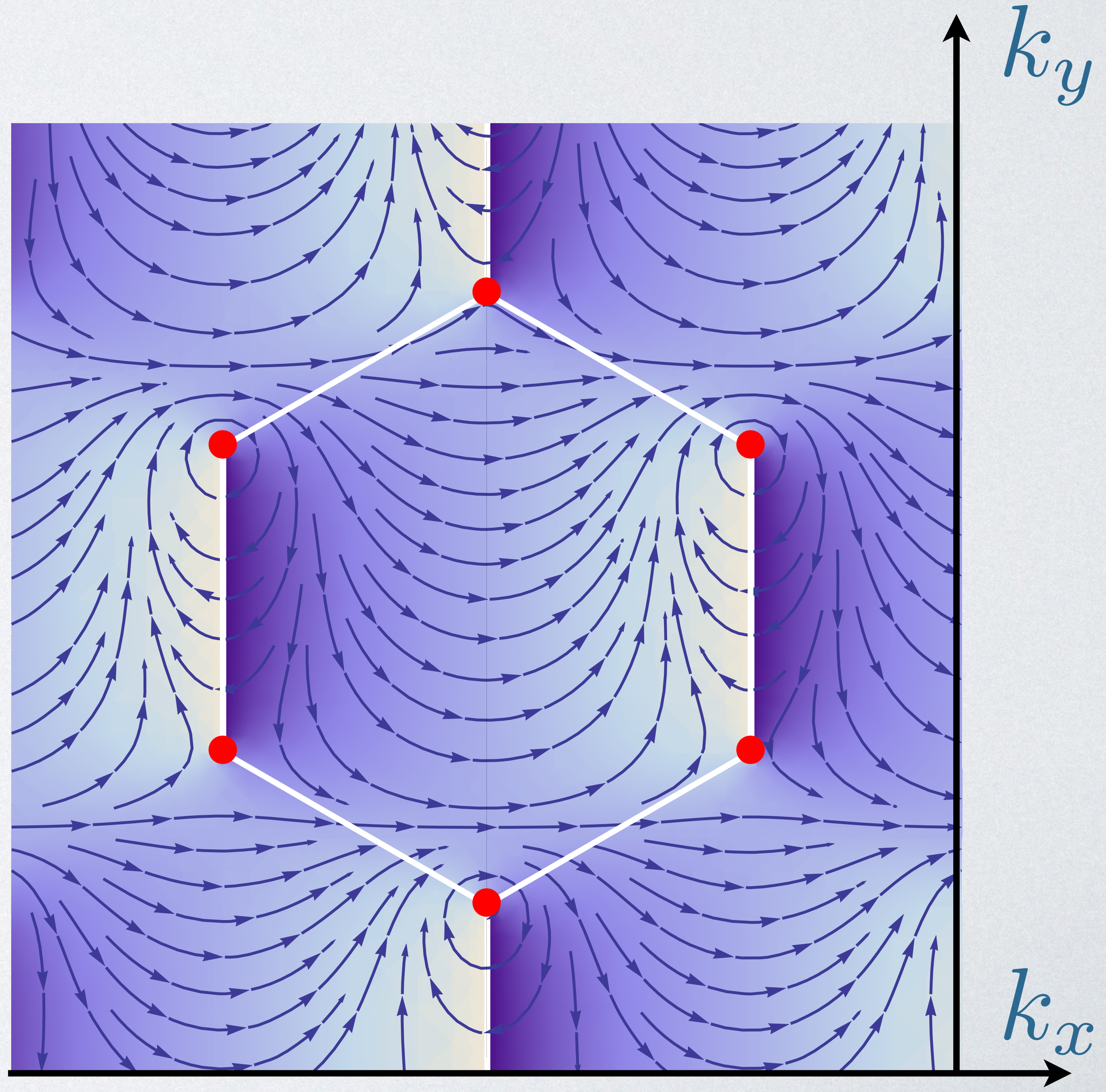

Topology of Dirac points

$$\mathcal{H}_{\boldsymbol{k}} = -t \begin{pmatrix} 0 & f^*(\boldsymbol{k}) \\ f(\boldsymbol{k}) & 0 \end{pmatrix} \qquad f(\mathbf{k}) = \beta + \mathrm{e}^{\mathrm{i}\mathbf{k}\cdot\mathbf{a}_1} + \mathrm{e}^{\mathrm{i}\mathbf{k}\cdot\mathbf{a}_2} \qquad \varepsilon(\boldsymbol{k}) = \pm|f(\boldsymbol{k})|^{1/2}$$

$$\boxed{\phi_{\boldsymbol{k}} = \arg[f(\boldsymbol{k})]}$$

Eigenstates:

$$\psi^{\pm}_{\boldsymbol{k}}(\boldsymbol{r}) = \frac{1}{\sqrt{2}} \begin{pmatrix} \pm 1 \\ \mathrm{e}^{\mathrm{i}\phi_{\boldsymbol{k}}} \end{pmatrix} \mathrm{e}^{\mathrm{i}\boldsymbol{k}\cdot\boldsymbol{r}}$$

Berry phase:

$$\phi_B = \frac{1}{2} \oint \nabla_{\boldsymbol{k}} \phi_{\boldsymbol{k}} \cdot \mathrm{d}\boldsymbol{k}$$

$\phi_B = -\pi$

Phase singularity around Dirac points

$\phi_B = +\pi$

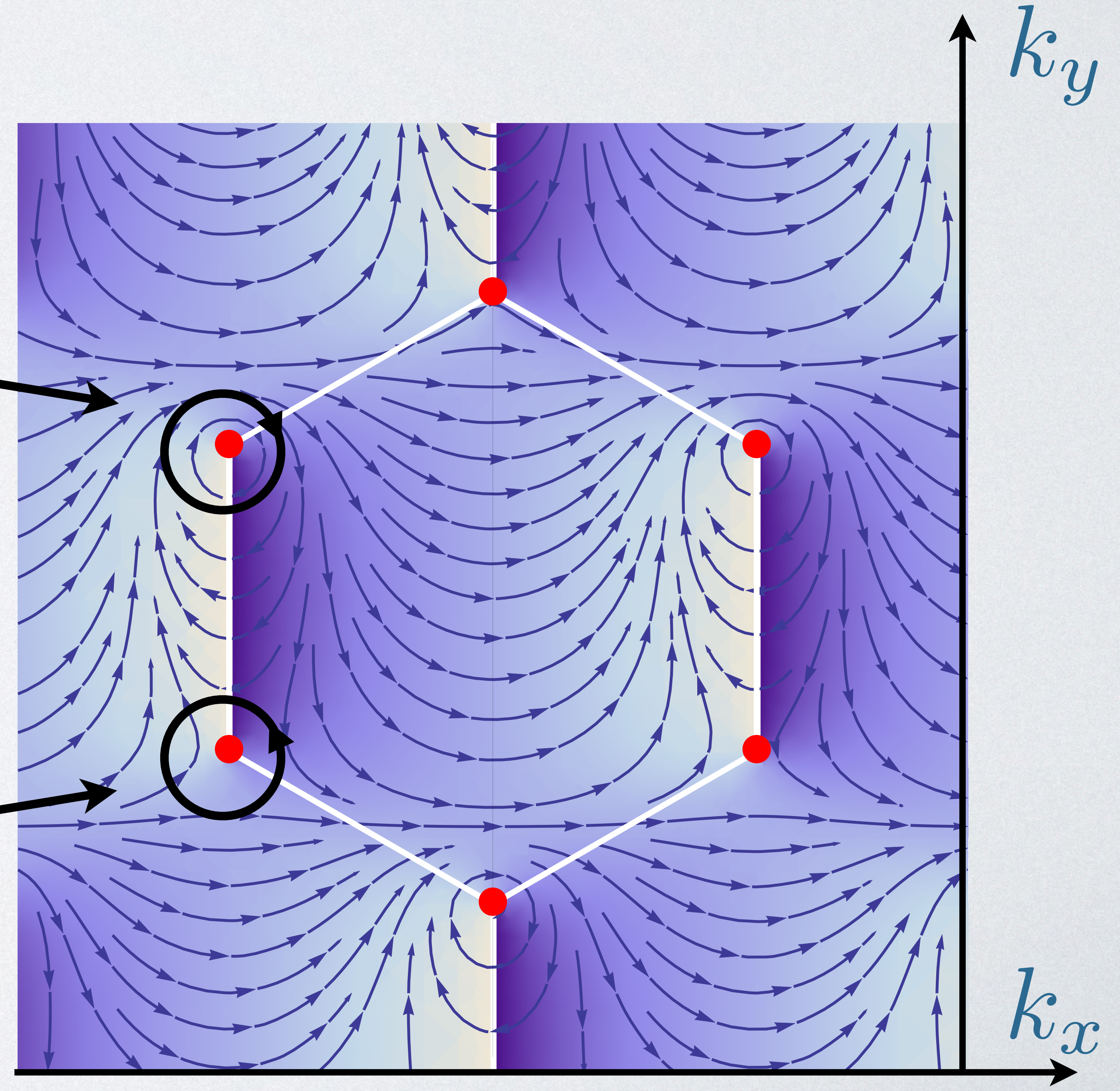

Topology of Dirac points

$$\mathcal{H}_{\boldsymbol{k}} = -t \begin{pmatrix} 0 & f^*(\boldsymbol{k}) \\ f(\boldsymbol{k}) & 0 \end{pmatrix} \qquad f(\mathbf{k}) = \beta + \mathrm{e}^{\mathrm{i}\mathbf{k}\cdot\mathbf{a}_1} + \mathrm{e}^{\mathrm{i}\mathbf{k}\cdot\mathbf{a}_2} \qquad \varepsilon(\boldsymbol{k}) = \pm|f(\boldsymbol{k})|^{1/2}$$

$$\phi_{\boldsymbol{k}} = \arg[f(\boldsymbol{k})]$$

Eigenstates:

$$\psi_{\boldsymbol{k}}^{\pm}(\boldsymbol{r}) = \frac{1}{\sqrt{2}} \begin{pmatrix} \pm 1 \\ \mathrm{e}^{\mathrm{i}\phi_{\boldsymbol{k}}} \end{pmatrix} \mathrm{e}^{\mathrm{i}\boldsymbol{k}\cdot\boldsymbol{r}}$$

Berry phase:

$$\phi_B = \frac{1}{2} \oint \nabla_{\boldsymbol{k}} \phi_{\boldsymbol{k}} \cdot \mathrm{d}\boldsymbol{k}$$

$\phi_B = -\pi$

Phase singularity around Dirac points

$\phi_B = +\pi$

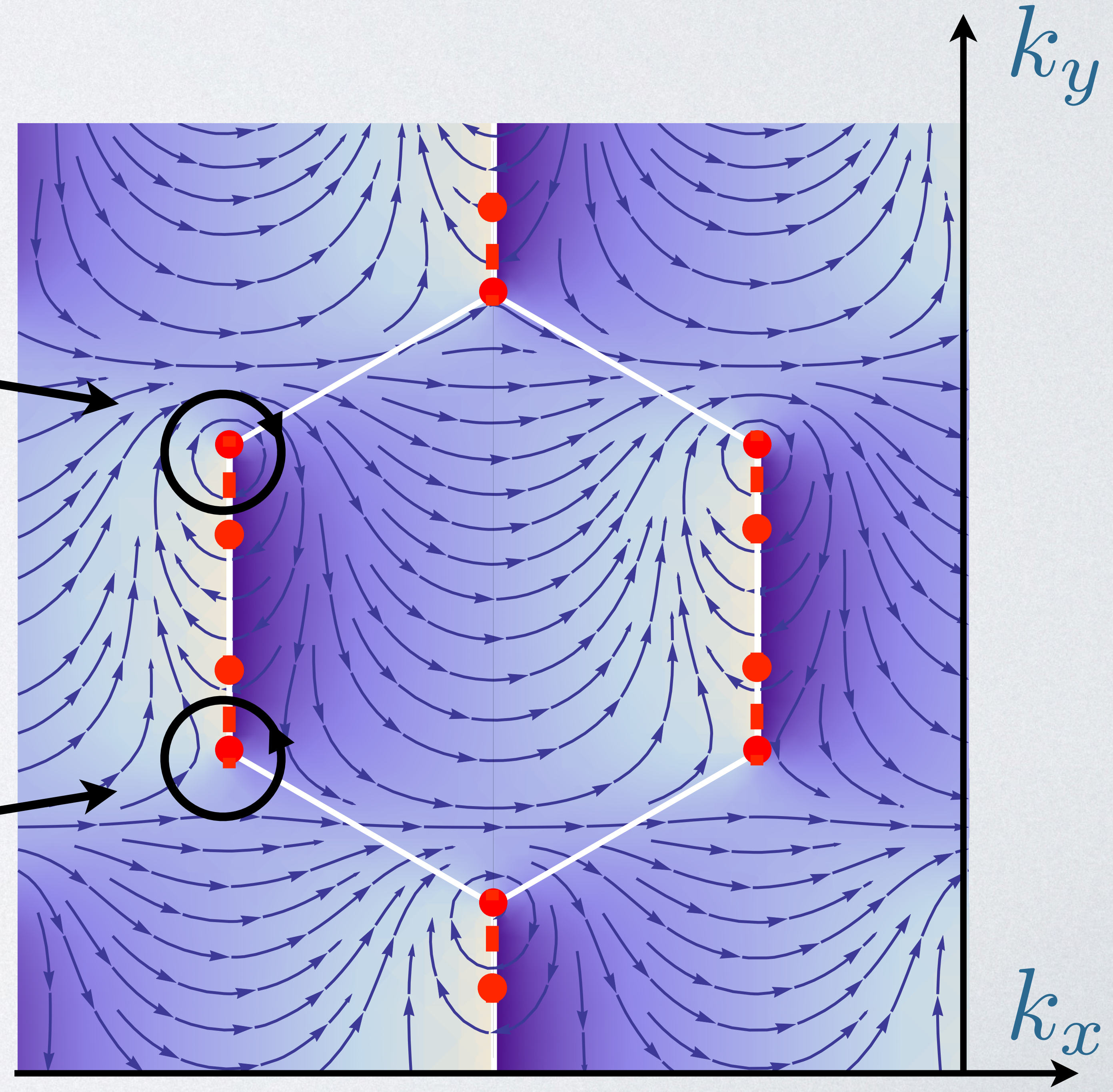

Topological Phase Transition

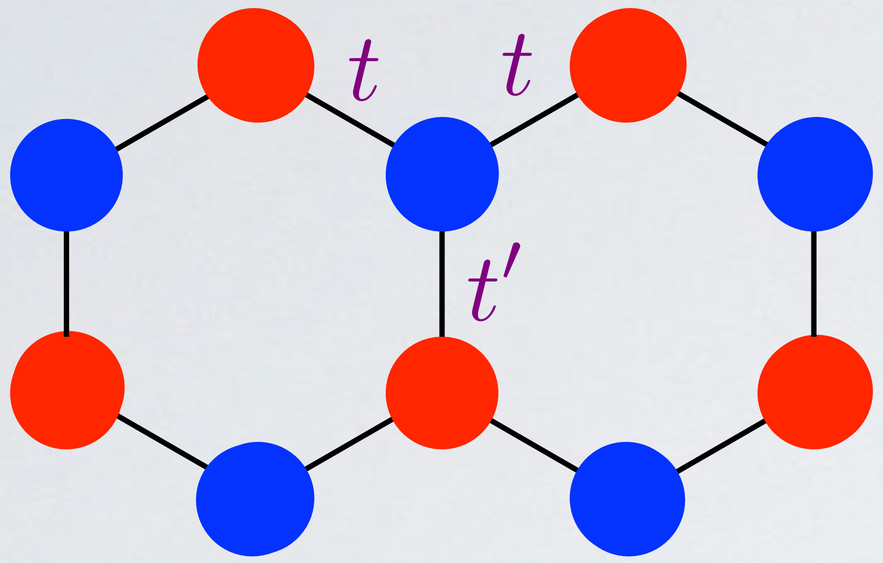

When anisotropy increases, Dirac points...

move... merge... disappear.

gapless phase — gapped phase

1 — β_c — β

semi-metal — insulator

anisotropy parameter:

$$\beta = \frac{t'}{t}$$

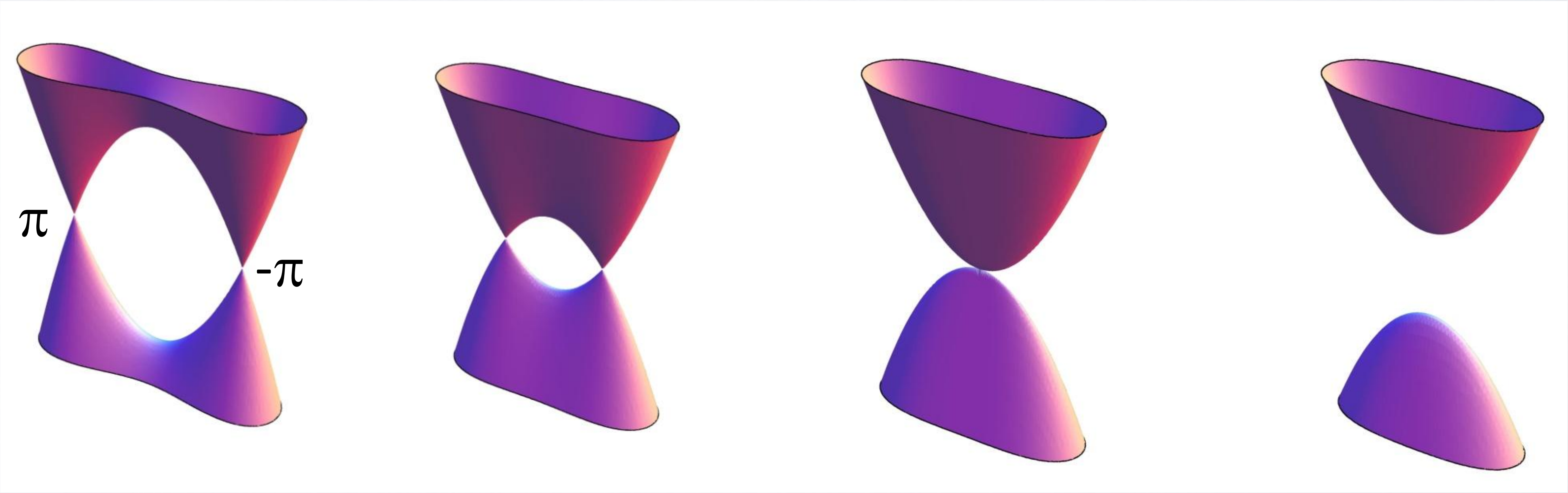

Montambaux, Piéchon, Fuchs, Goerbig (2009)
Hasegawa *et al.* (2006) ; Pereira *et al.* (2009)

Topological Phase Transition

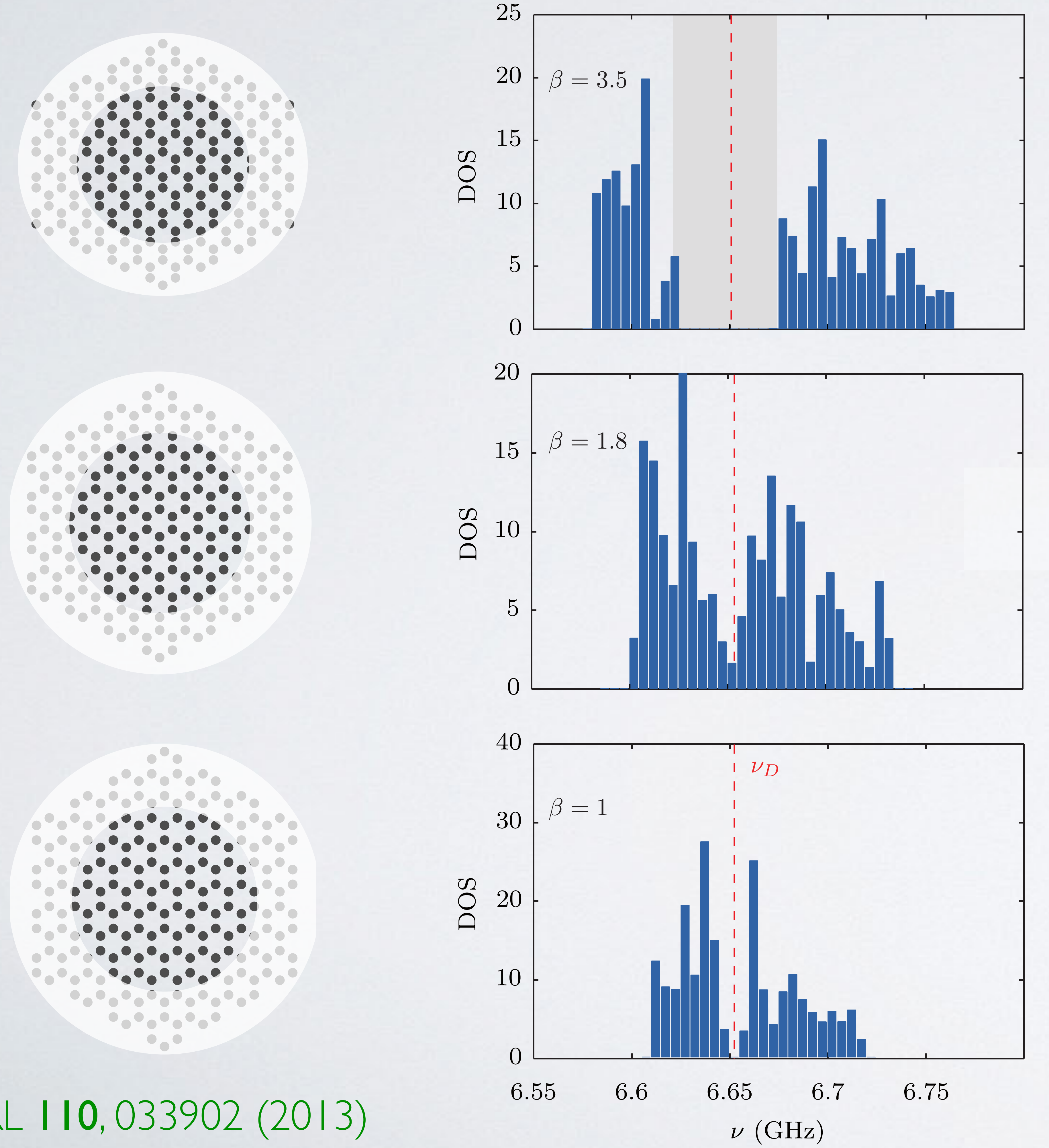

PRL **110**, 033902 (2013)

INPHYNI

Topological Phase Transition

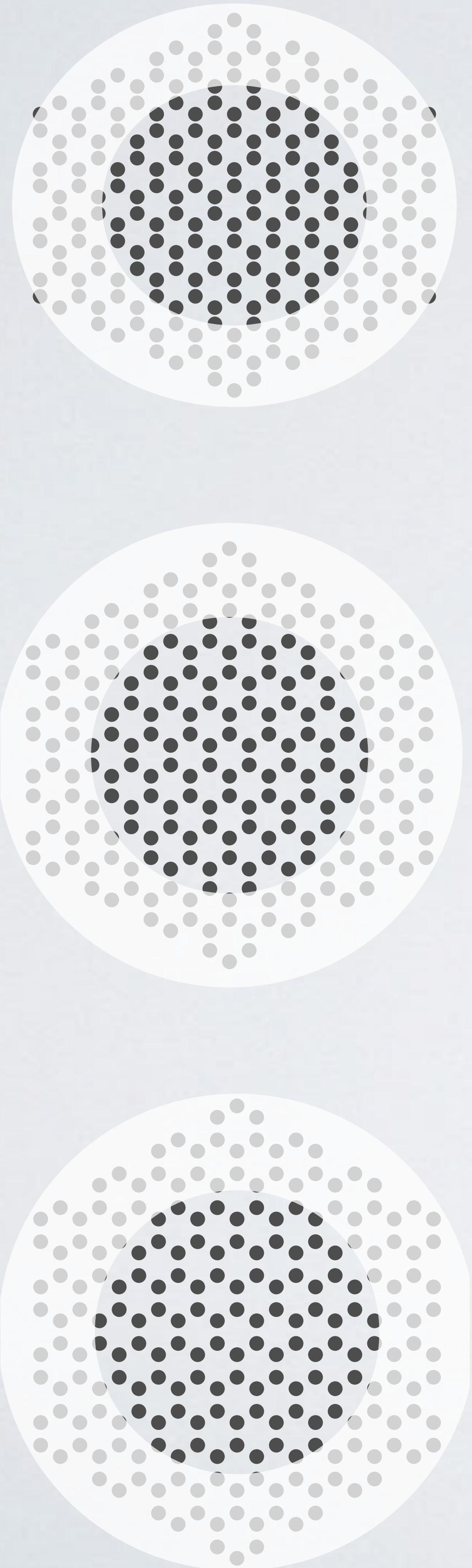

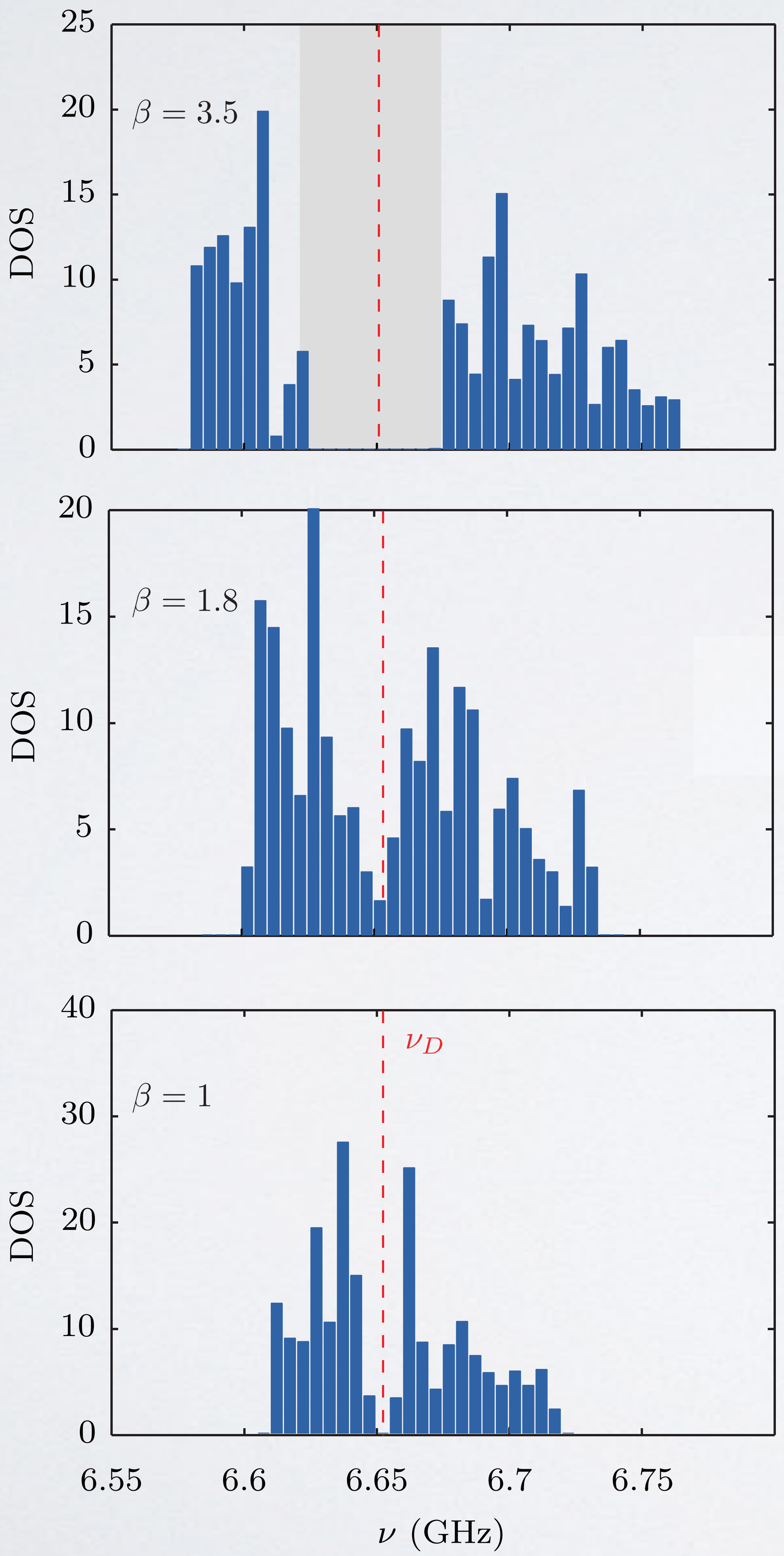

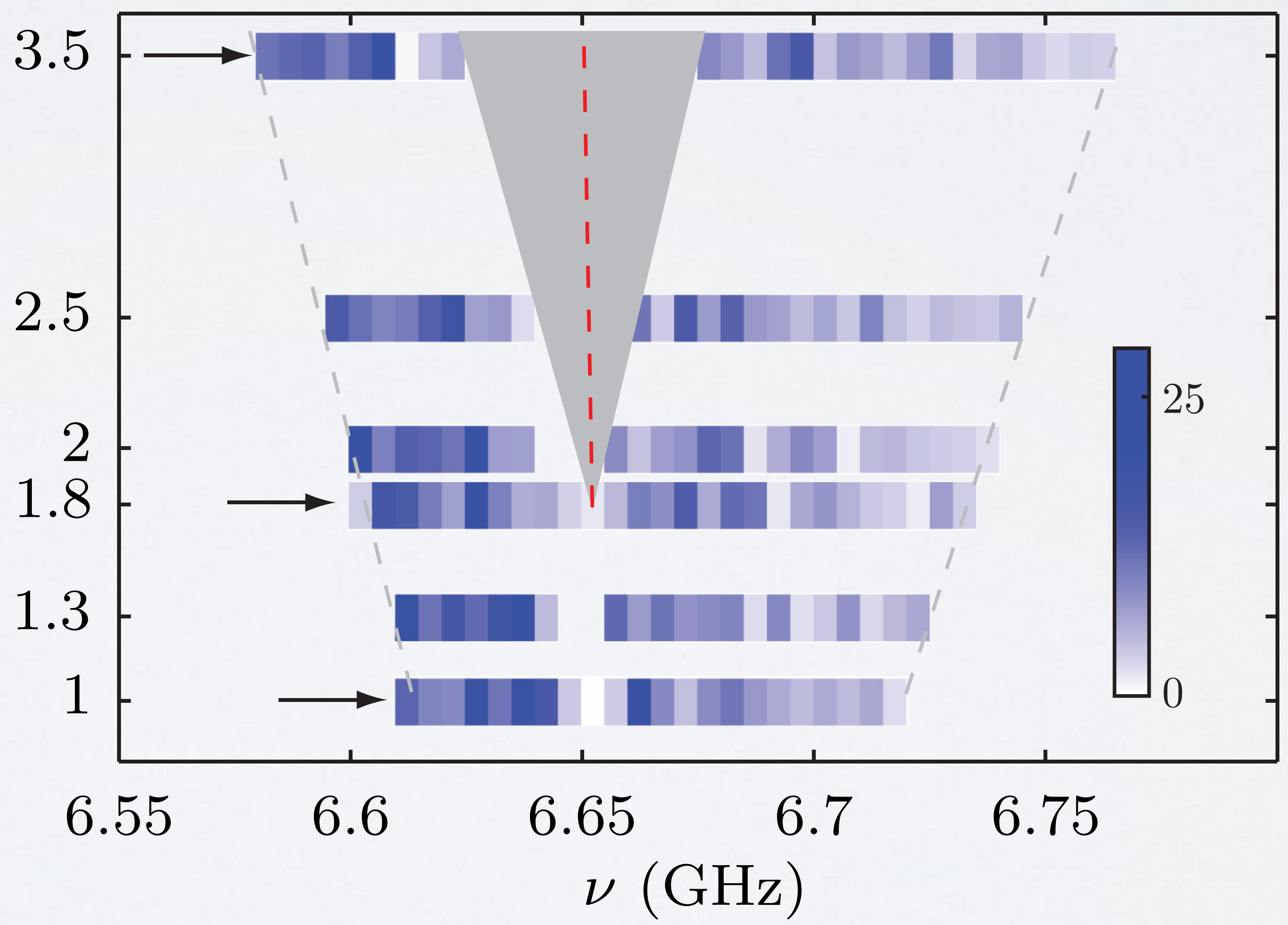

PRL **110**, 033902 (2013)

Topological Phase Transition

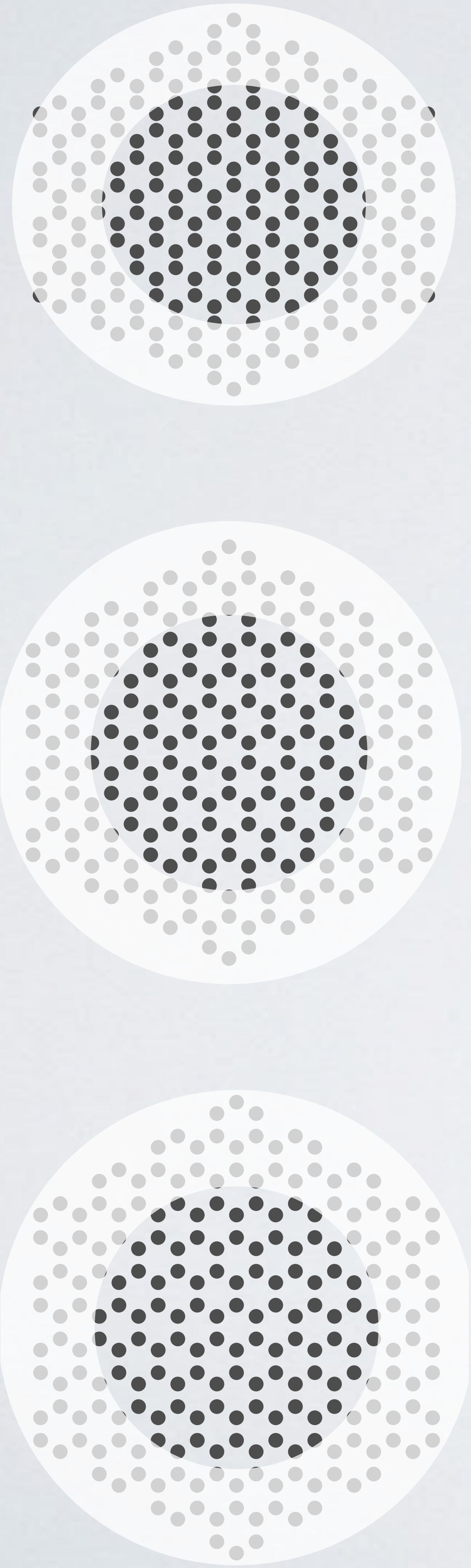

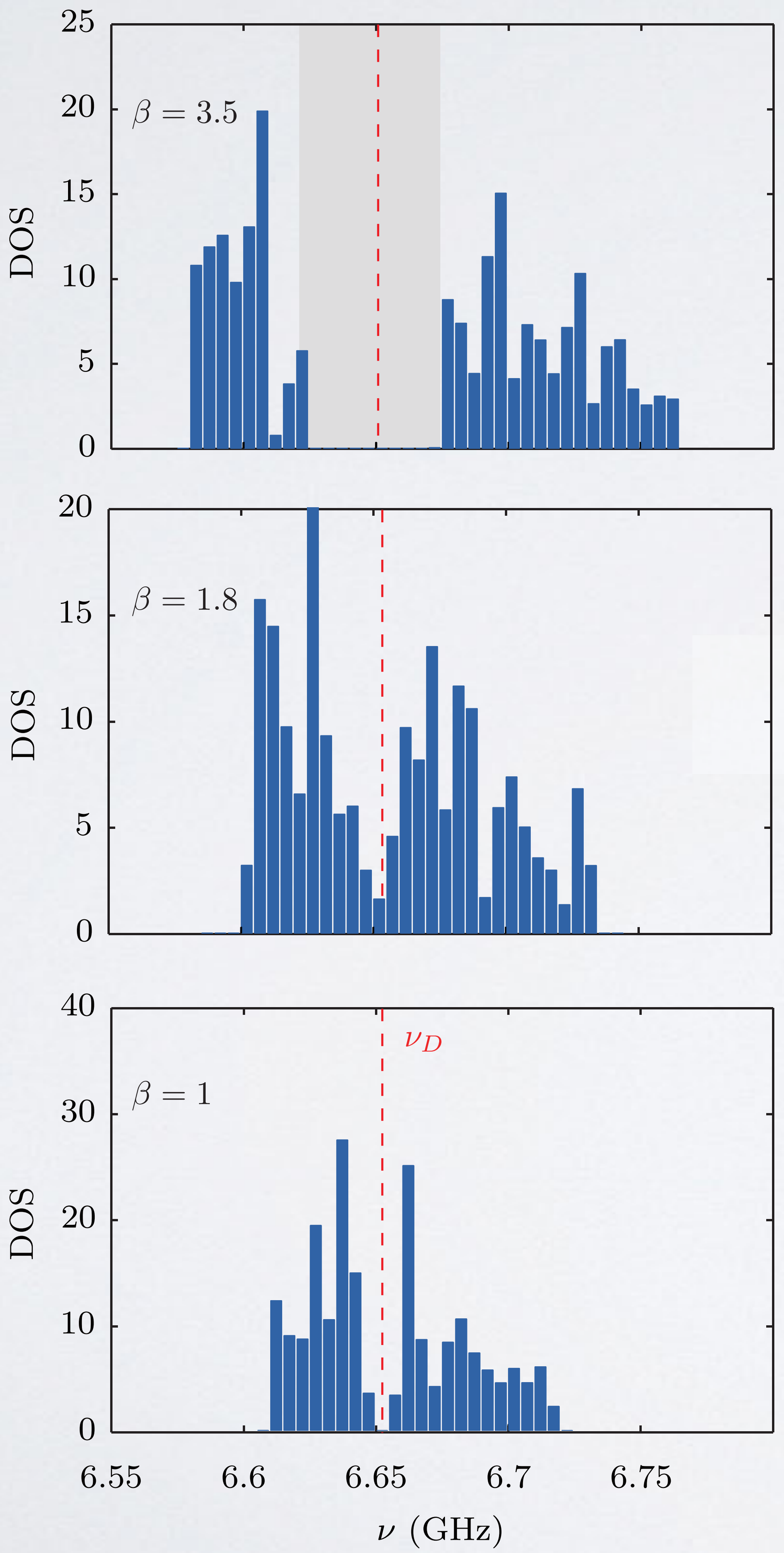

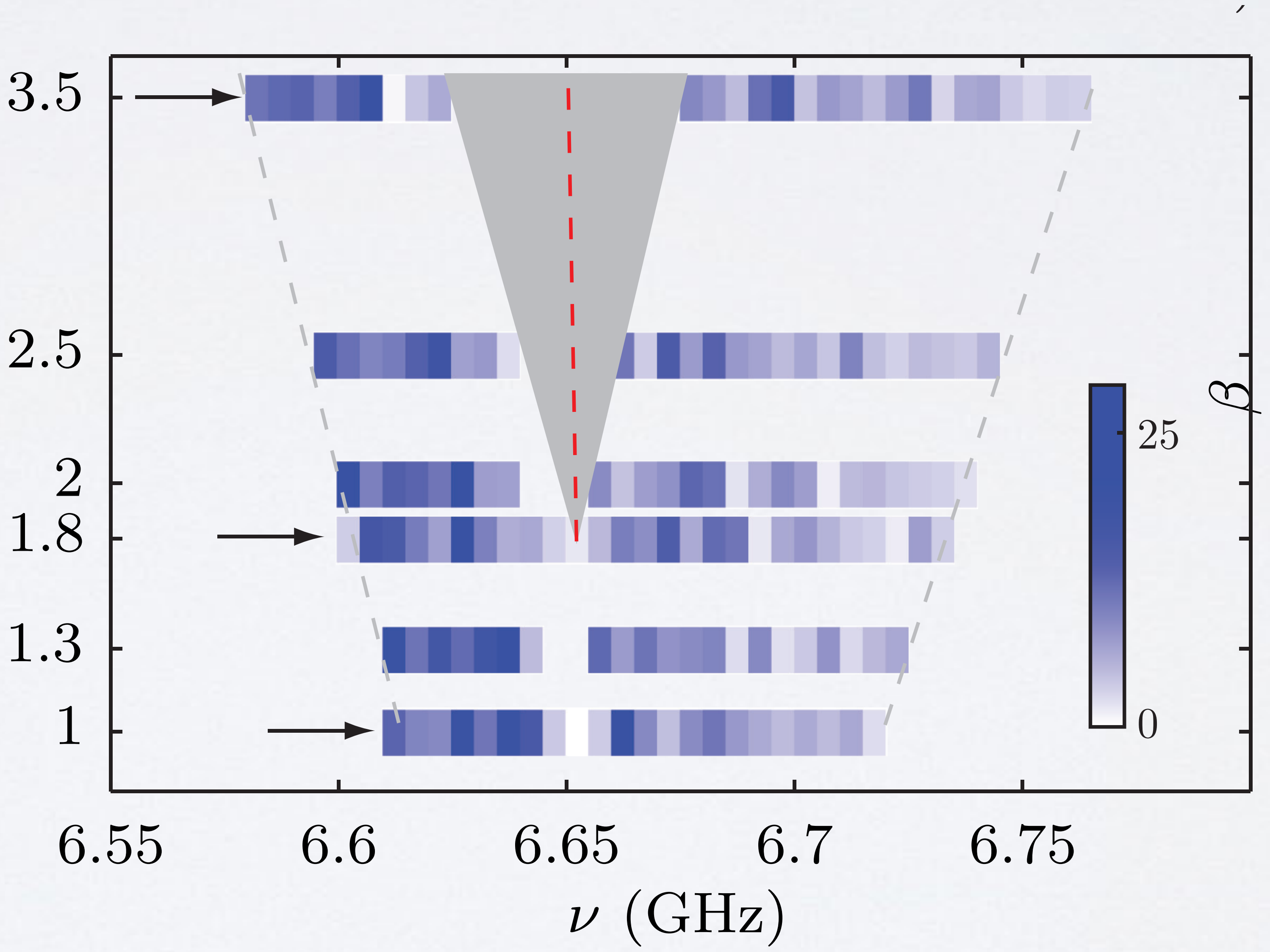

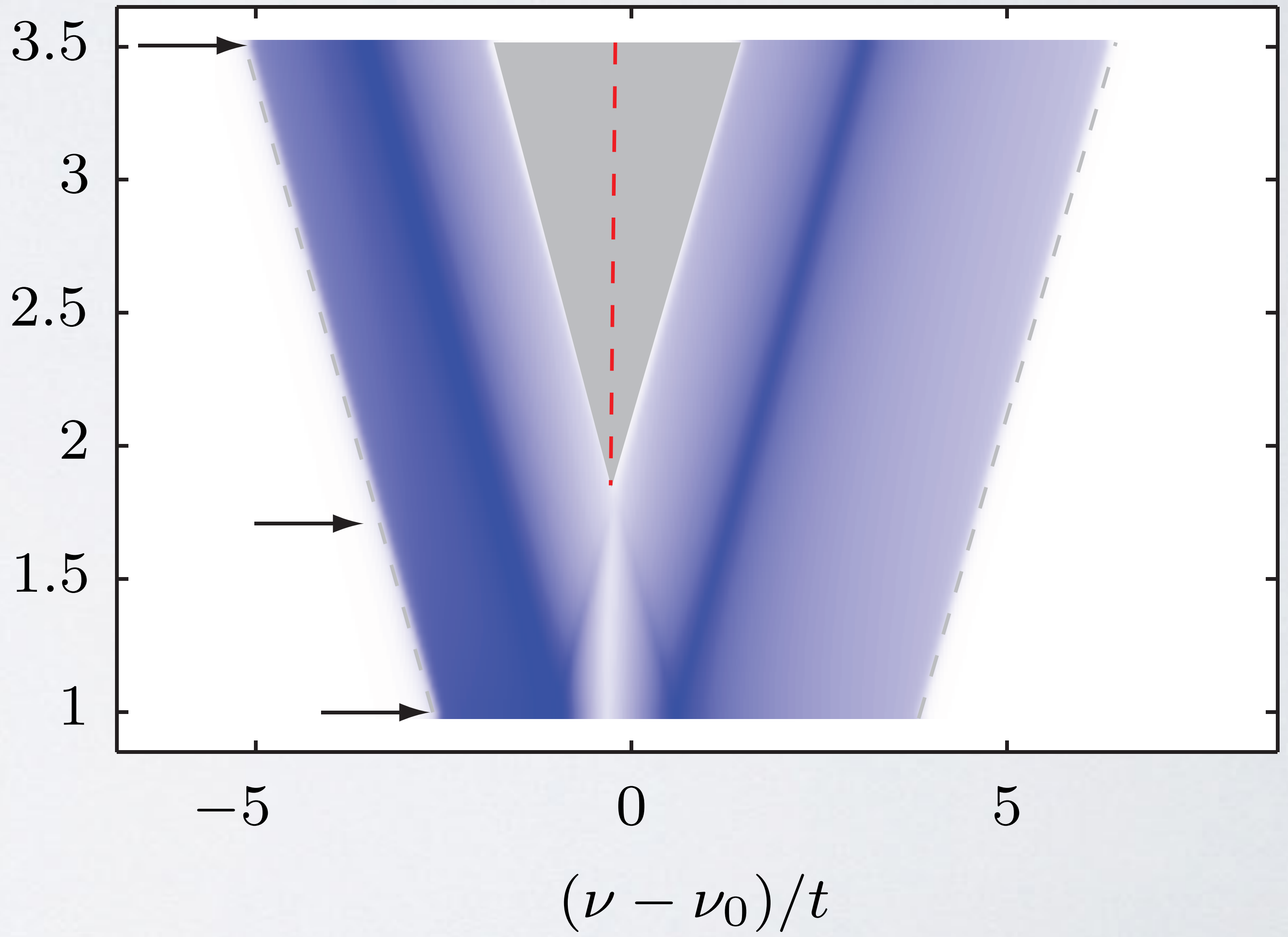

PRL **110**, 033902 (2013)

INPHYNI

Topological Phase Transition

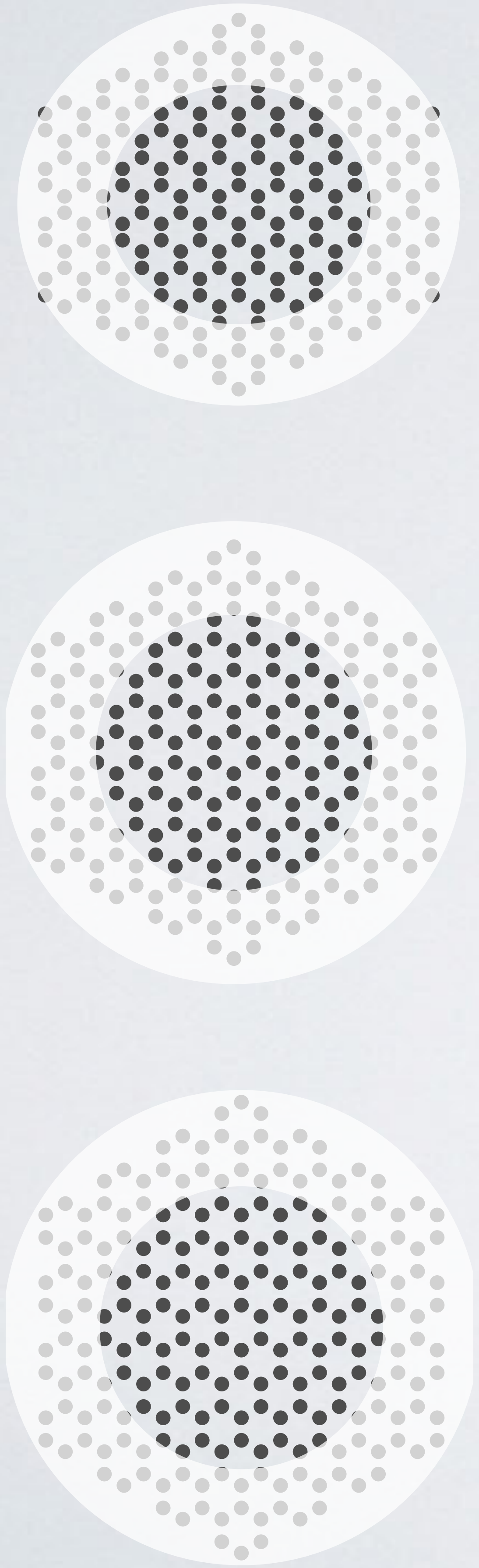

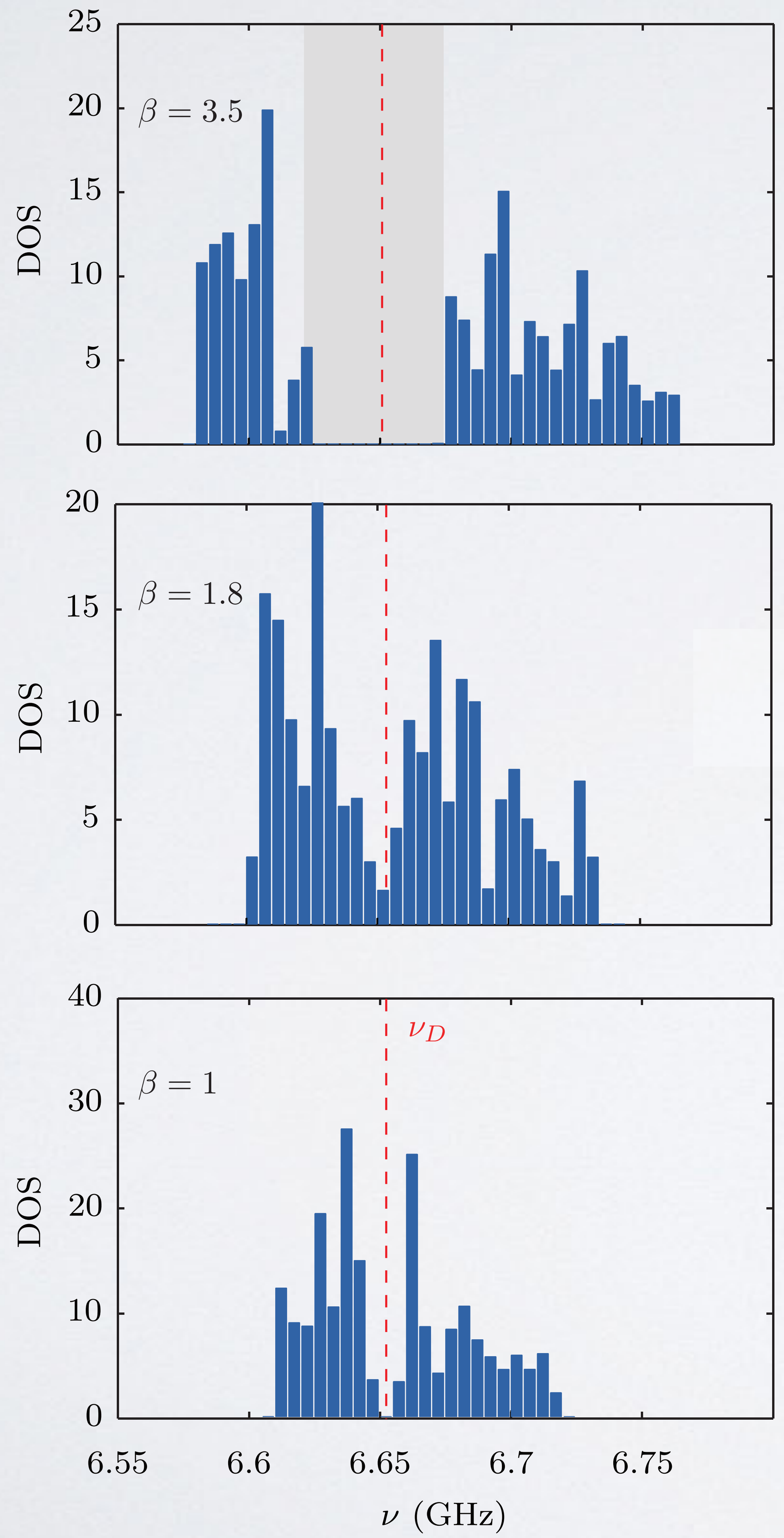

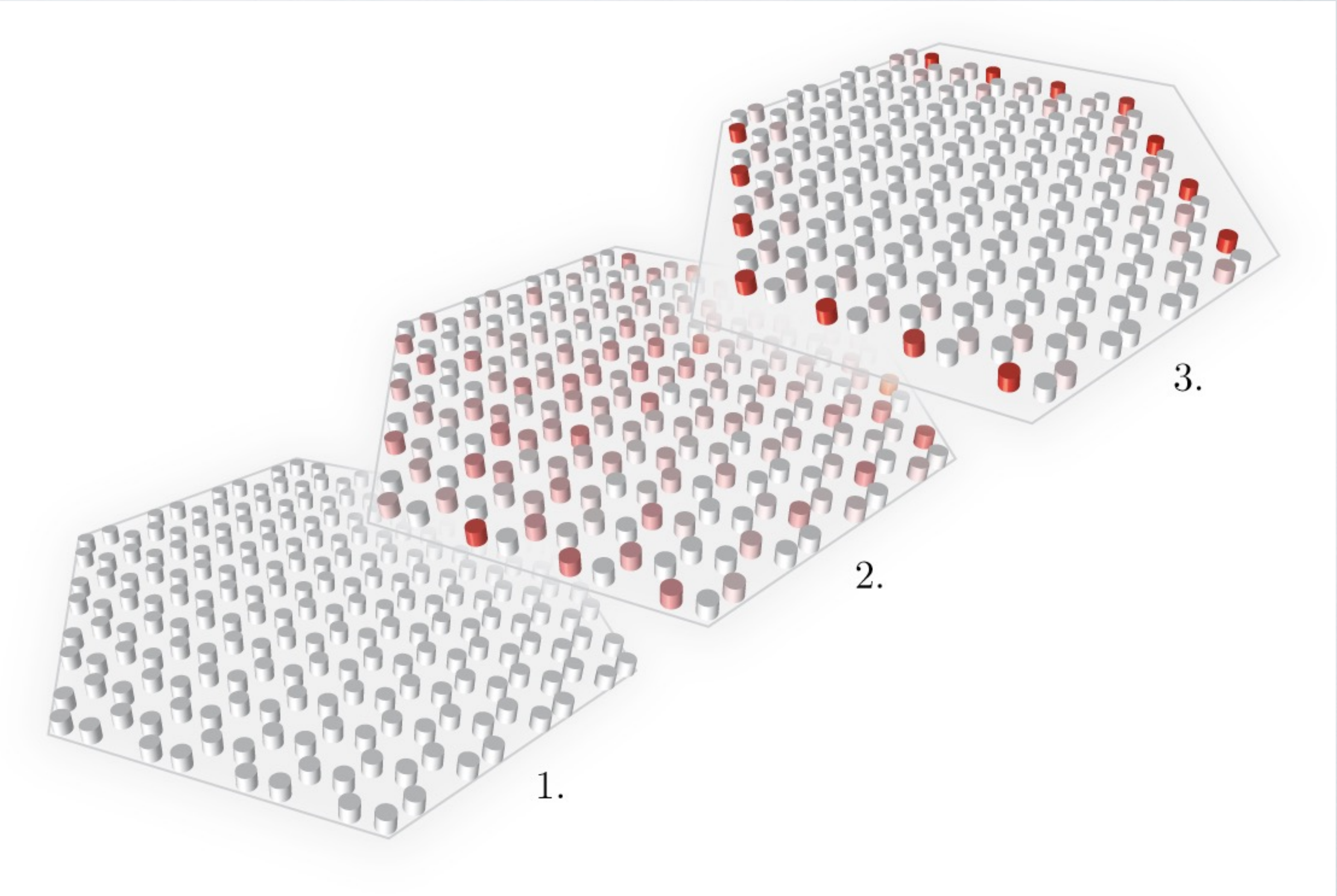

PRL **110**, 033902 (2013)

Edge states

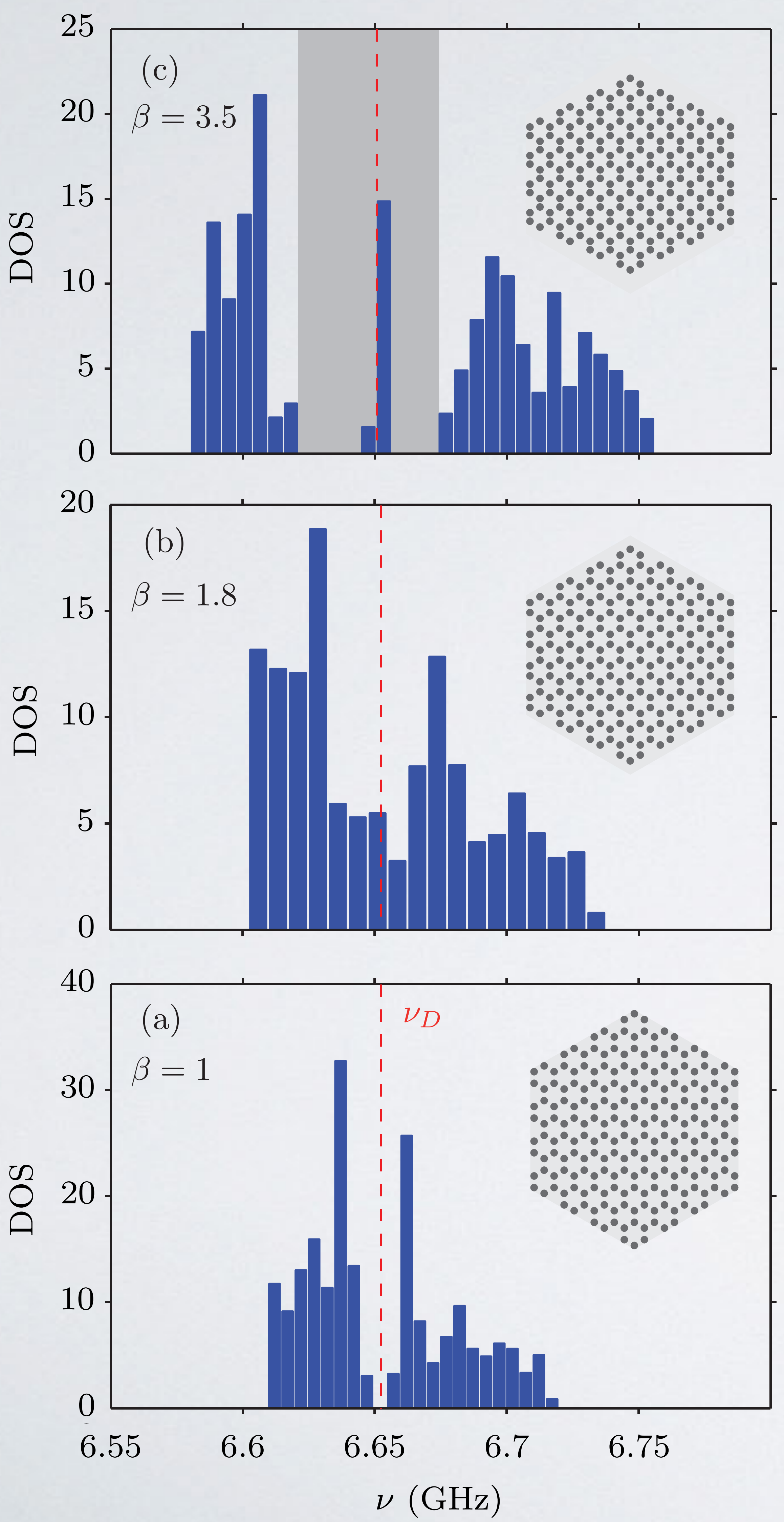

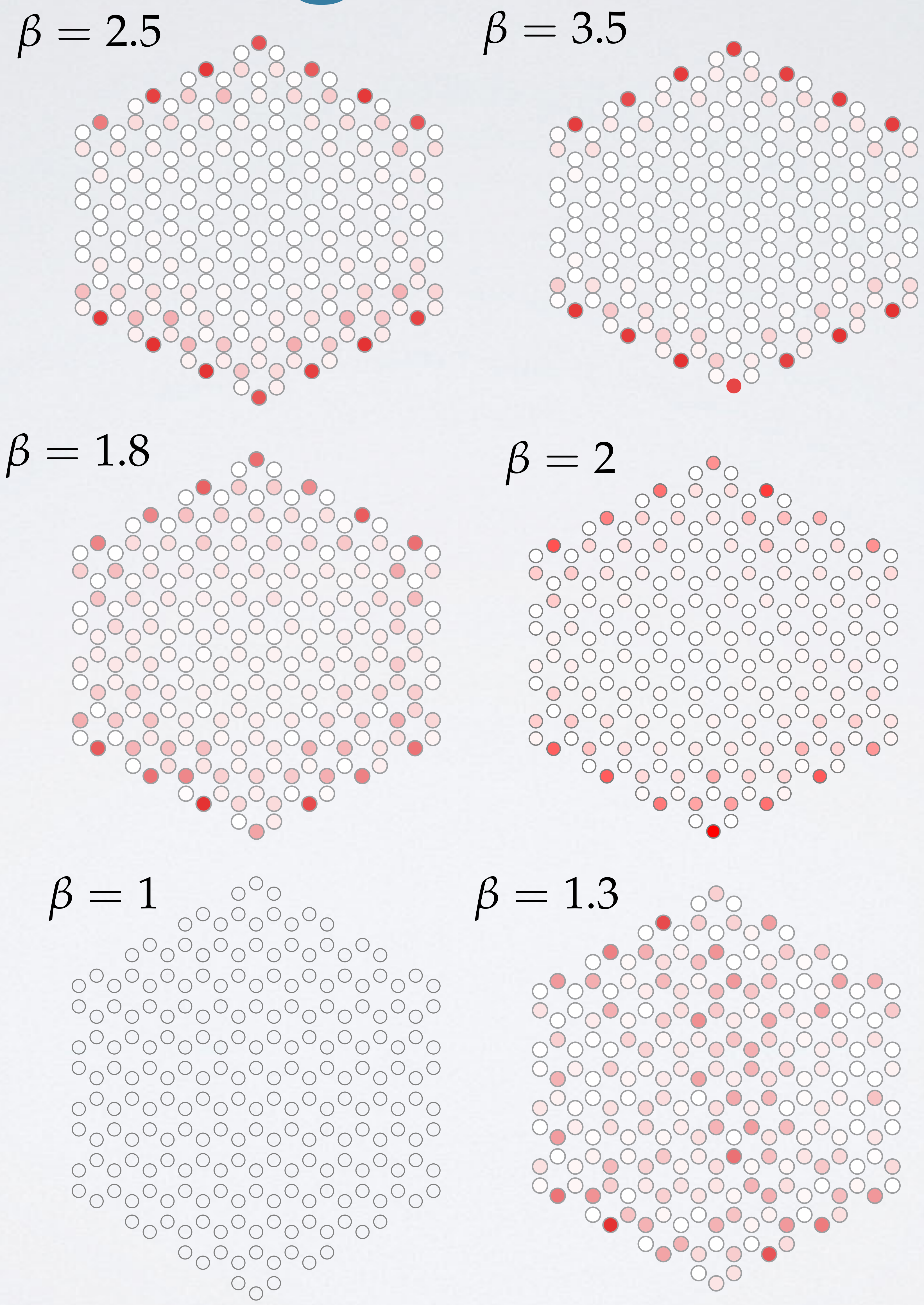

- no edge states along the compression axis
- edge states live only on one sublattice
- the higher the anisotropy the smaller the extension into the bulk

Edgde states in 'graphene' ribbons

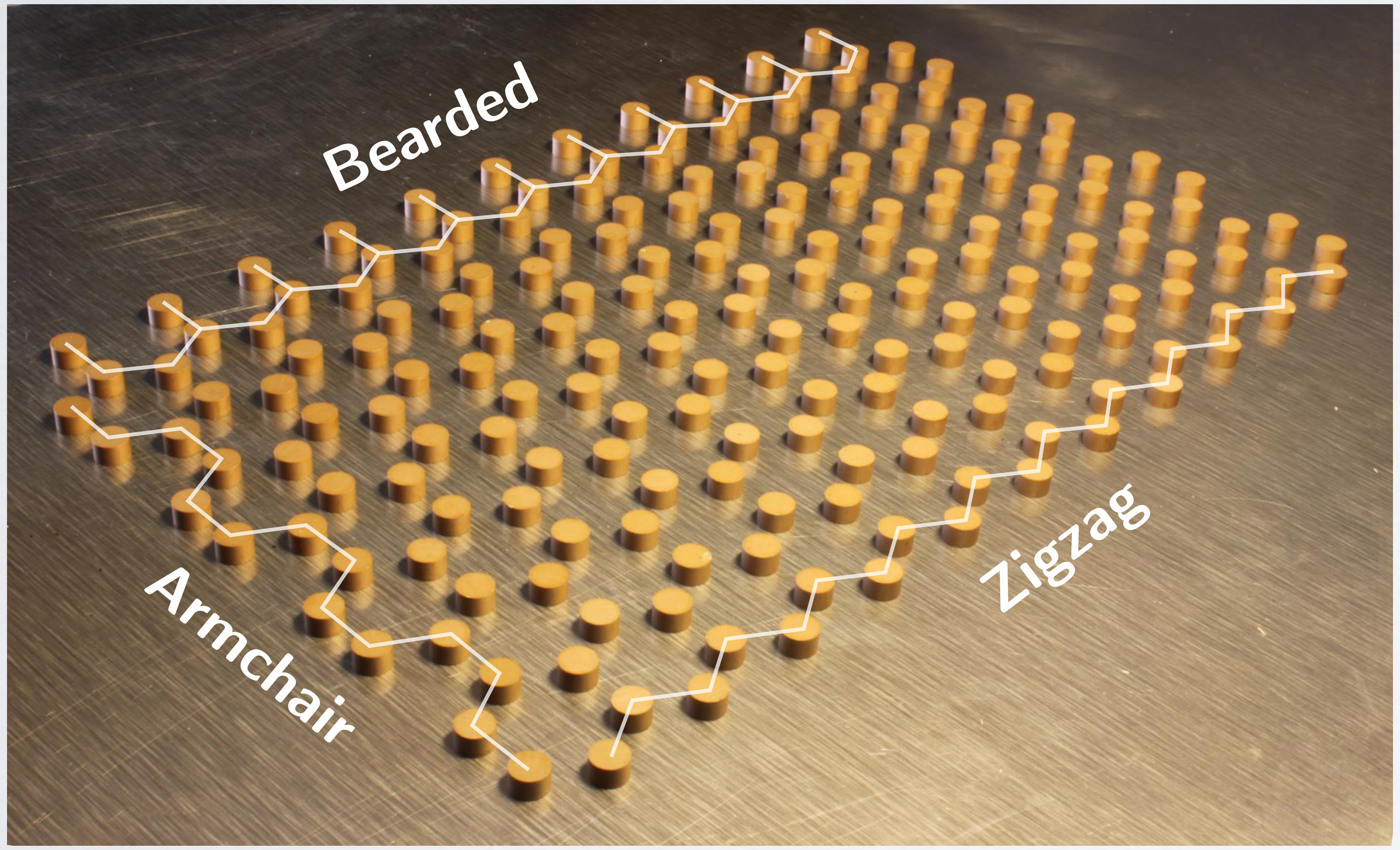

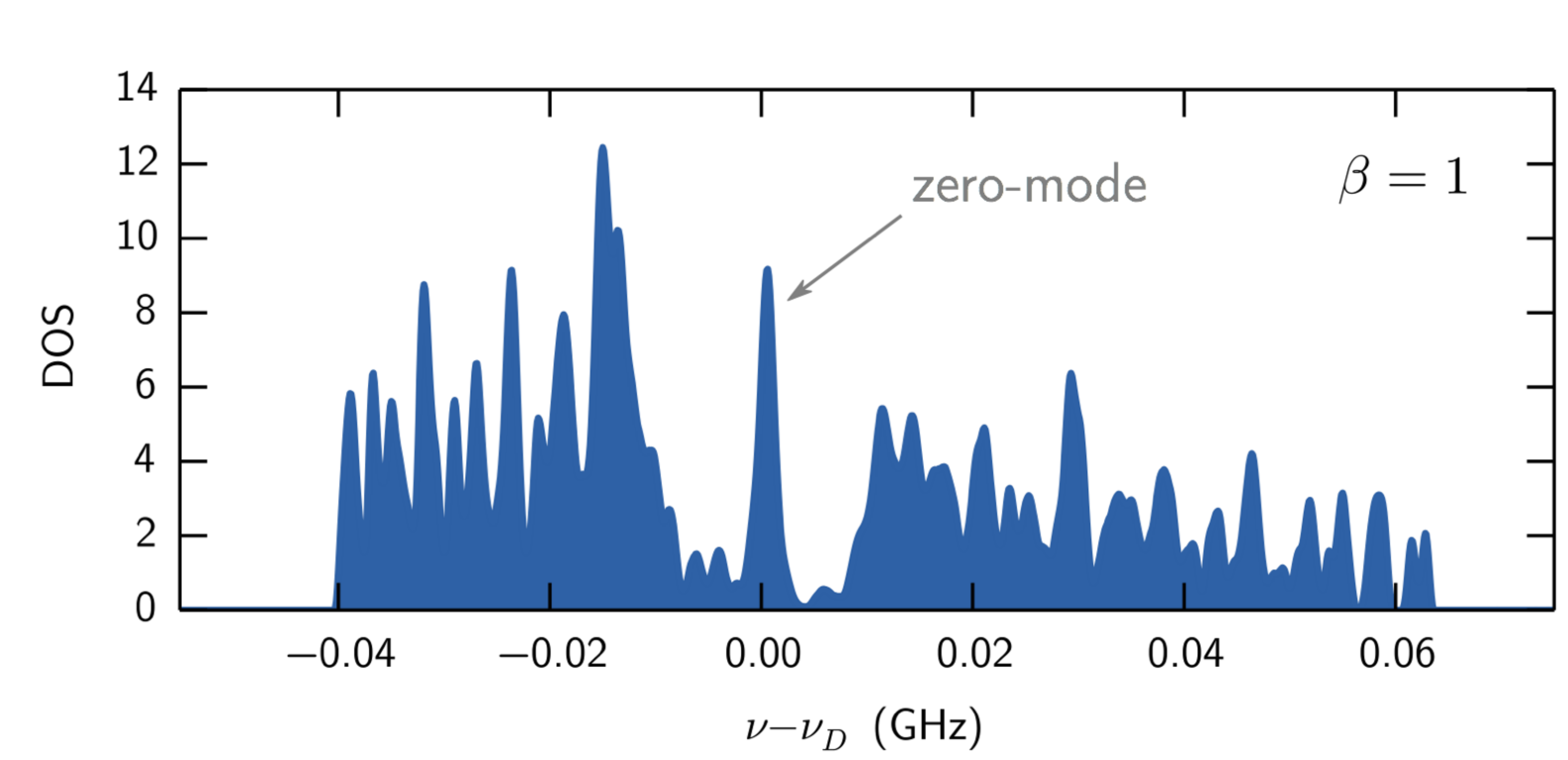

Edgde states in ‘graphene’ ribbons

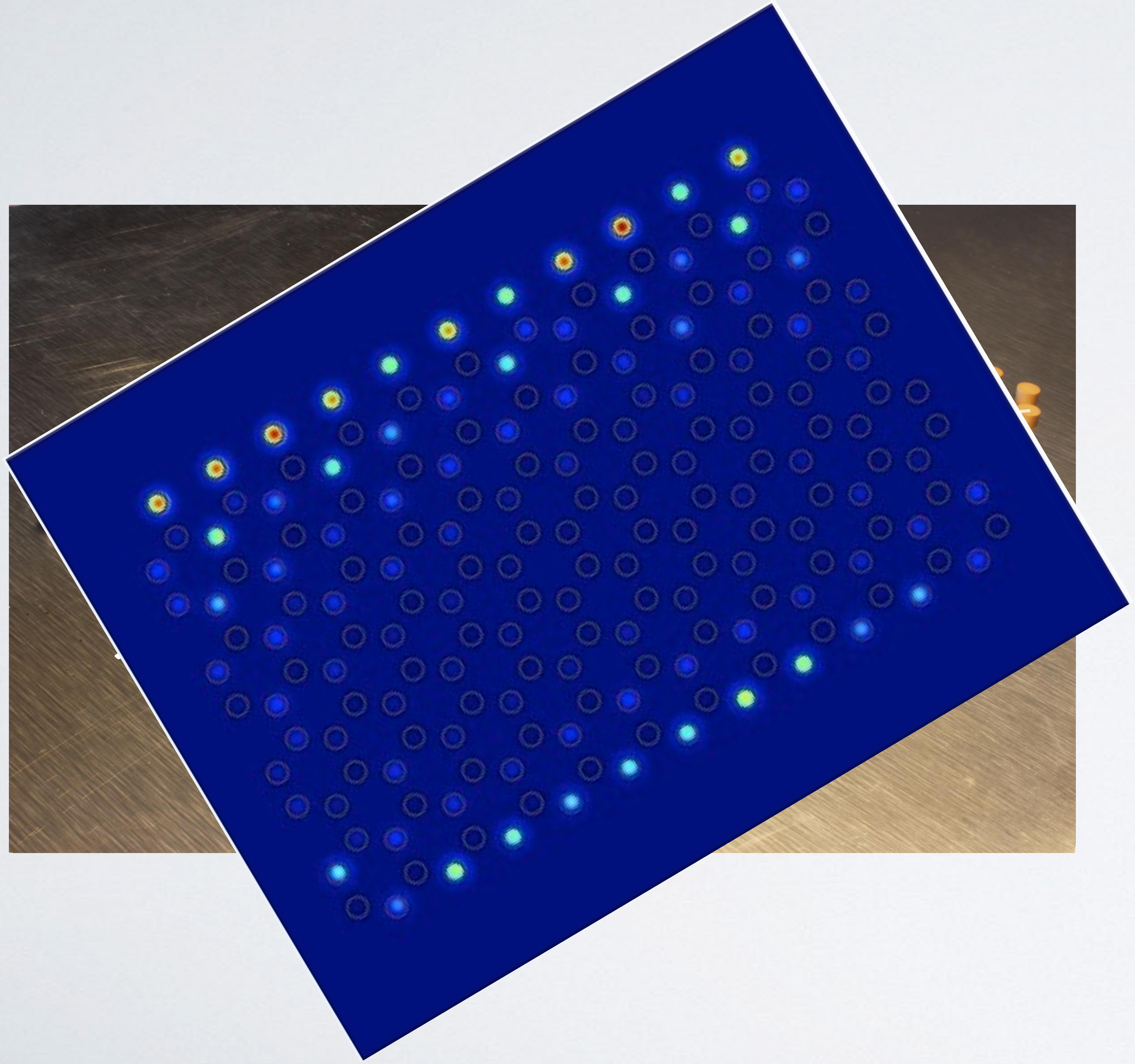

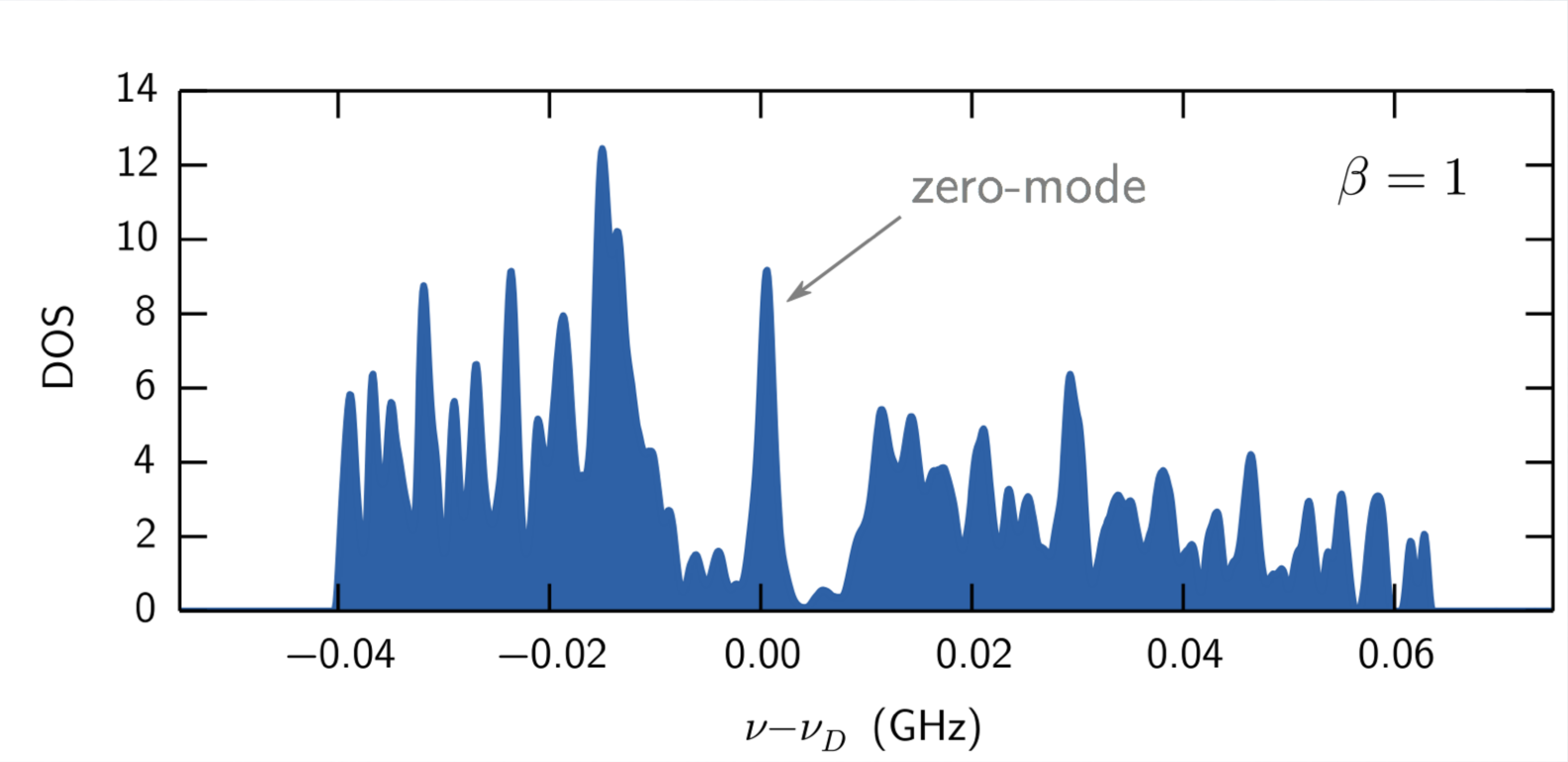

Zig-zag & Bearded edge states

Zak phase & edge states

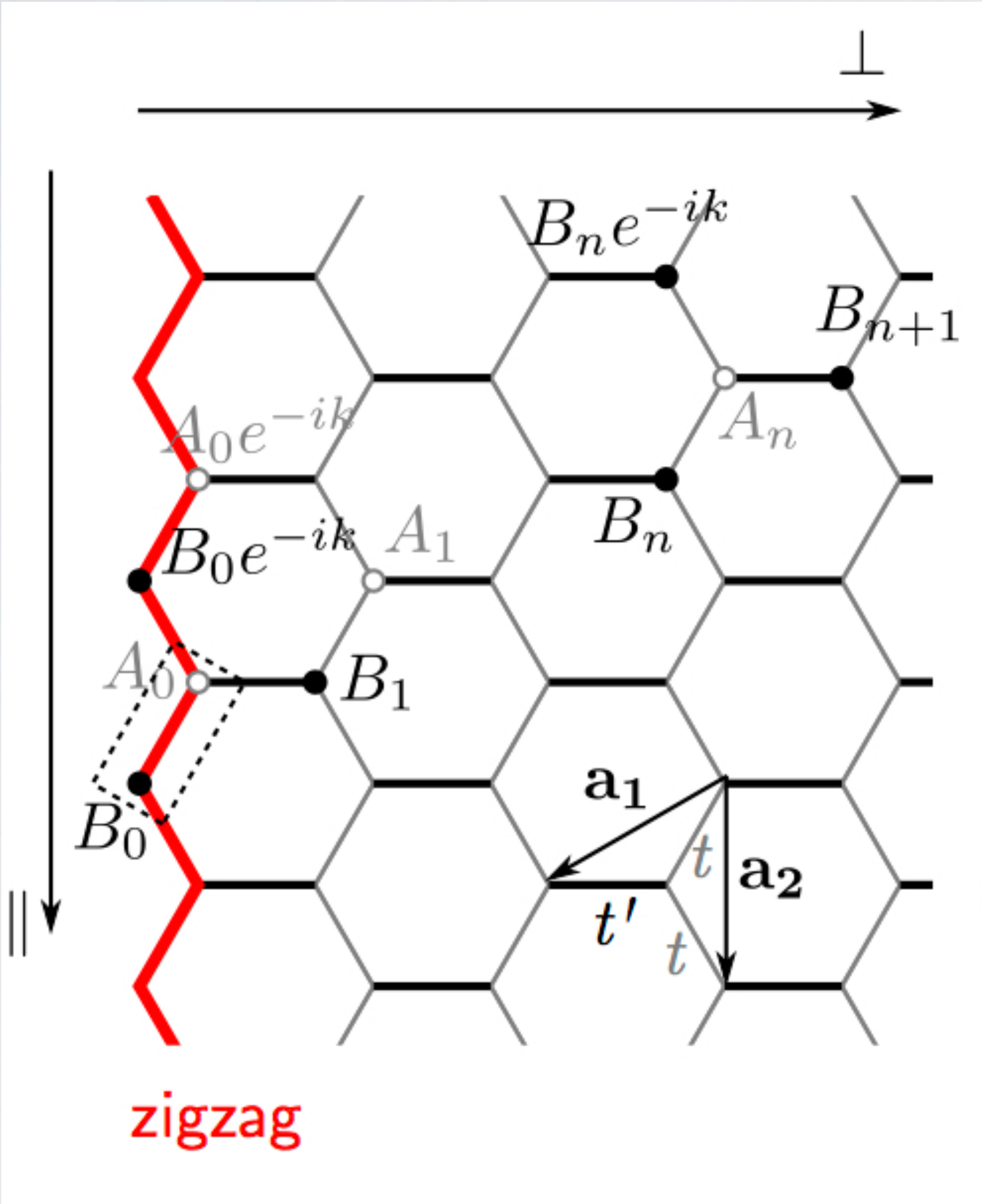

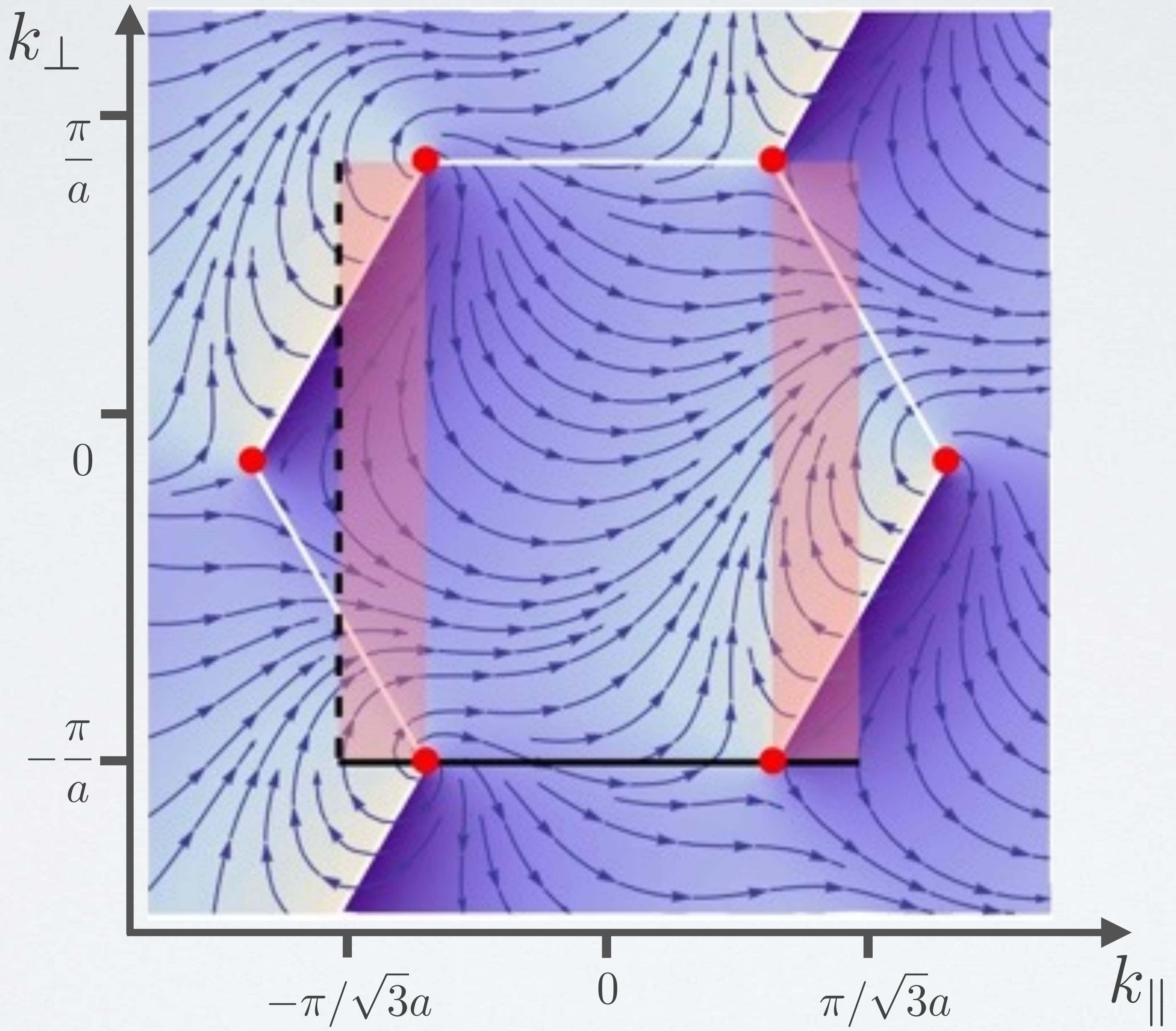

$$f^{zz}(\boldsymbol{k}) = 1 + \beta e^{i(\frac{\sqrt{3}}{2}k_\parallel - \frac{3}{2}k_\perp)a} + e^{i\sqrt{3}k_\parallel a}$$

Delplace et al. PRB (2011)

INPHYNI

Zak phase & edge states

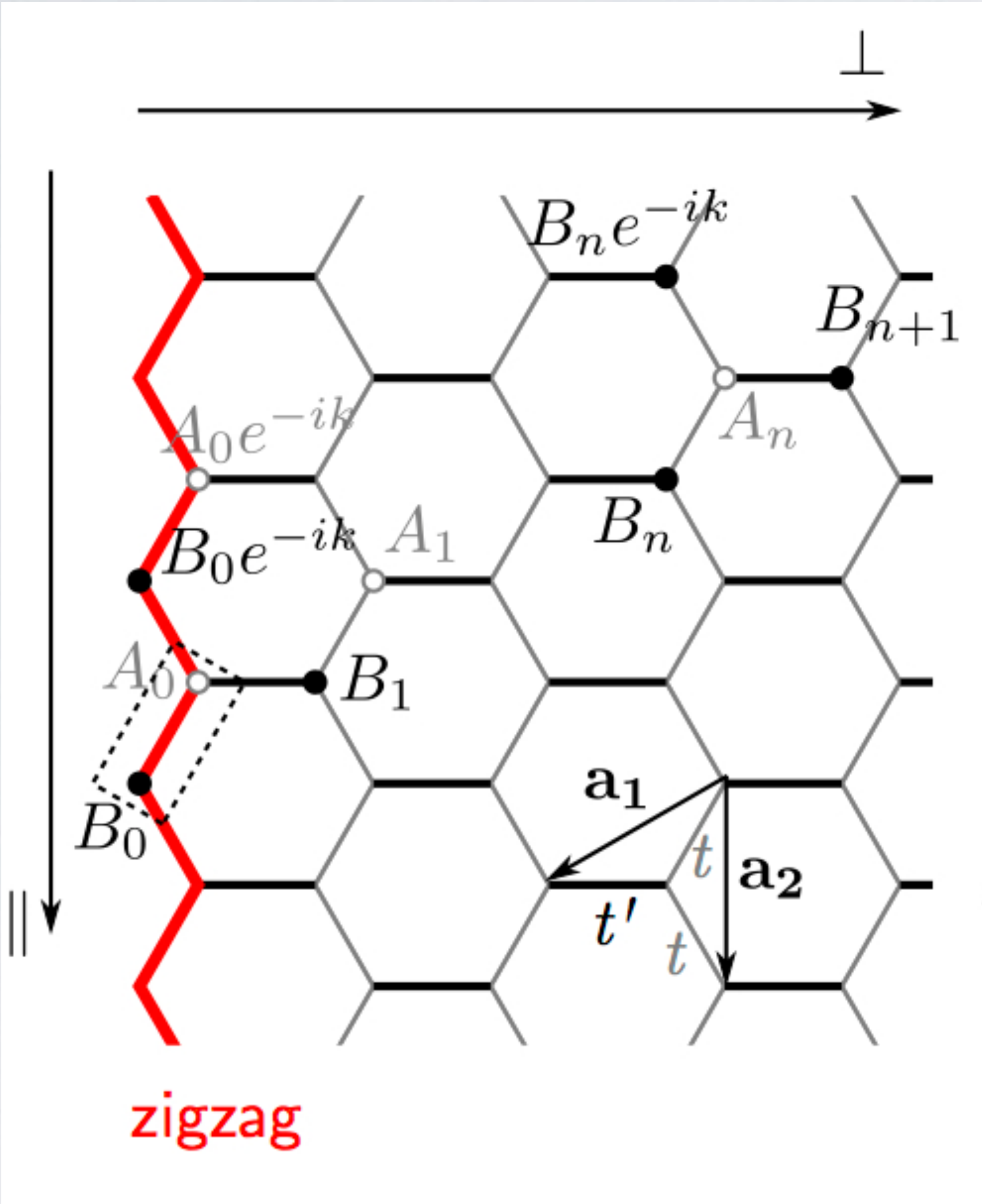

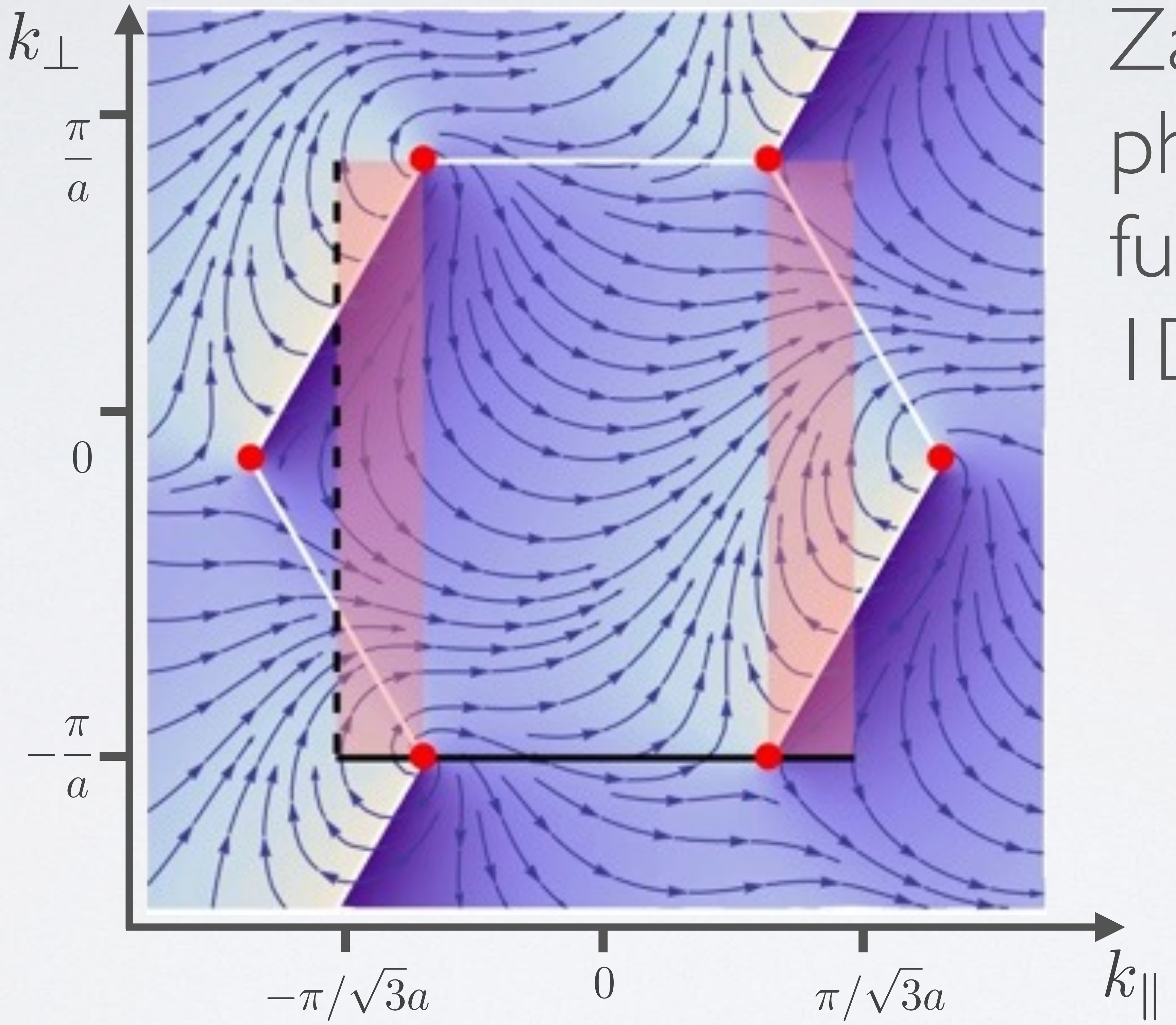

Zak phase corresponds to the Berry phase accumulated by the wave-function along a path exploring the 1D Brillouin zone.

$$\mathcal{Z}(k_\parallel) = \frac{1}{2}\int_{BZ} dk_\perp \frac{\partial\phi(k_\parallel, k_\perp)}{\partial k_\perp}$$

$$\mathcal{Z}(k_\parallel) = \begin{cases} \pi & \text{edge states} \\ 0 & \text{no edge states} \end{cases}$$

$$f^{zz}(\boldsymbol{k}) = 1 + \beta e^{i(\frac{\sqrt{3}}{2}k_\parallel - \frac{3}{2}k_\perp)a} + e^{i\sqrt{3}k_\parallel a}$$

Delplace et al. PRB (2011)

BD & ZZ existence diagram

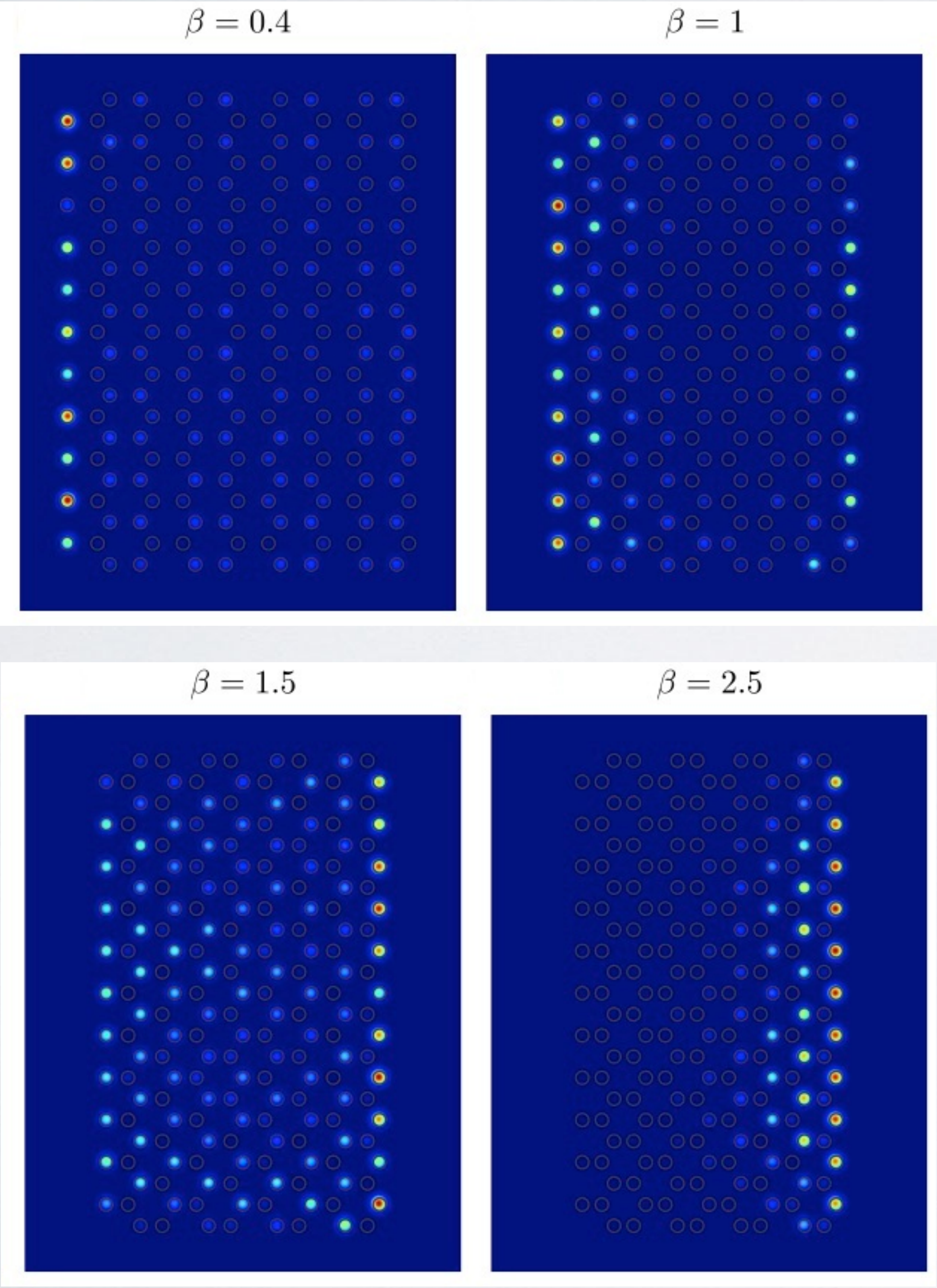

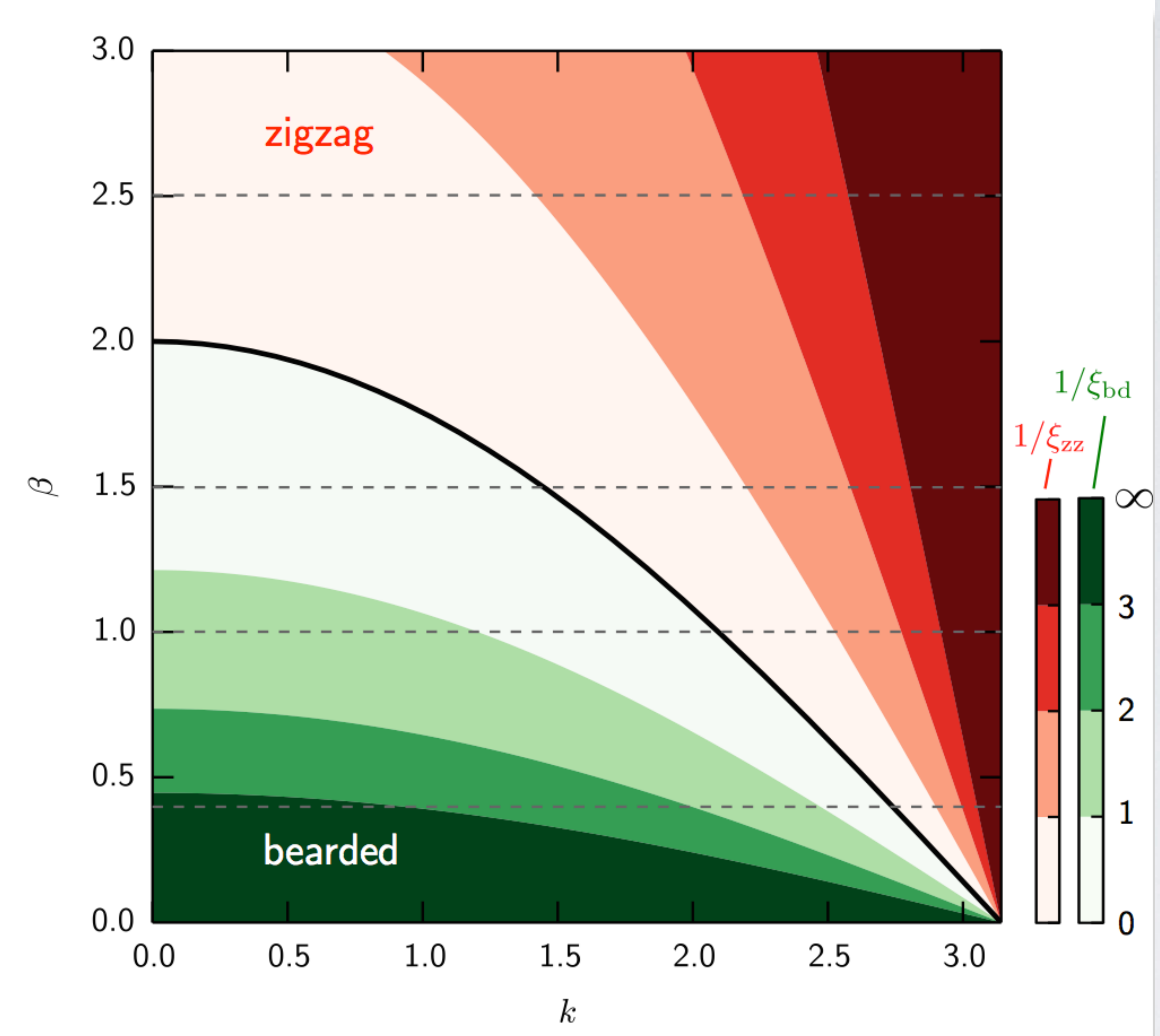

ξ_{zz}
ξ_{bd}
localization lengths (TB analysis)

Armchair edge states existence diagram

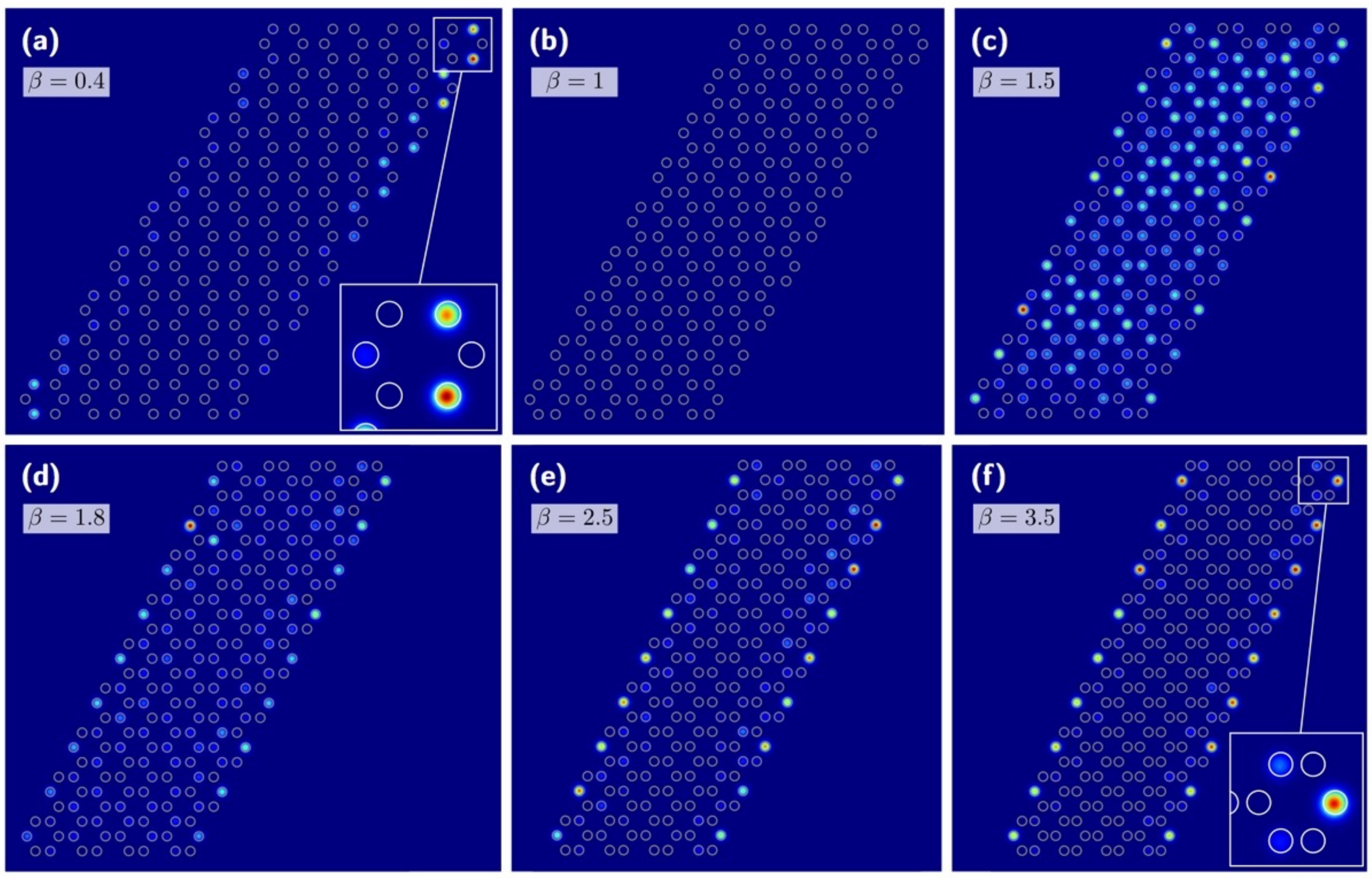

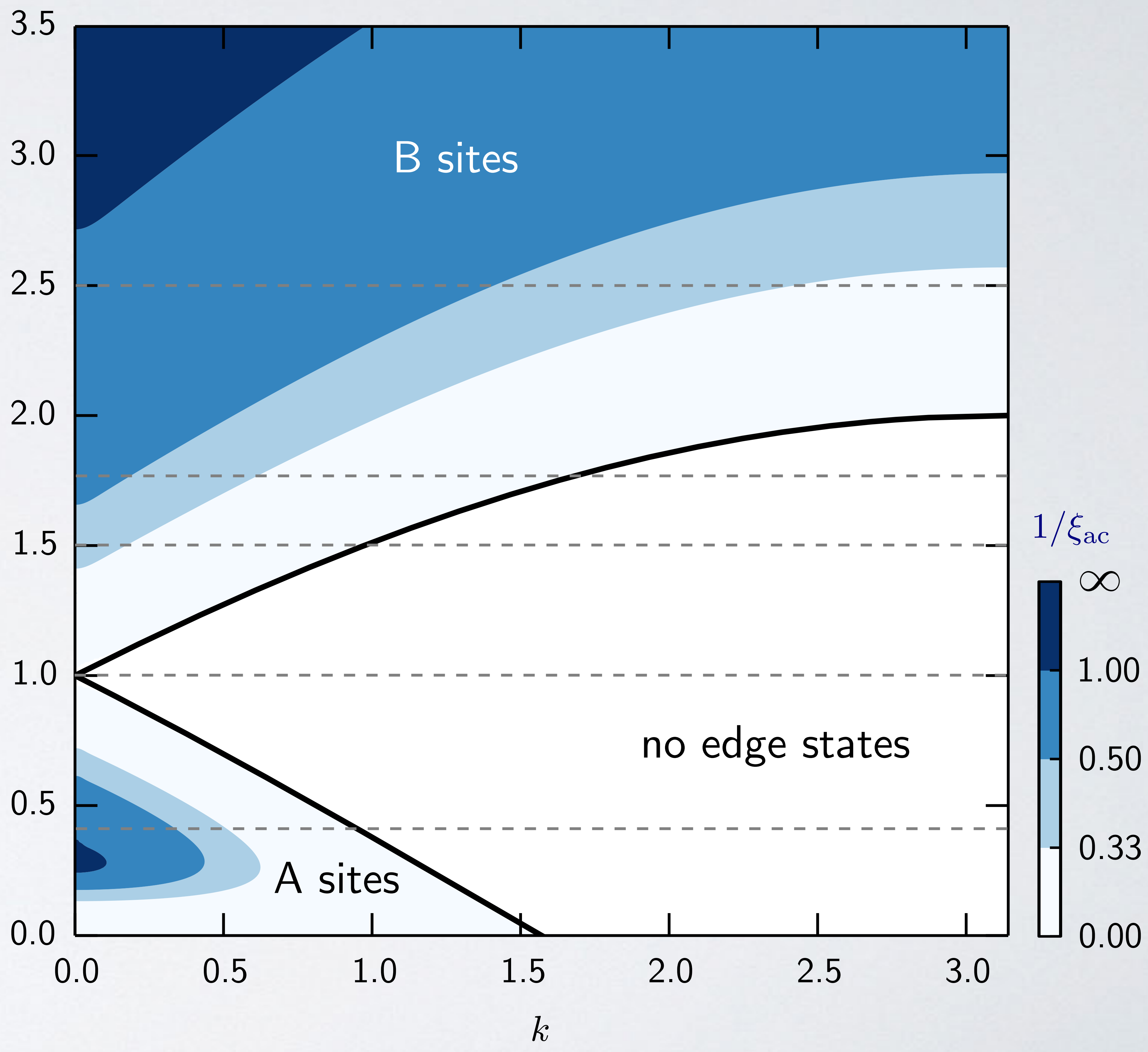

NJP **16**, 113023 (2014)

INPHYNI

Outline

1. The playground: coupled microwave resonator lattices

   dielectric resonators, TE modes, evanescent coupling, LDOS & eigenstates

2. Initiatory game: topological phase transition in strained graphene

   Berry phase, merging of Dirac points, Zak phase, manipulation of edge states

3. ‘Flat games’: Lieb lattice & Pseudo-Landau levels

   flat band, sublattice polarization, gigantic pseudo-magnetic field, supersymmetric oscillator

INPHYNI

Lieb lattice

The paradigmatic example of bipartite system with flat band

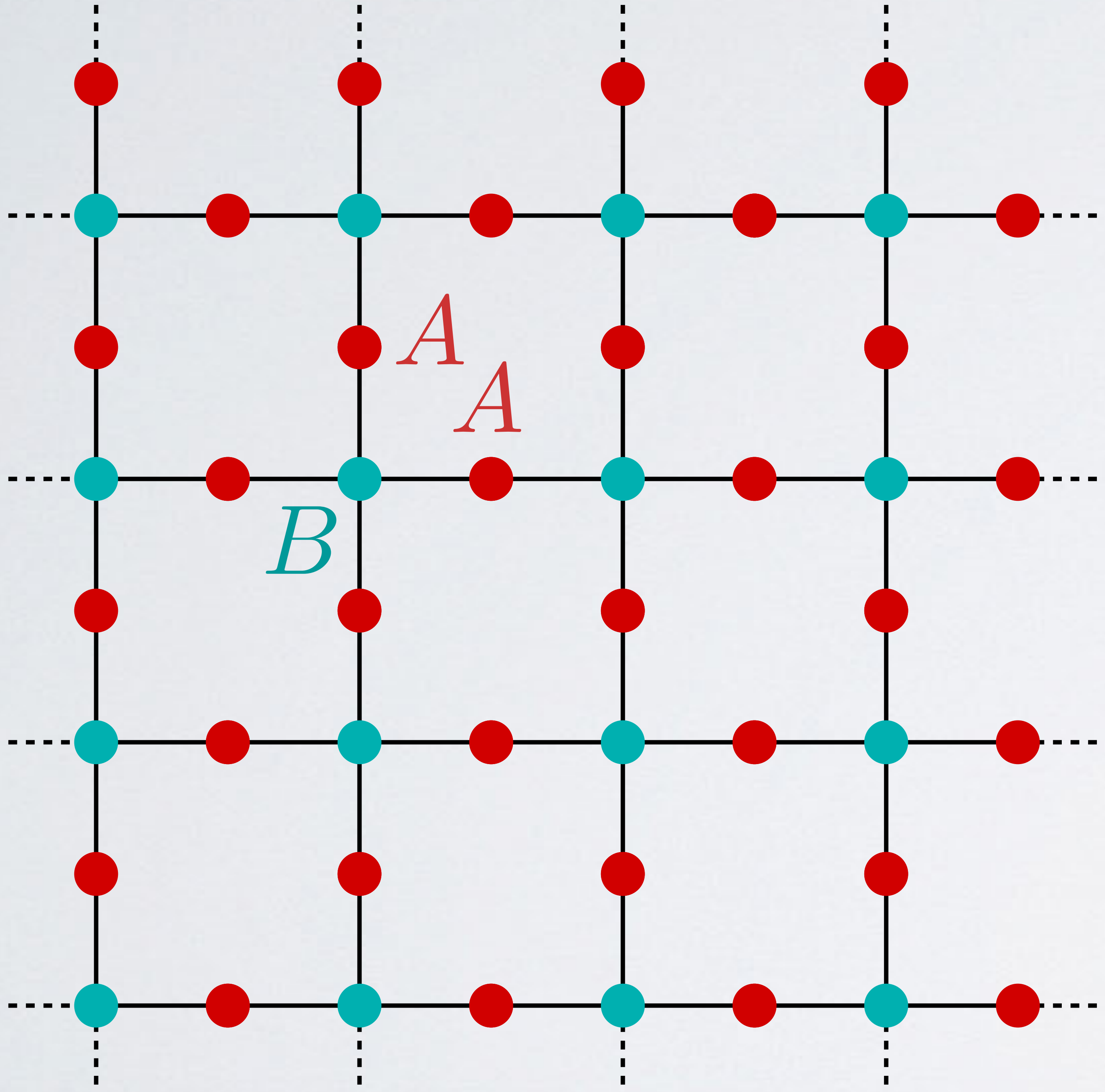

- A sites: majority sublattice, B sites: minority sublattice
- Two dispersive bands forming a Dirac cone at the M point
- Flat band at zero energy living on the majority sublattice (sublattice polarized compacton states)
- 2 additional zero modes at the Dirac point supported by opposite sublattices

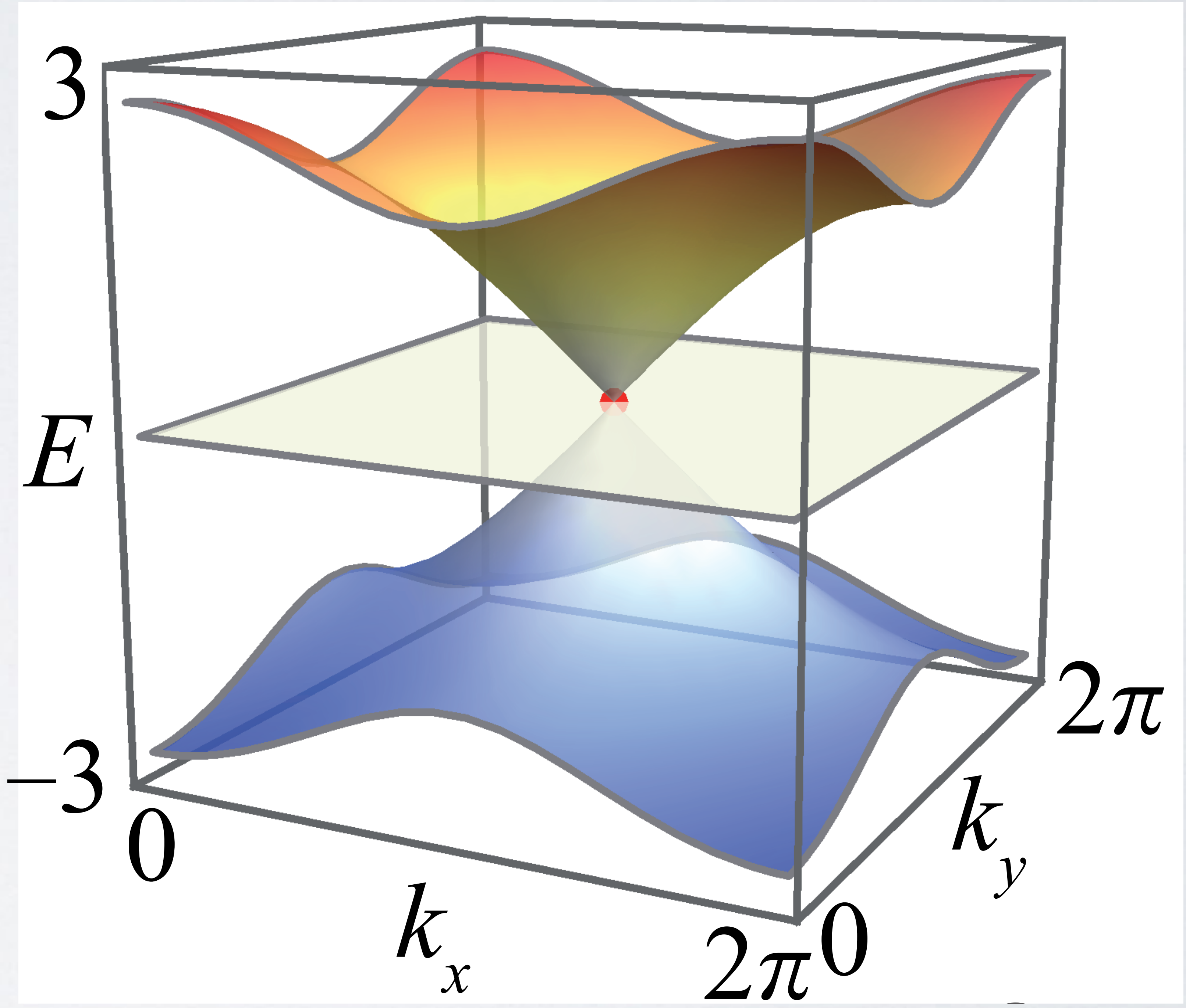

Global chiral symmetry: $H_{\mathrm{TB}}(\vec{k}) = \begin{pmatrix} 0 & t_{AB}(\vec{k}) \\ t_{BA}(\vec{k}) & 0 \end{pmatrix}$ $\sigma_z H_{\mathrm{TB}}(\vec{k}) \sigma_z = -H_{\mathrm{TB}}(\vec{k})$

INPHYNI

Dimerized and finite-size Lieb lattice

2 steps to select and spatially confined one (polarized) zero mode

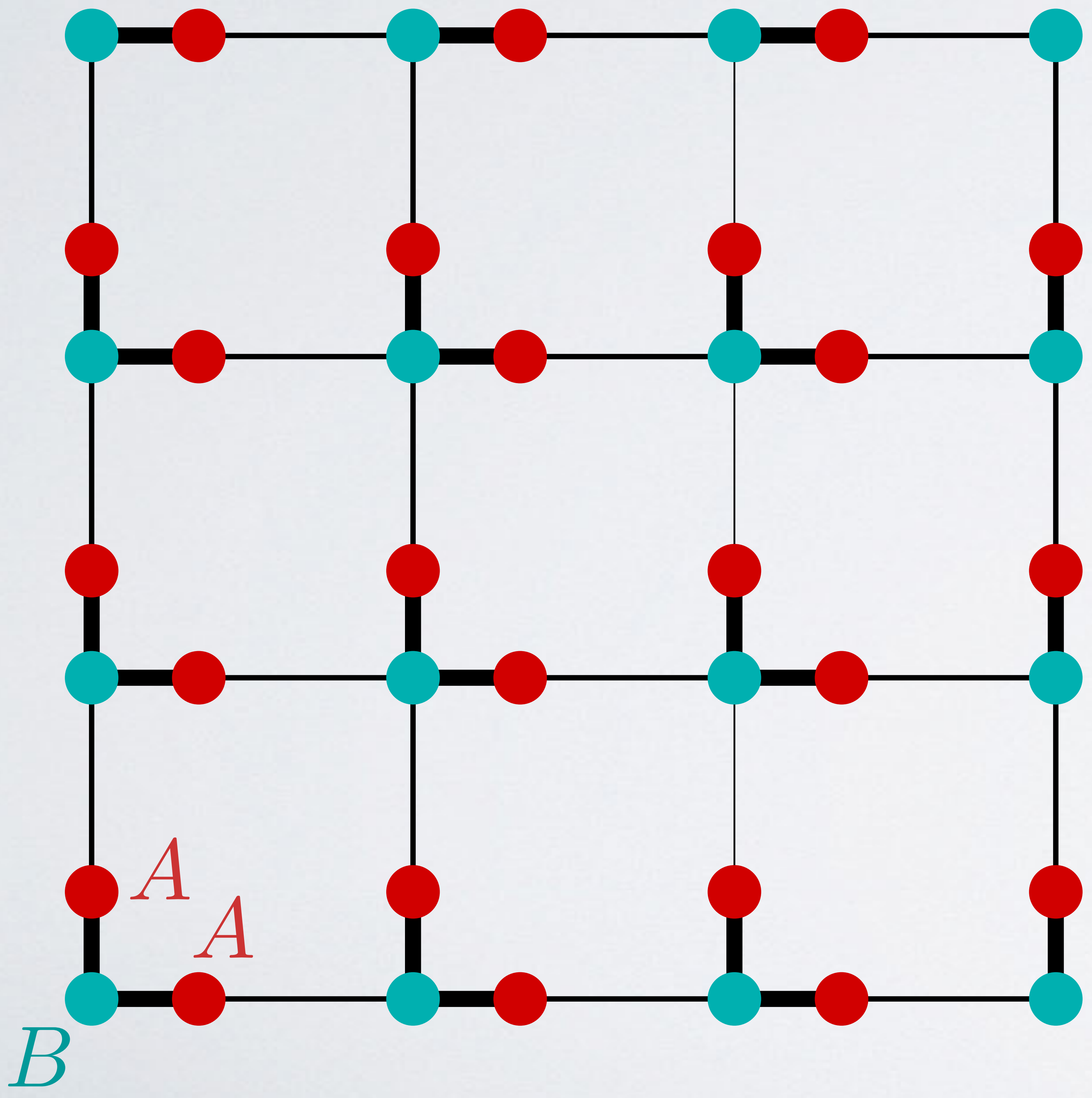

- Dirac point is lifted by dimerization of the couplings
- In a finite lattice only one of the defect modes is compatible with the boundary conditions
- We select the zero mode polarized on the minority sublattice (*B* sites)

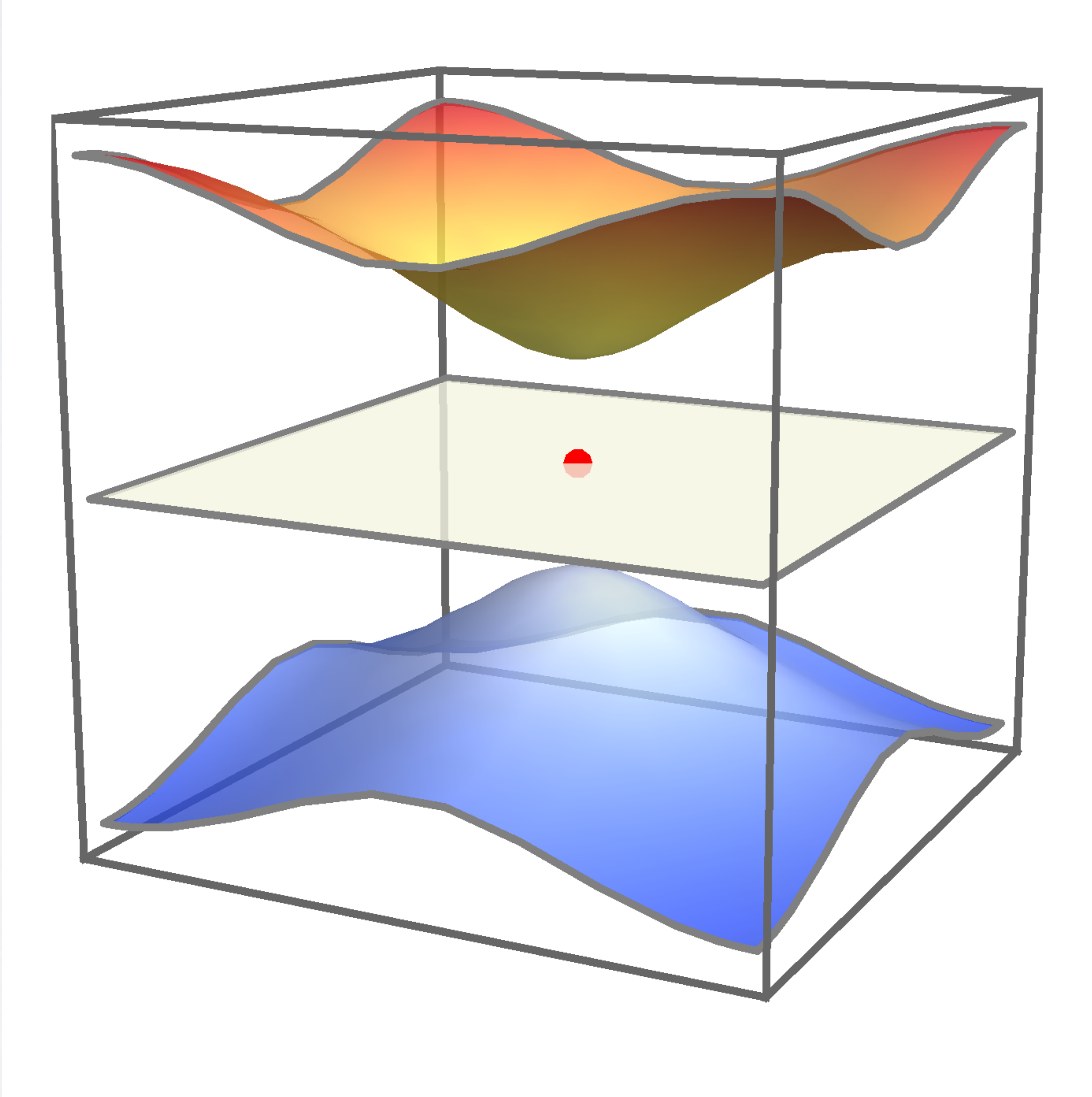

The selected zero mode is still spectrally degenerated with the flat band

INPHYNI

Partial breaking of chiral symmetry

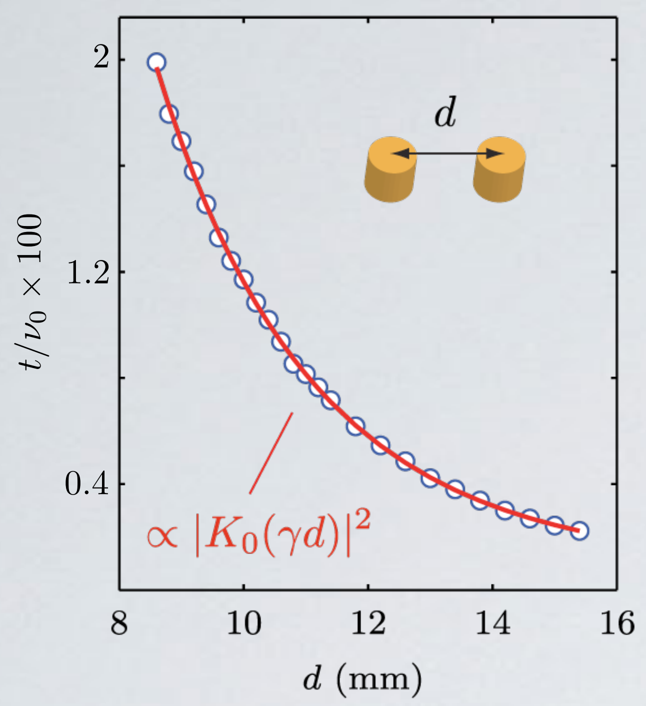

Depending on the lattice parameters,
next-nearest-neigbor couplings can be induced

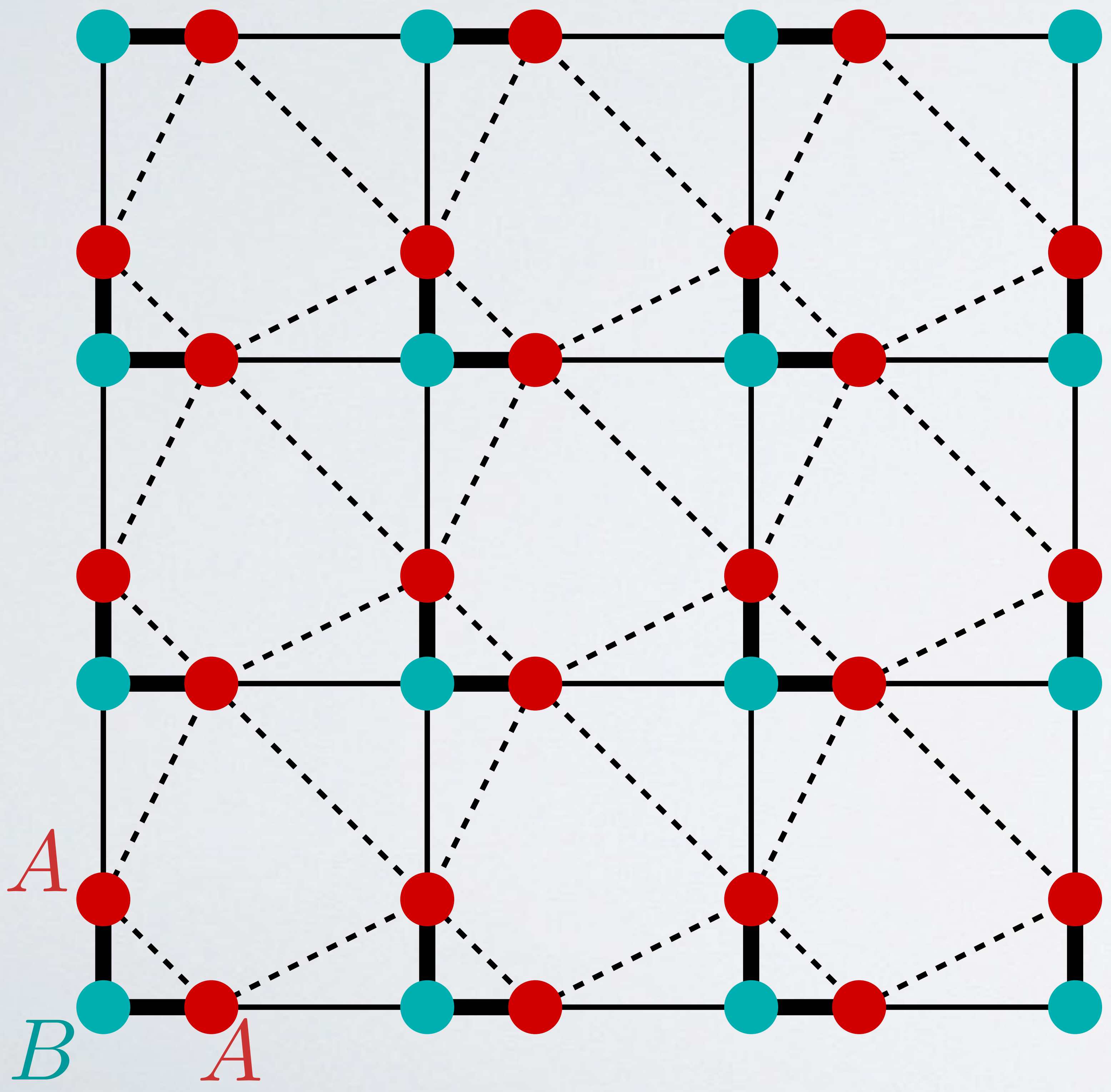

- the chiral symmetry of the majority sublattice is broken
- minority sublattice preserves its chirality
- the flat band becomes dispersive
- the zero-mode is lifted away

$$H_{\mathrm{TB}}(\vec{k}) = \begin{pmatrix} t_{AA}(\vec{k}) & t_{AB}(\vec{k}) \\ t_{BA}(\vec{k}) & 0 \end{pmatrix}$$

$$\left[\sigma_z H_{\mathrm{TB}}(\vec{k})\sigma_z\right]_{BB} = \left[-H_{\mathrm{TB}}(\vec{k})\right]_{BB}$$

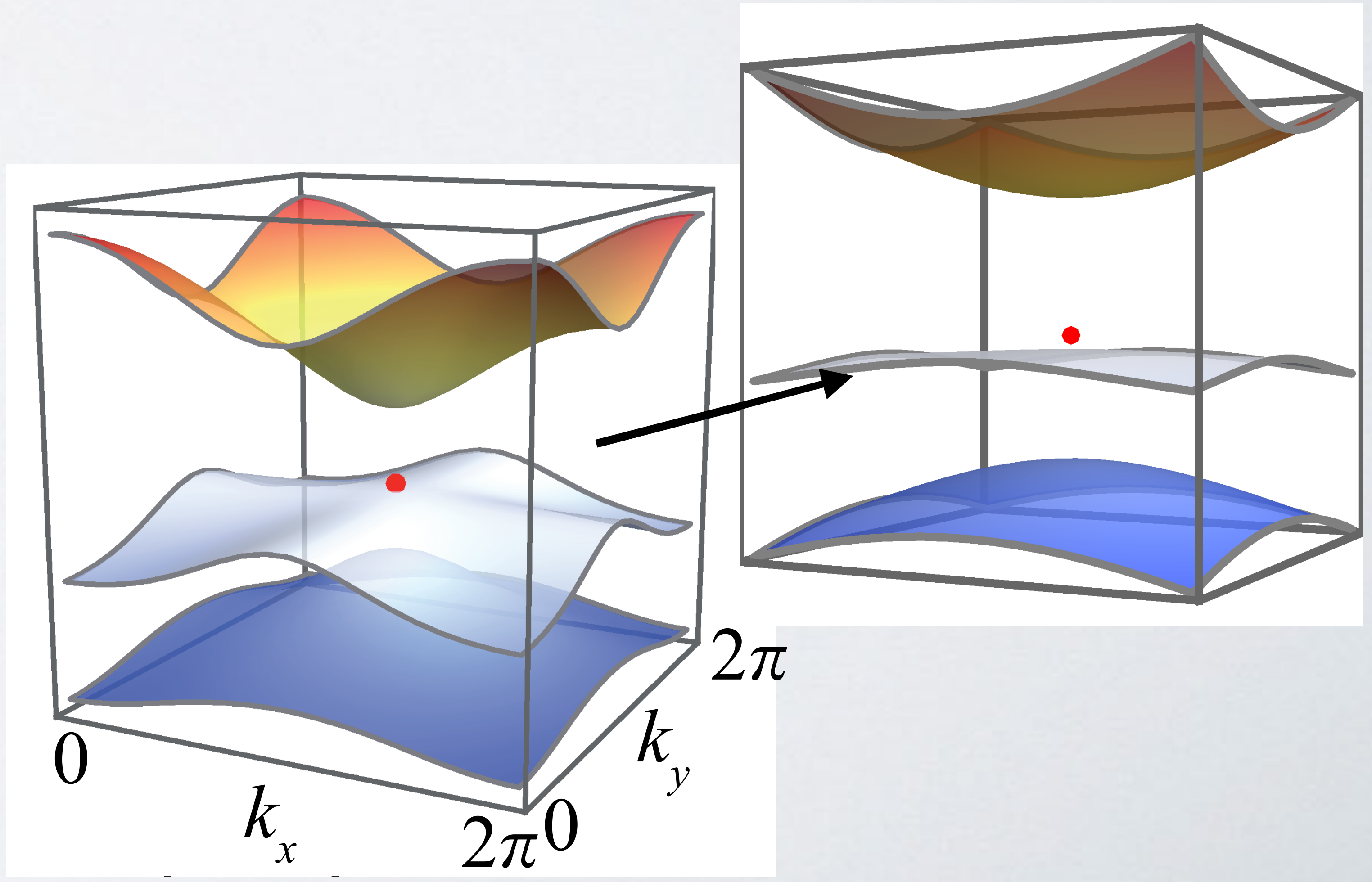

INPHYNI

Microwave Lieb Lattice

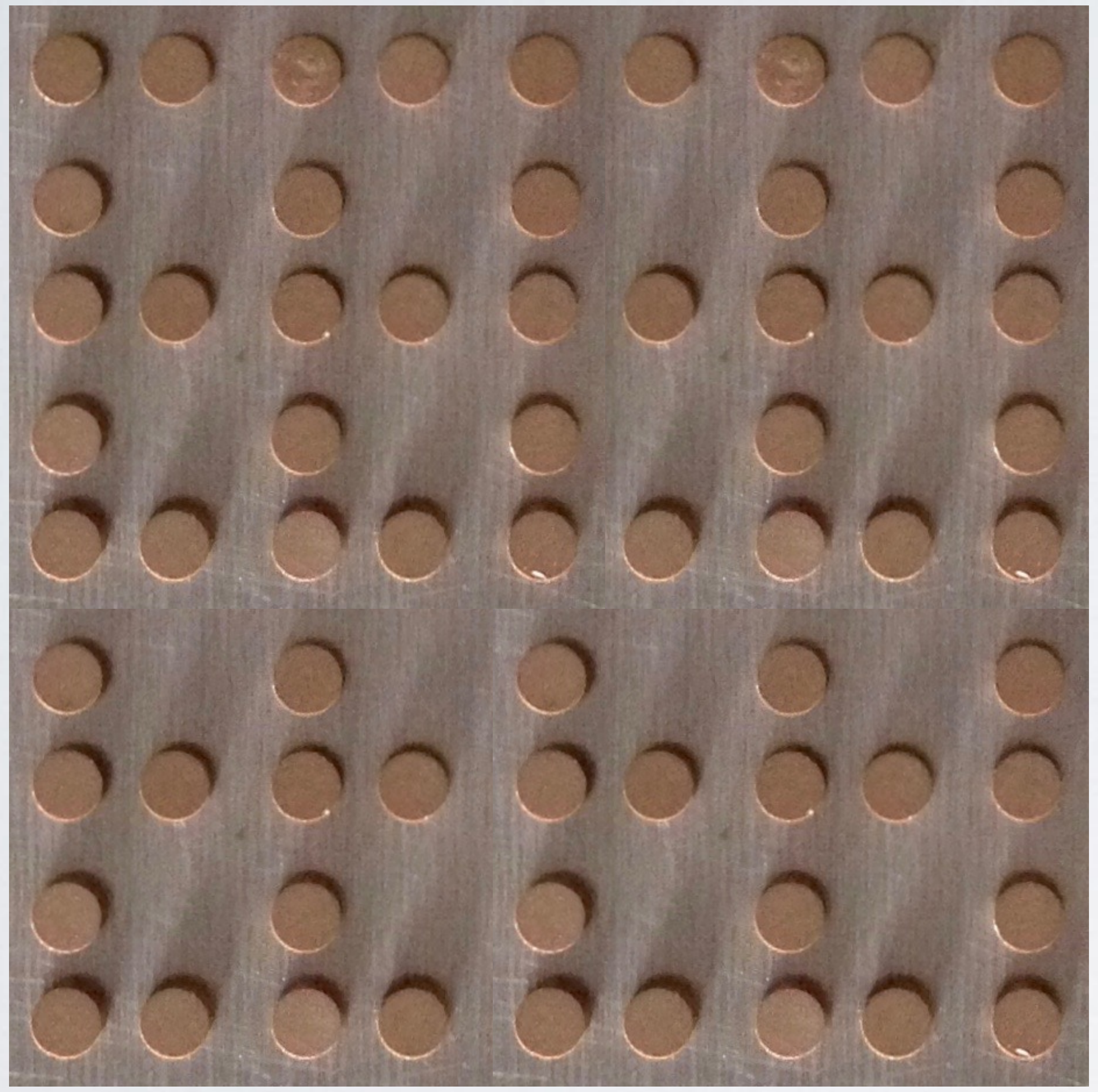

- 65 resonators
- 2 distances: 12 & 15 mm
- 2 couplings: 37 & 12 MHz

Microwave Lieb Lattice

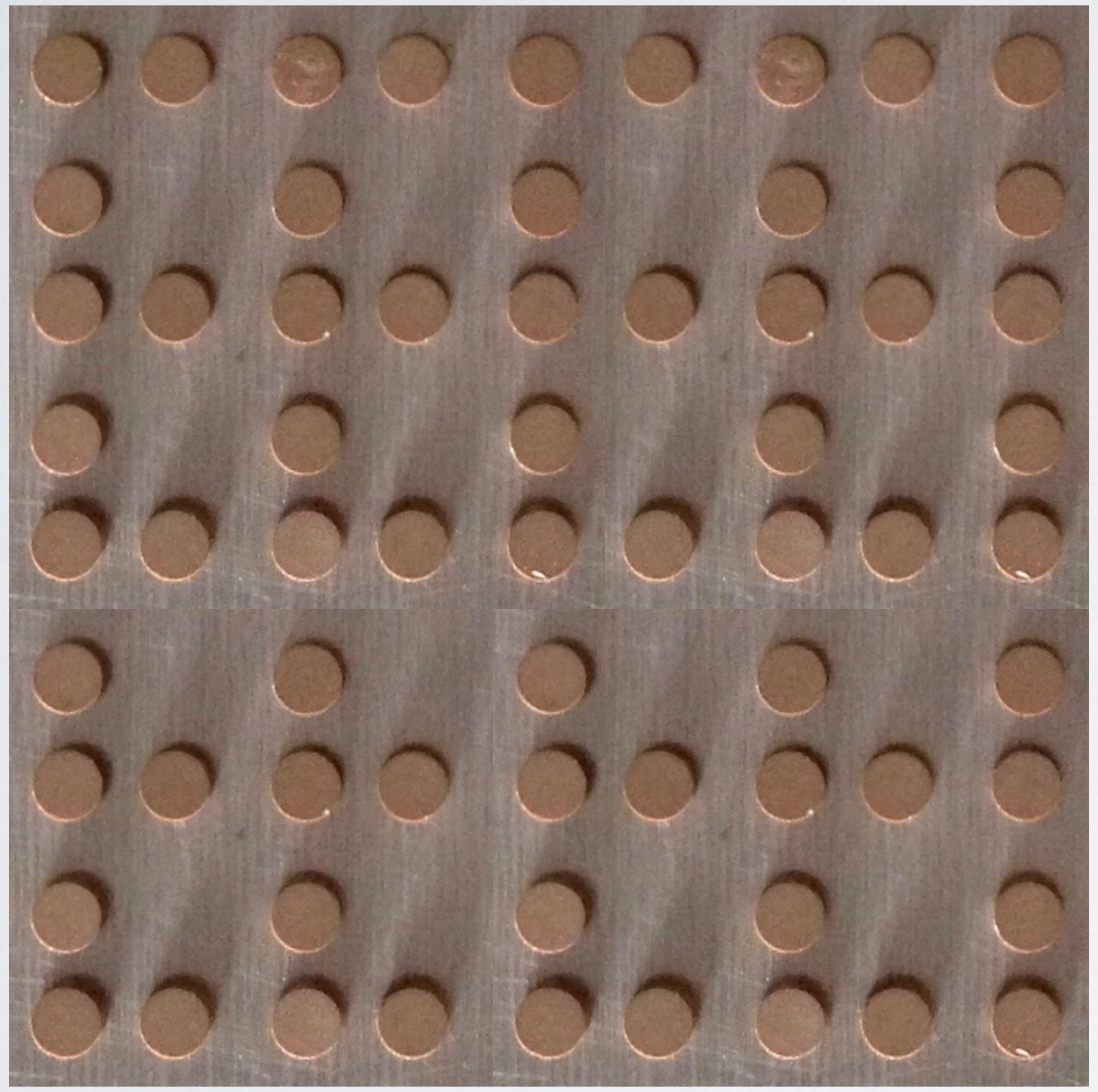

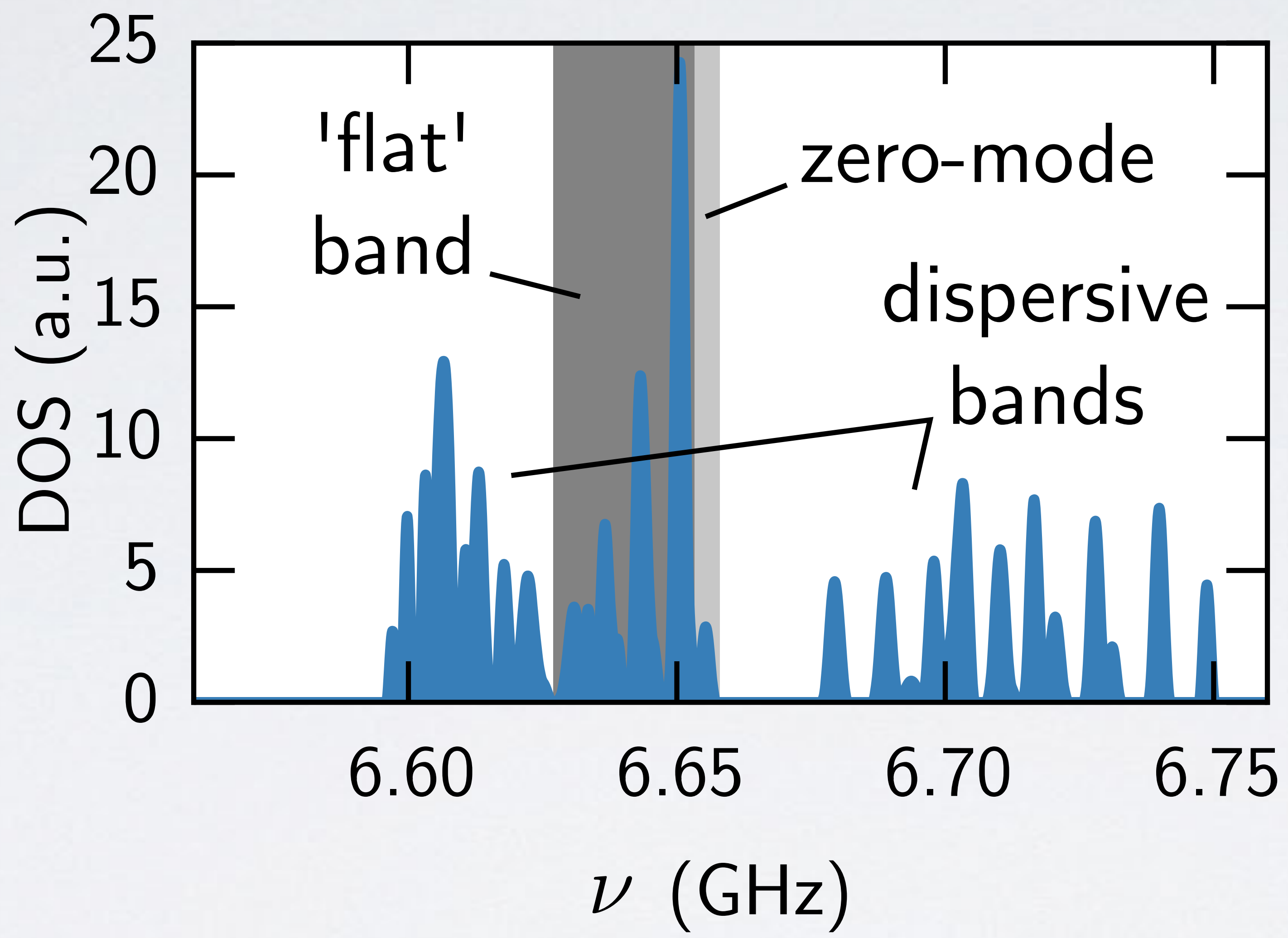

- 65 resonators
- 2 distances: 12 & 15 mm
- 2 couplings: 37 & 12 MHz

Microwave Lieb Lattice

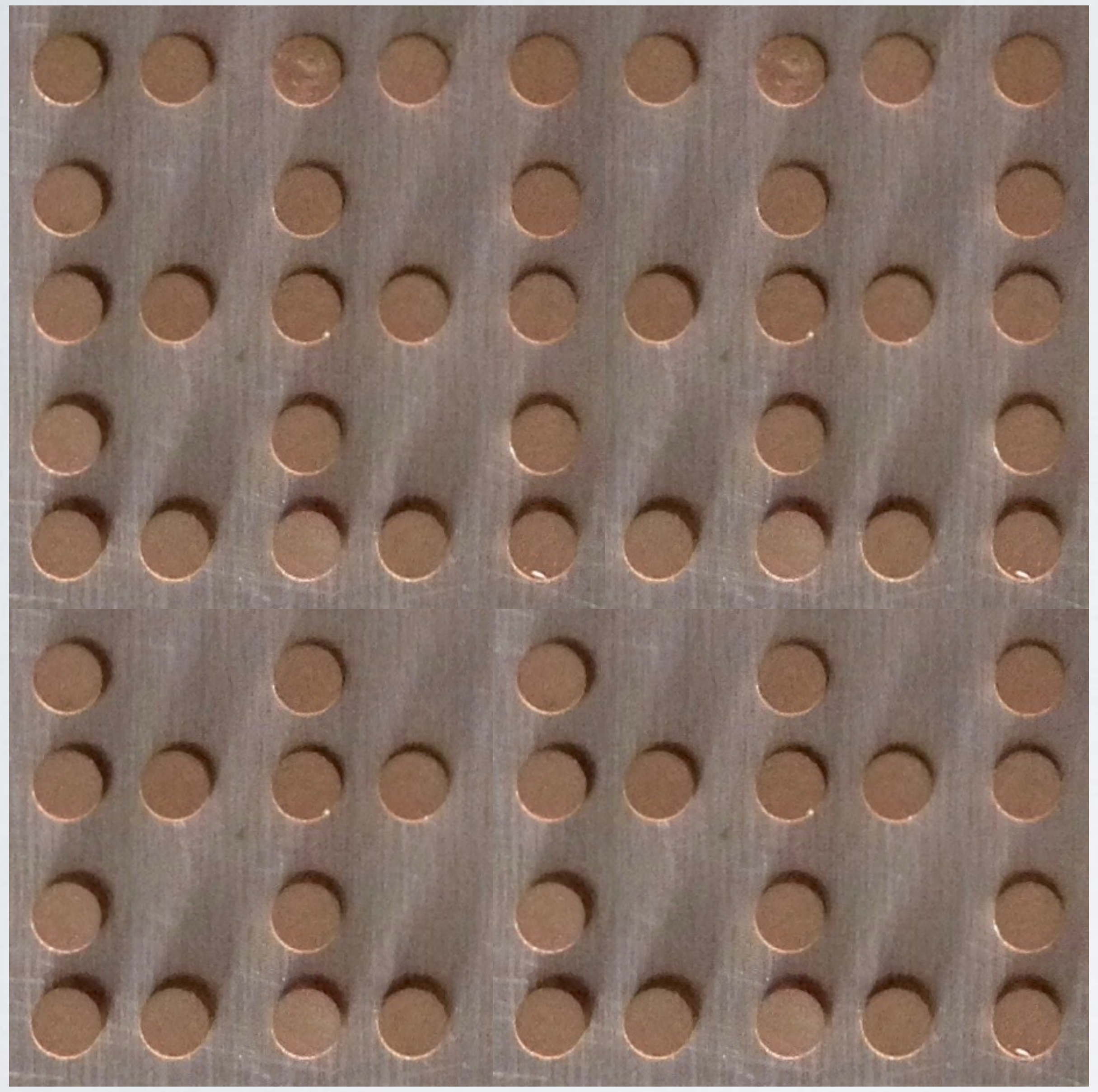

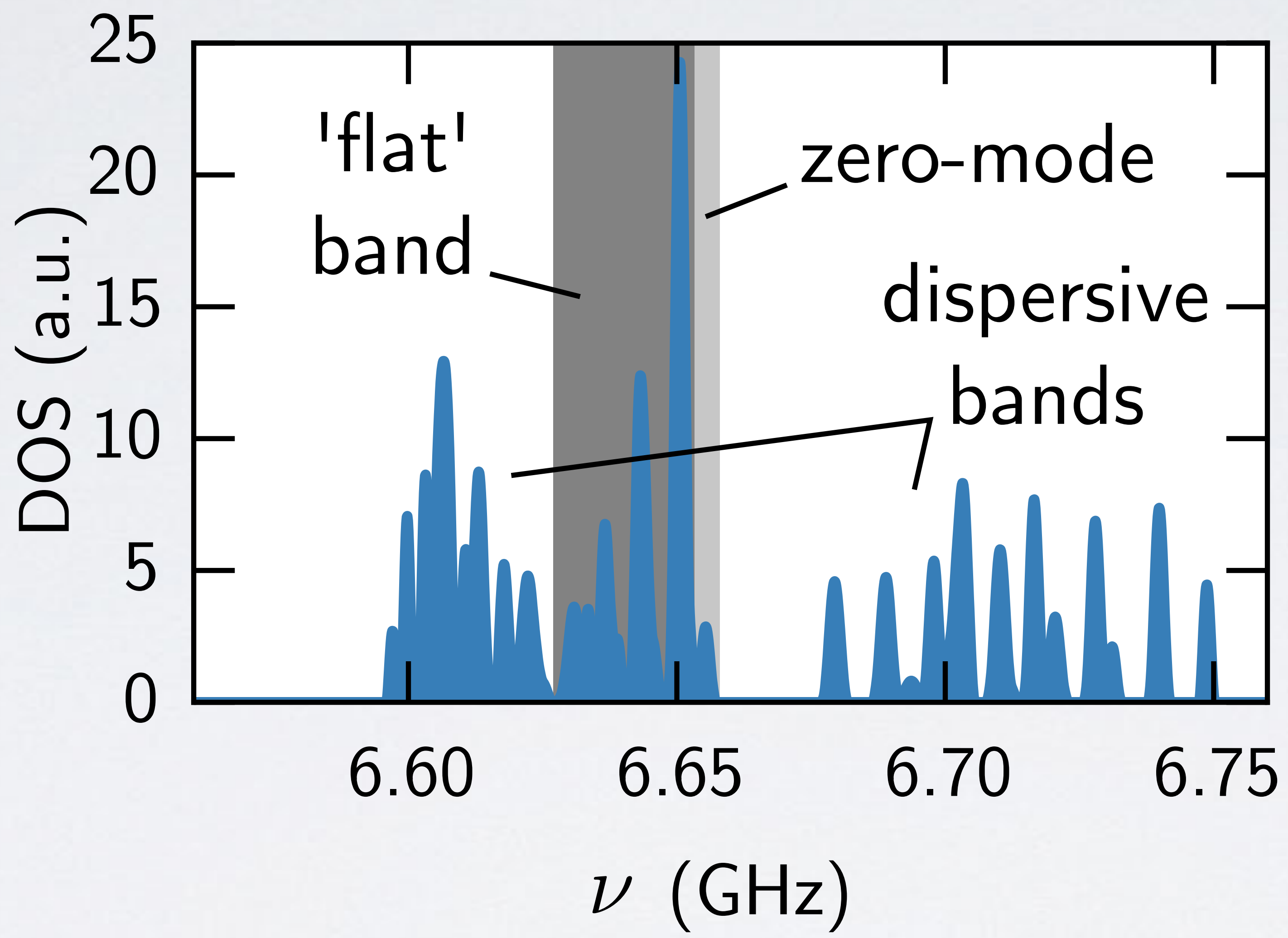

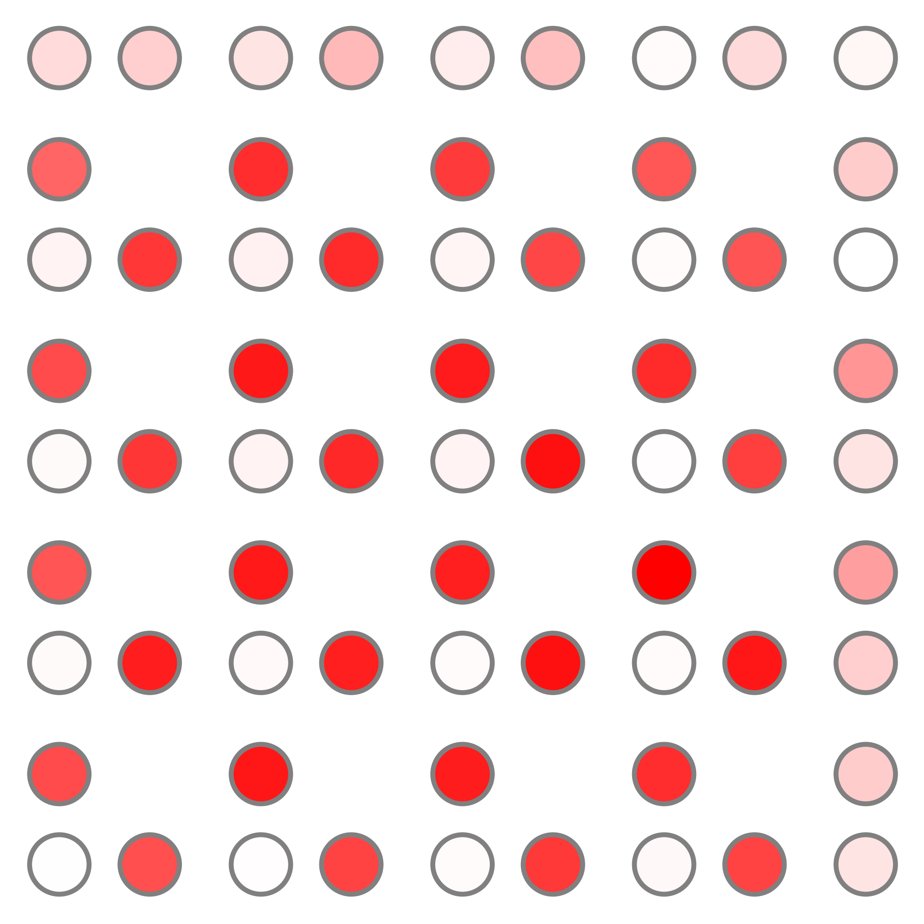

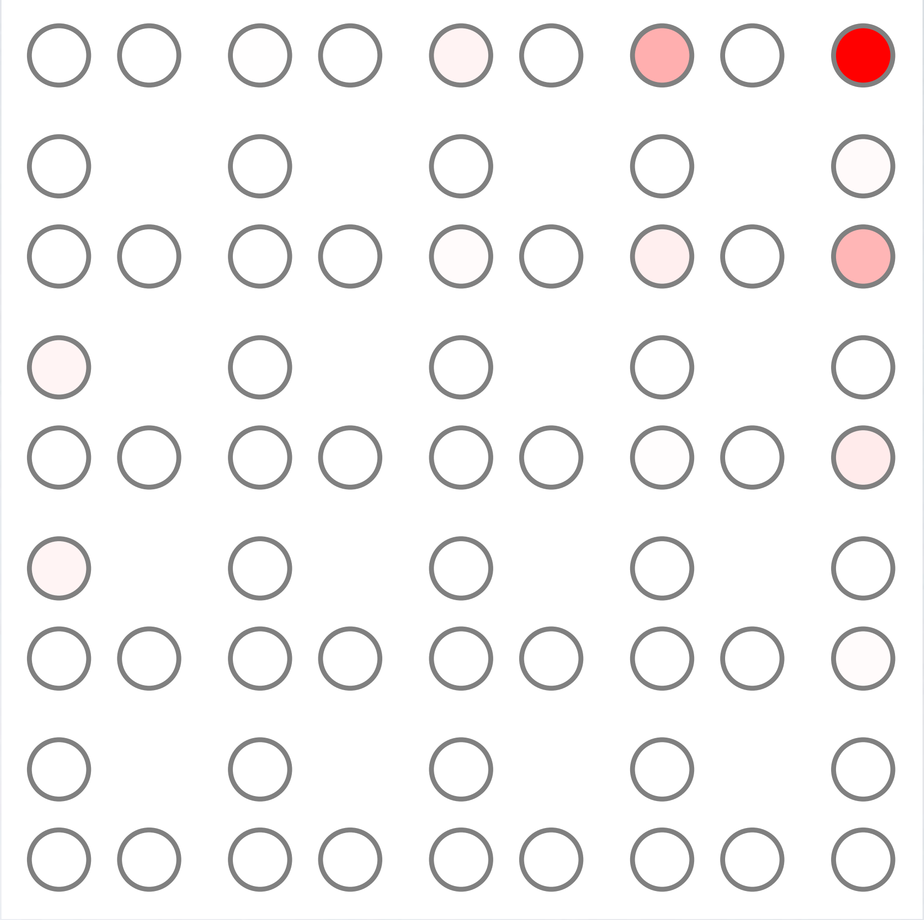

- 65 resonators
- 2 distances: 12 & 15 mm
- 2 couplings: 37 & 12 MHz

Microwave Lieb Lattice

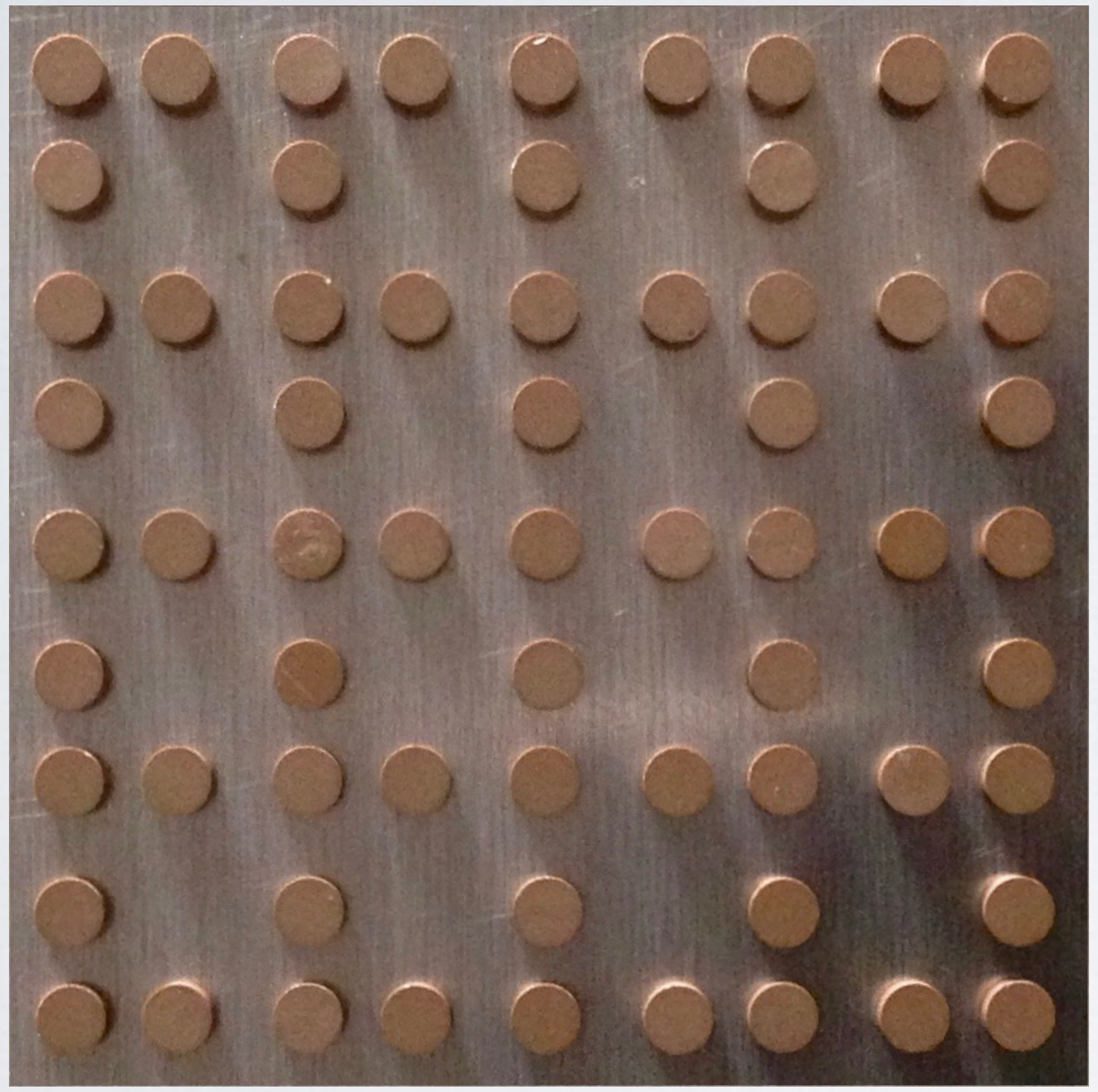

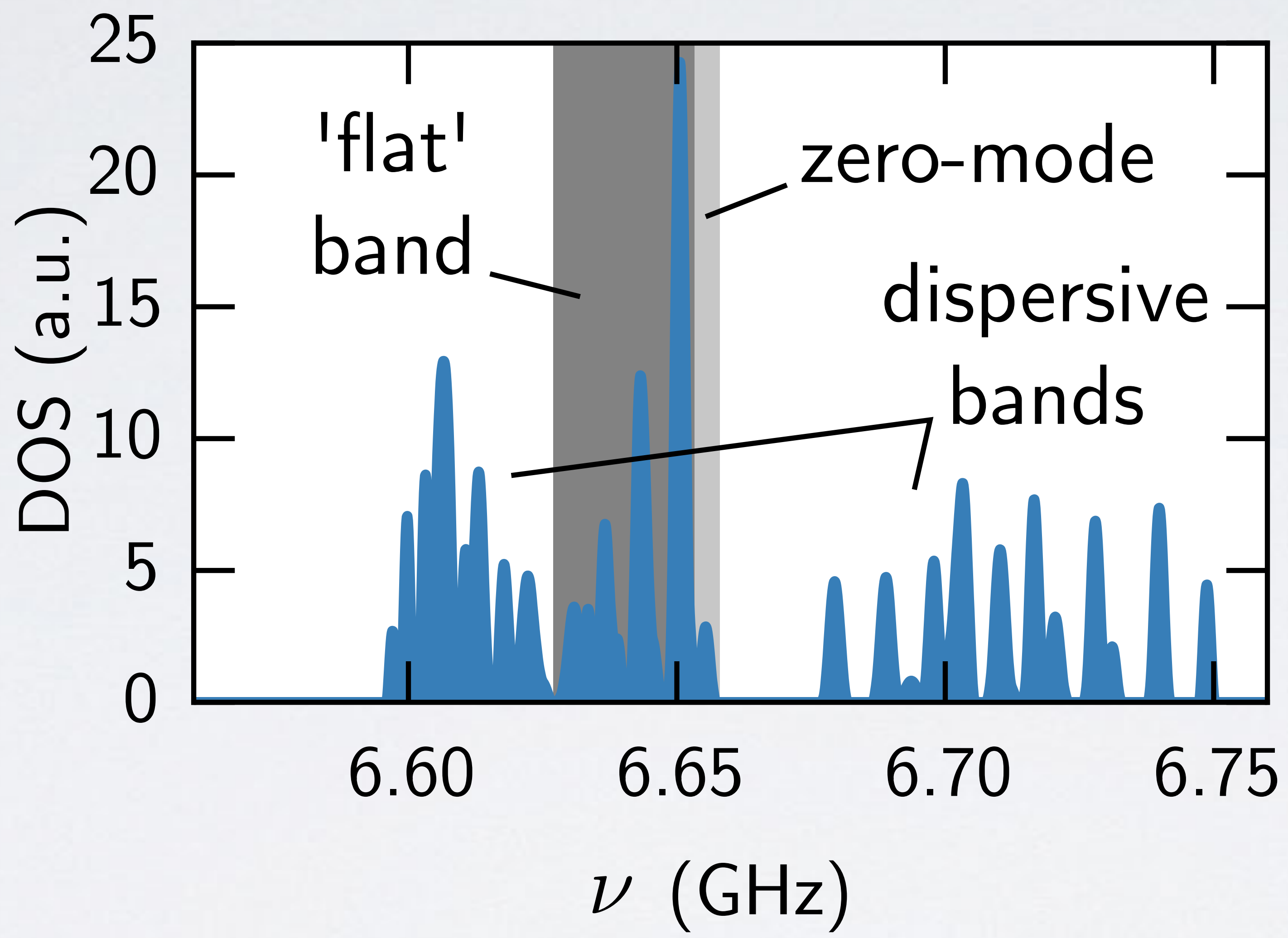

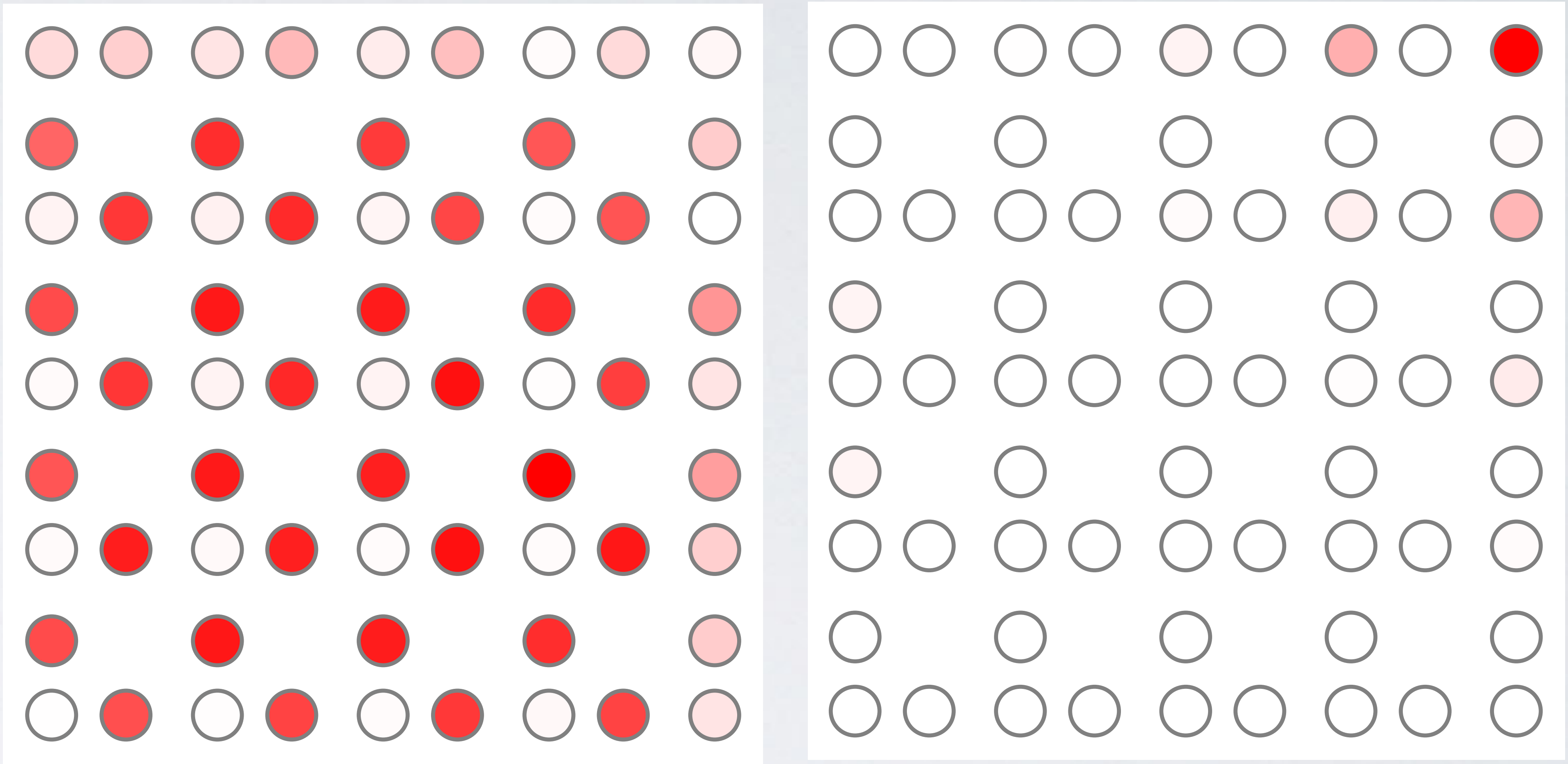

- 65 resonators
- 2 distances: 12 & 15 mm
- 2 couplings: 37 & 12 MHz

Microwave Lieb Lattice

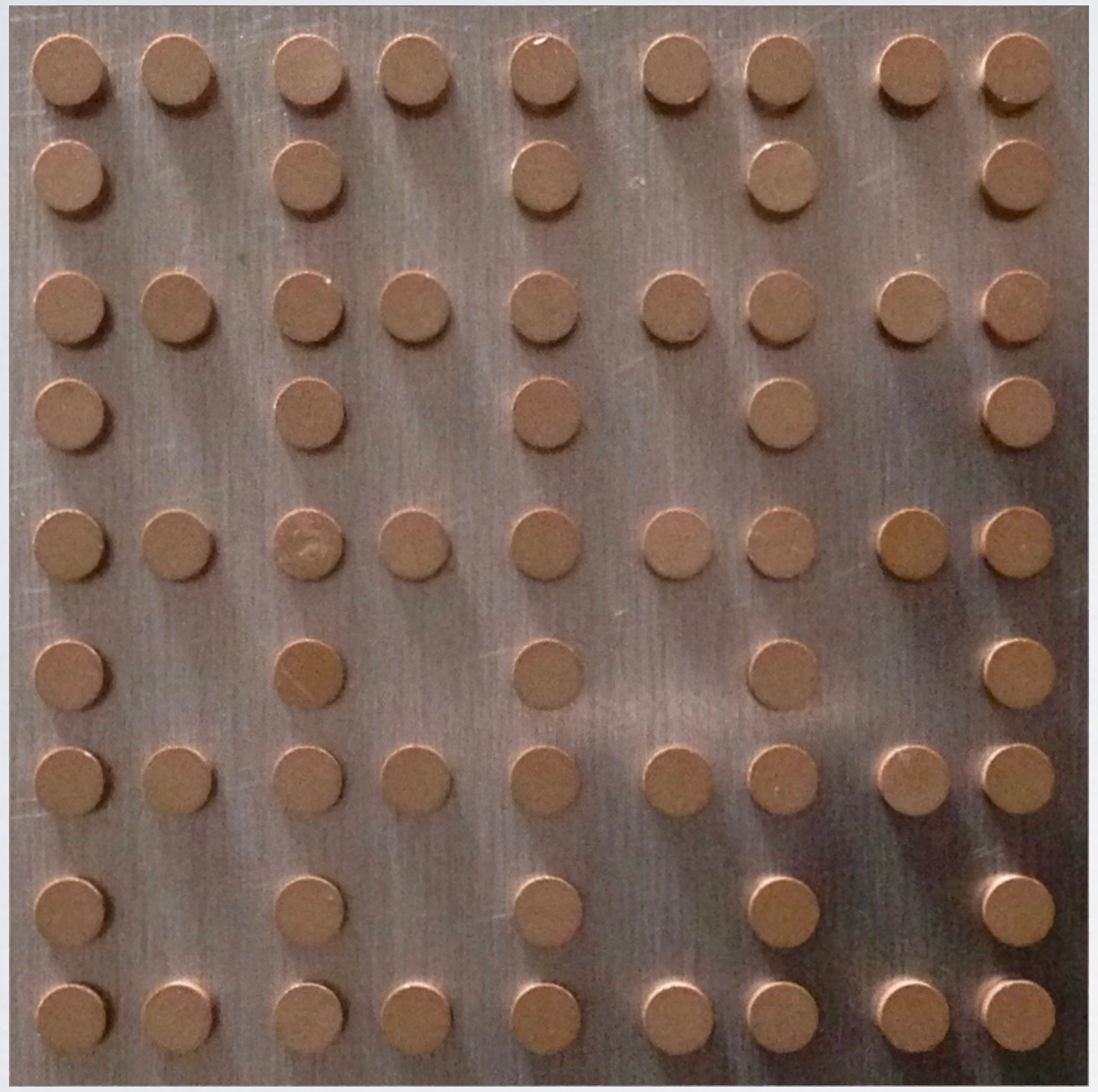

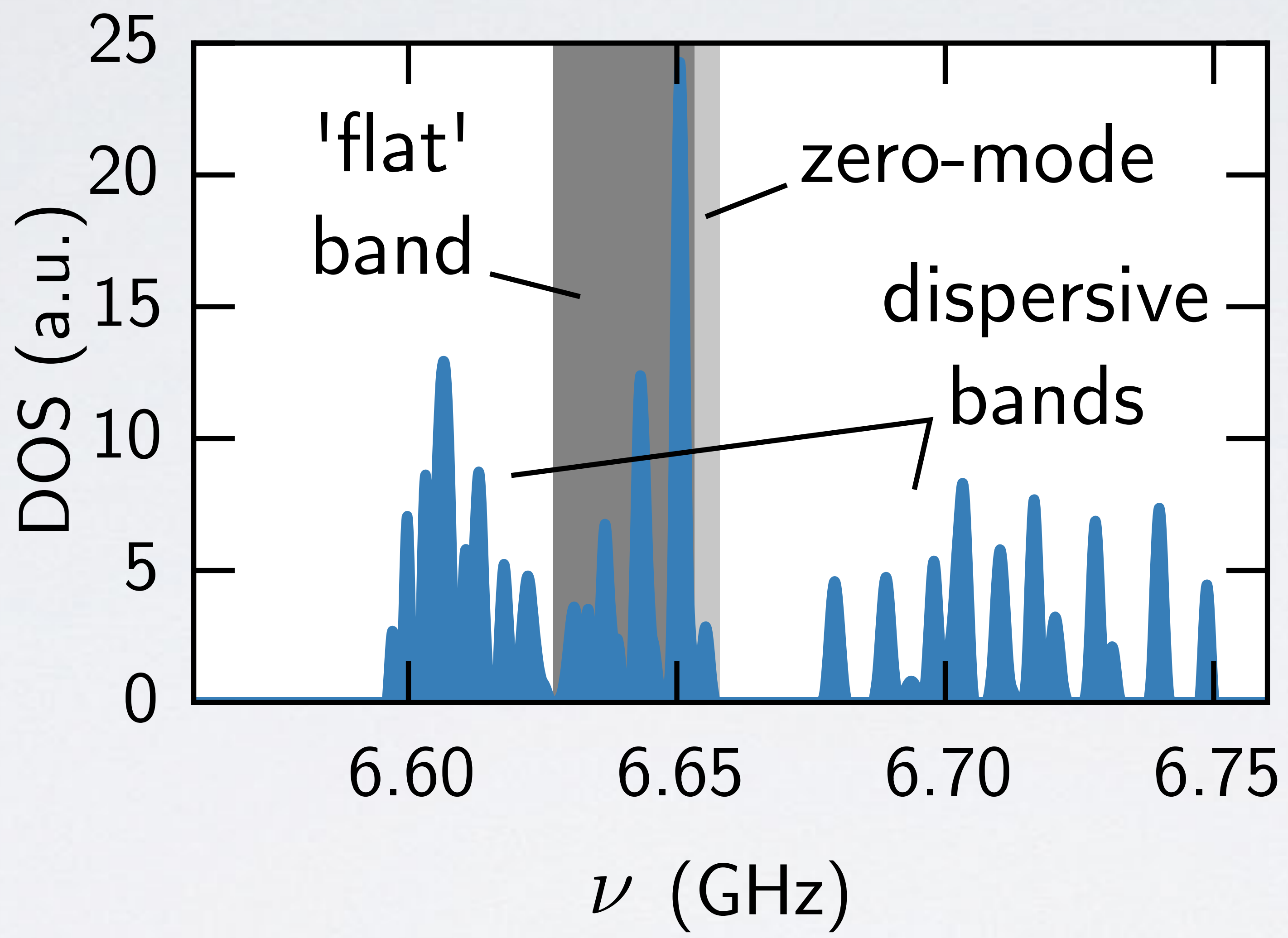

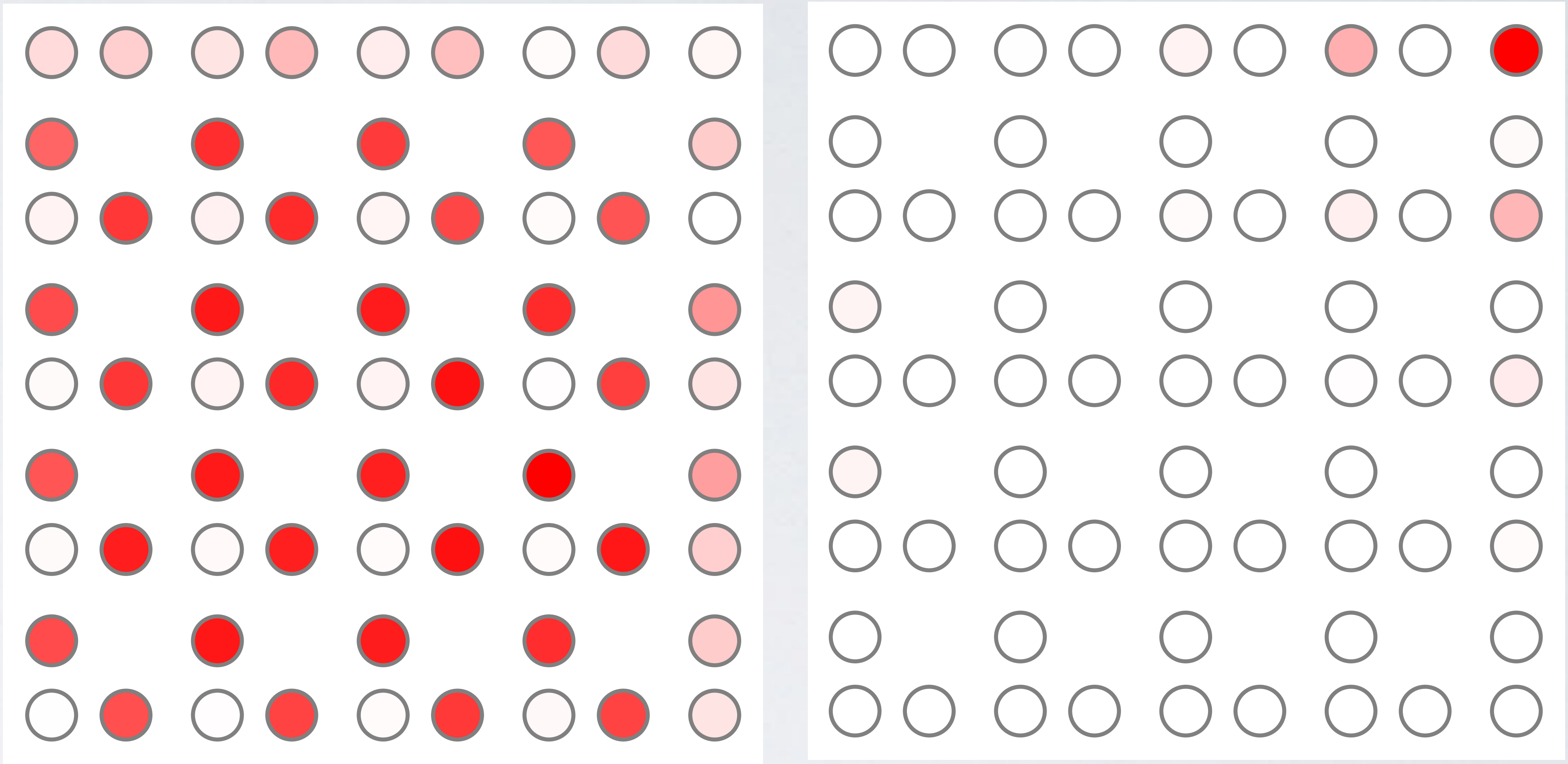

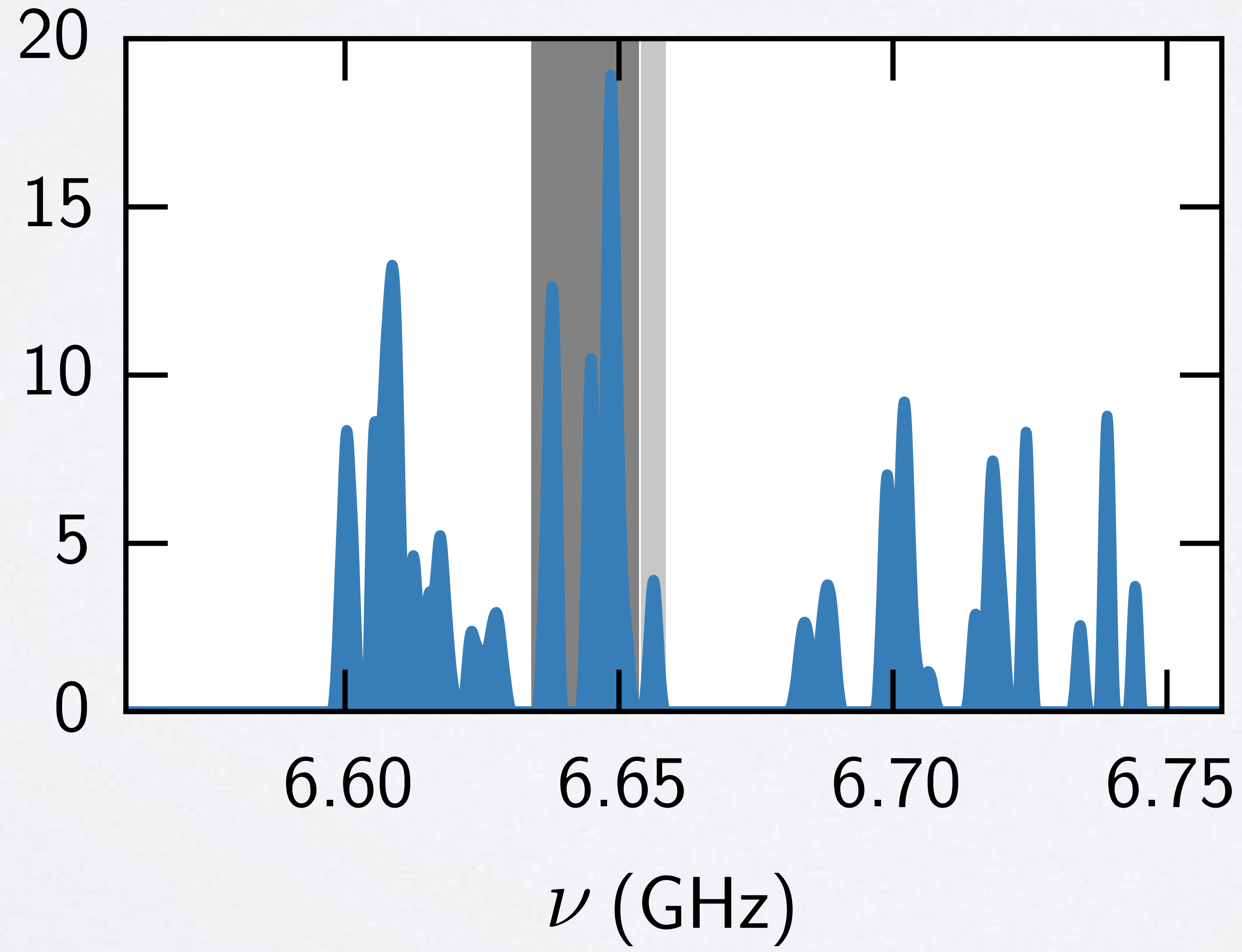

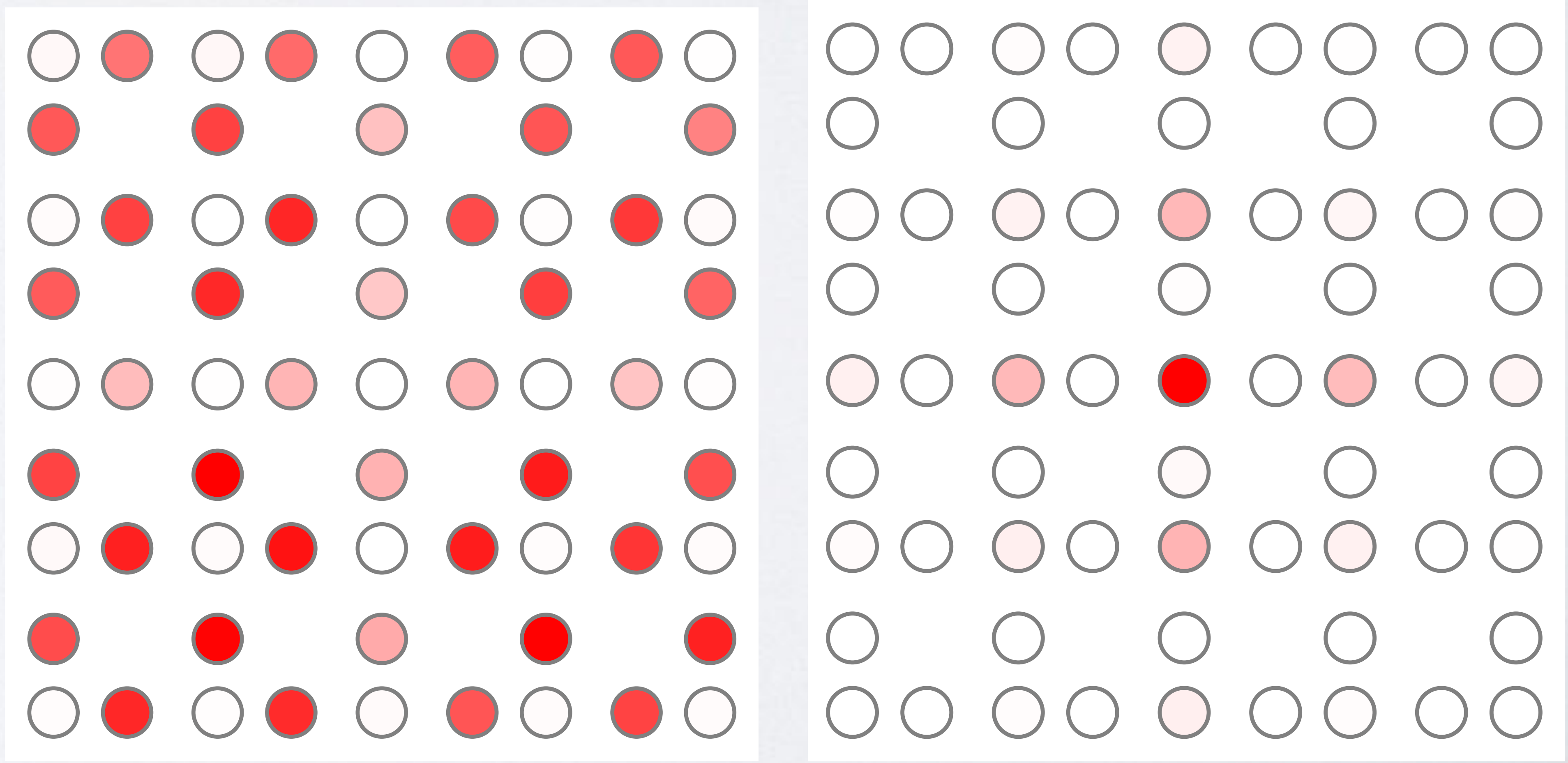

- 65 resonators
- 2 distances: 12 & 15 mm
- 2 couplings: 37 & 12 MHz

2D Materials **4**, 025008 (2017)

Selective enhancement

Elastomer patches induce local losses on the majority sublattice

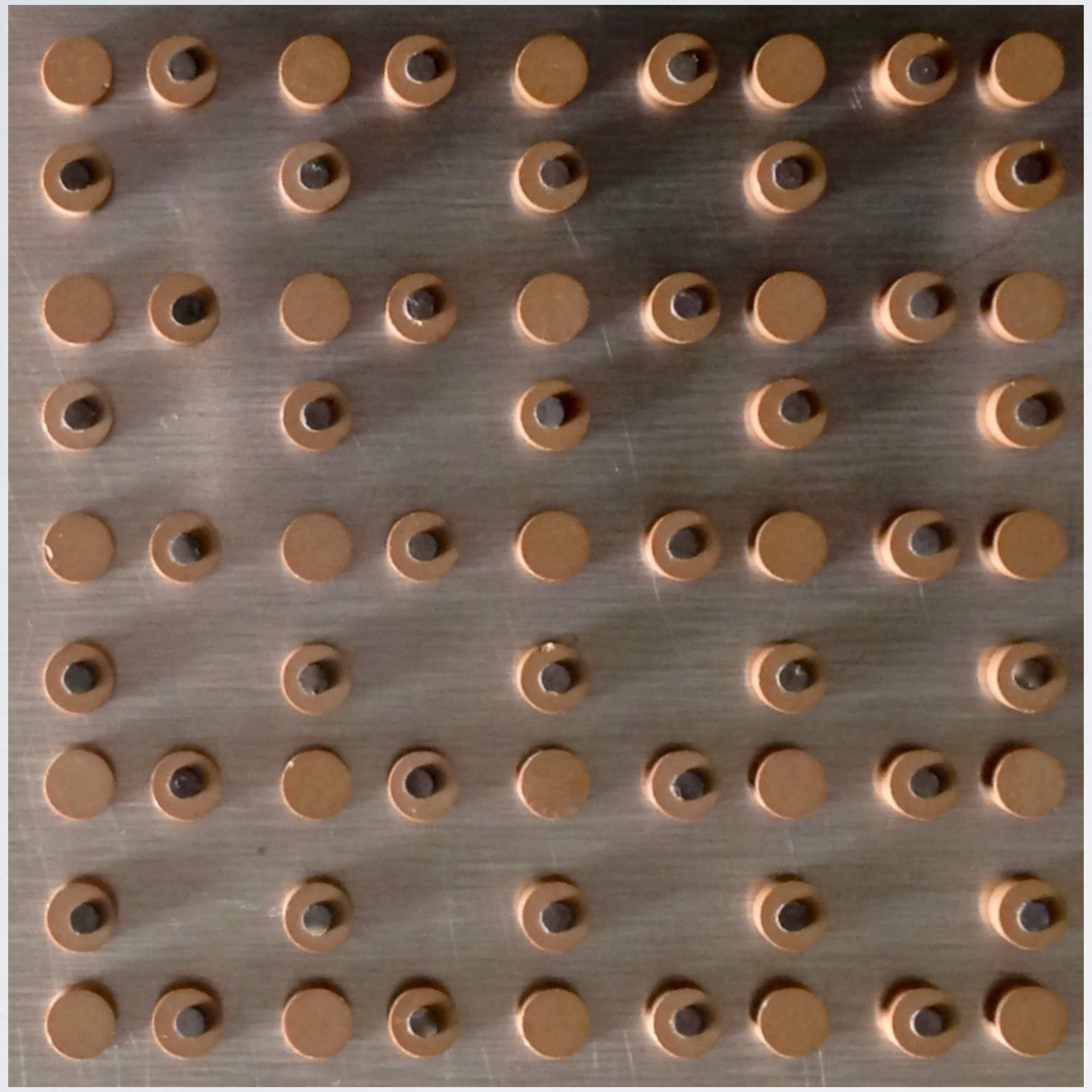

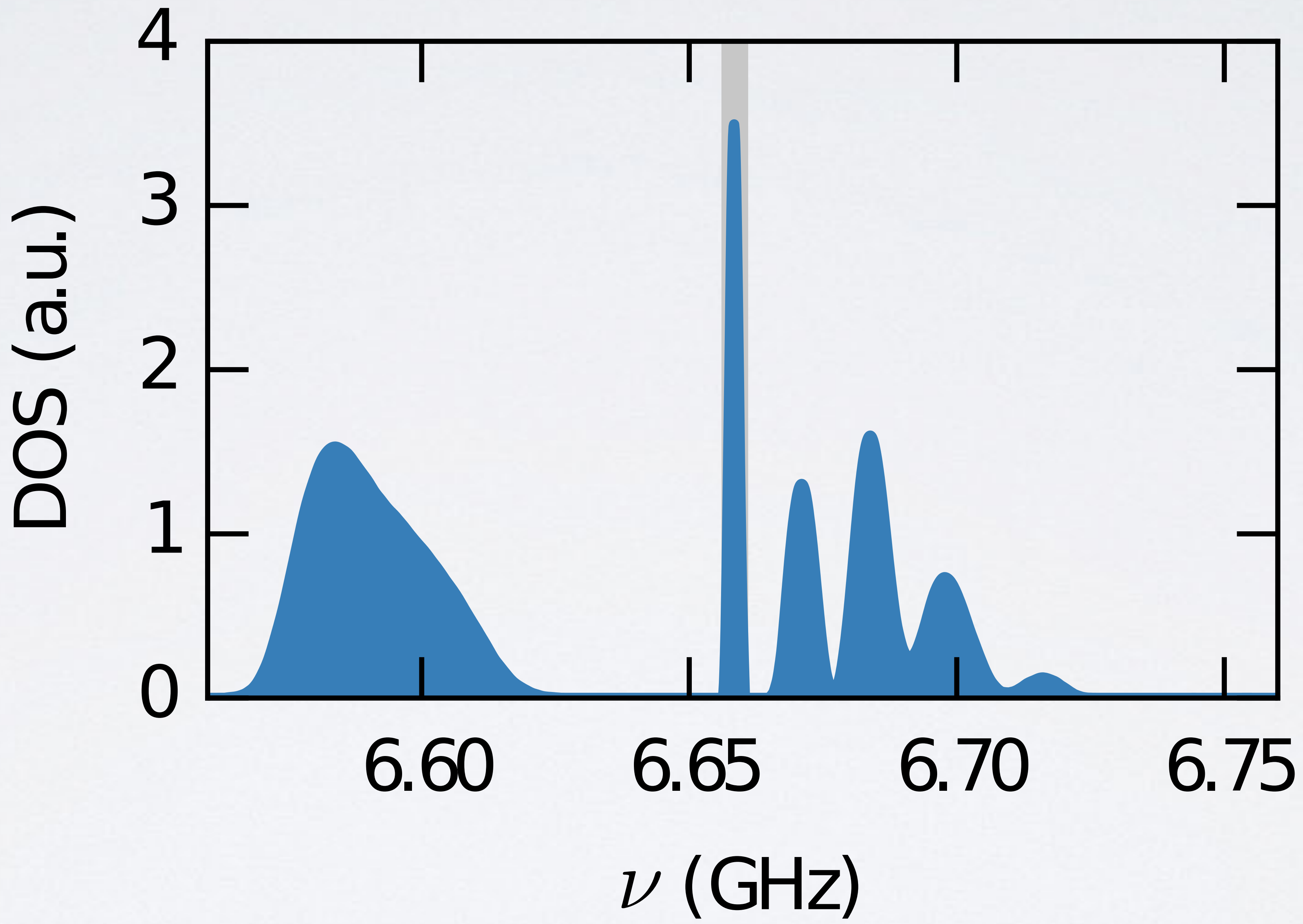

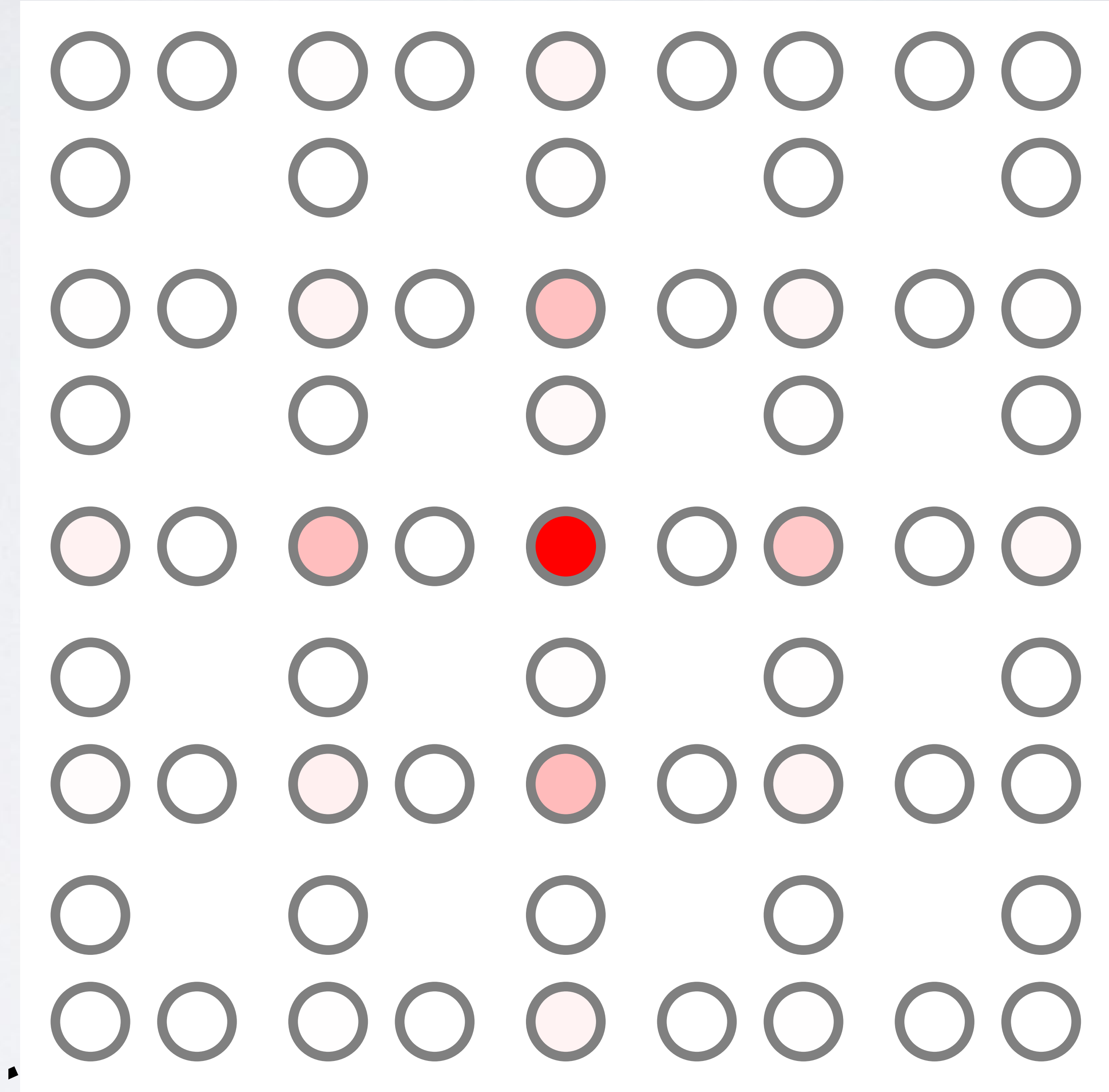

- the flat band disappears
- the half-polarized dispersive bands are drastically altered
- the defect state dominates the spectrum, while its shape is unaffected

Pseudo-Landau levels

Gigantic pseudomagnetic fields reveal the topological secrets of Landau levels

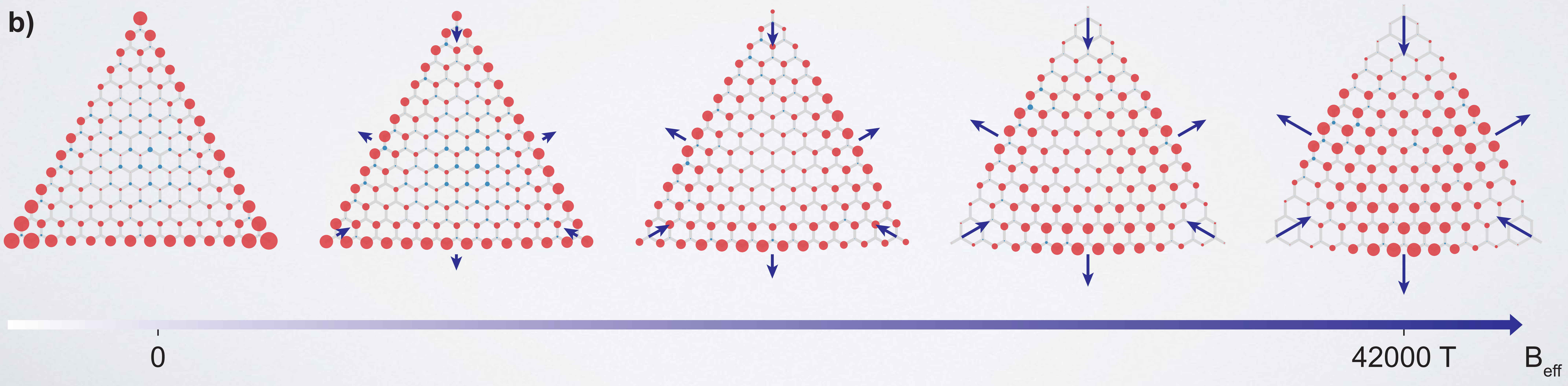

Non-uniformly strained graphene

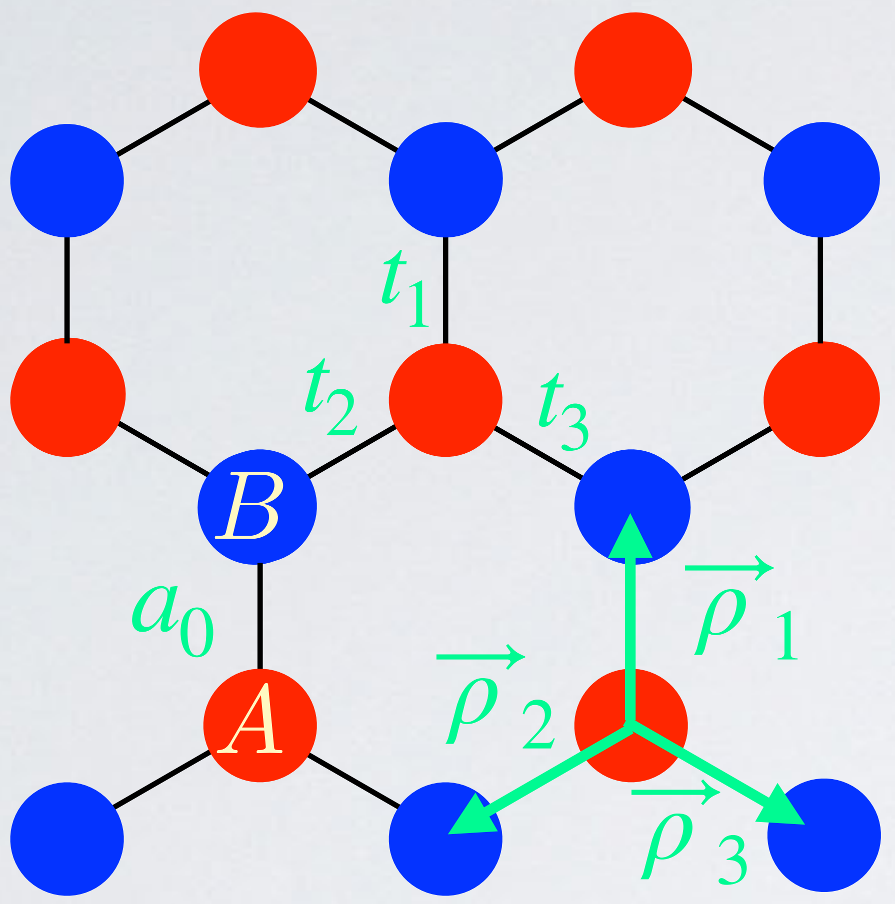

Effective Dirac Hamiltonian in the low-energy approximation

$$H = c\eta\sigma_x(px - A_x) + c\sigma_y(p_y - A_y)$$

$$A_x = \eta\frac{2t_1 - t_2 - t_3}{3a_0t_0}$$

$$A_y = \eta\frac{t_2 - t_3}{\sqrt{3}a_0t_0}$$

$$c = 3a_0t_0/2$$

Maximal pseudo-magnetic field obtained for a triaxial strain

$$t_i(\vec{r}) = t_0\left[1 - \frac{\beta}{2a_0^2}\rho_i \cdot \vec{r}\right]$$

β gives the strength of the magnetic field

$$\ell_M = \sqrt{1/|\beta|}$$

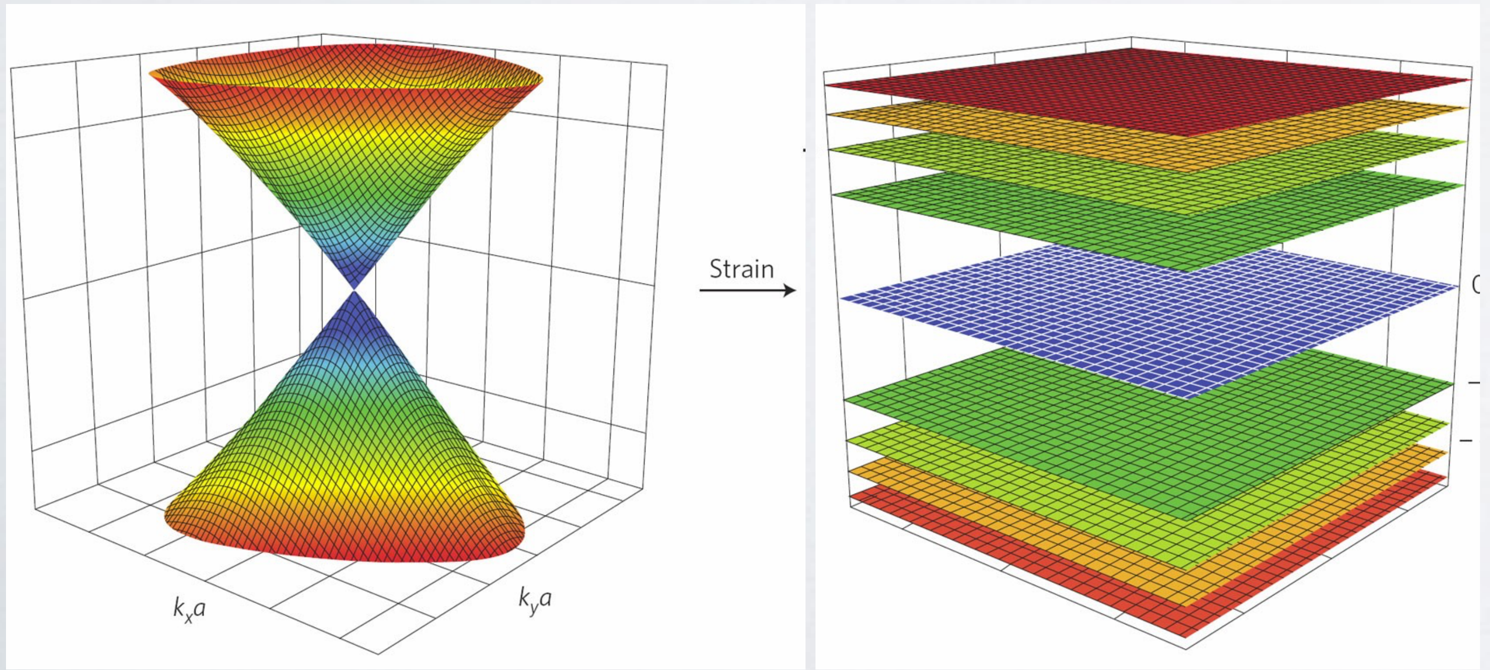

Pseudo-Landau level : $E_n = \text{sgn}(n)\hbar c\sqrt{2|n\beta|}$

INPHYNI

Finite lattice: optimal geometry

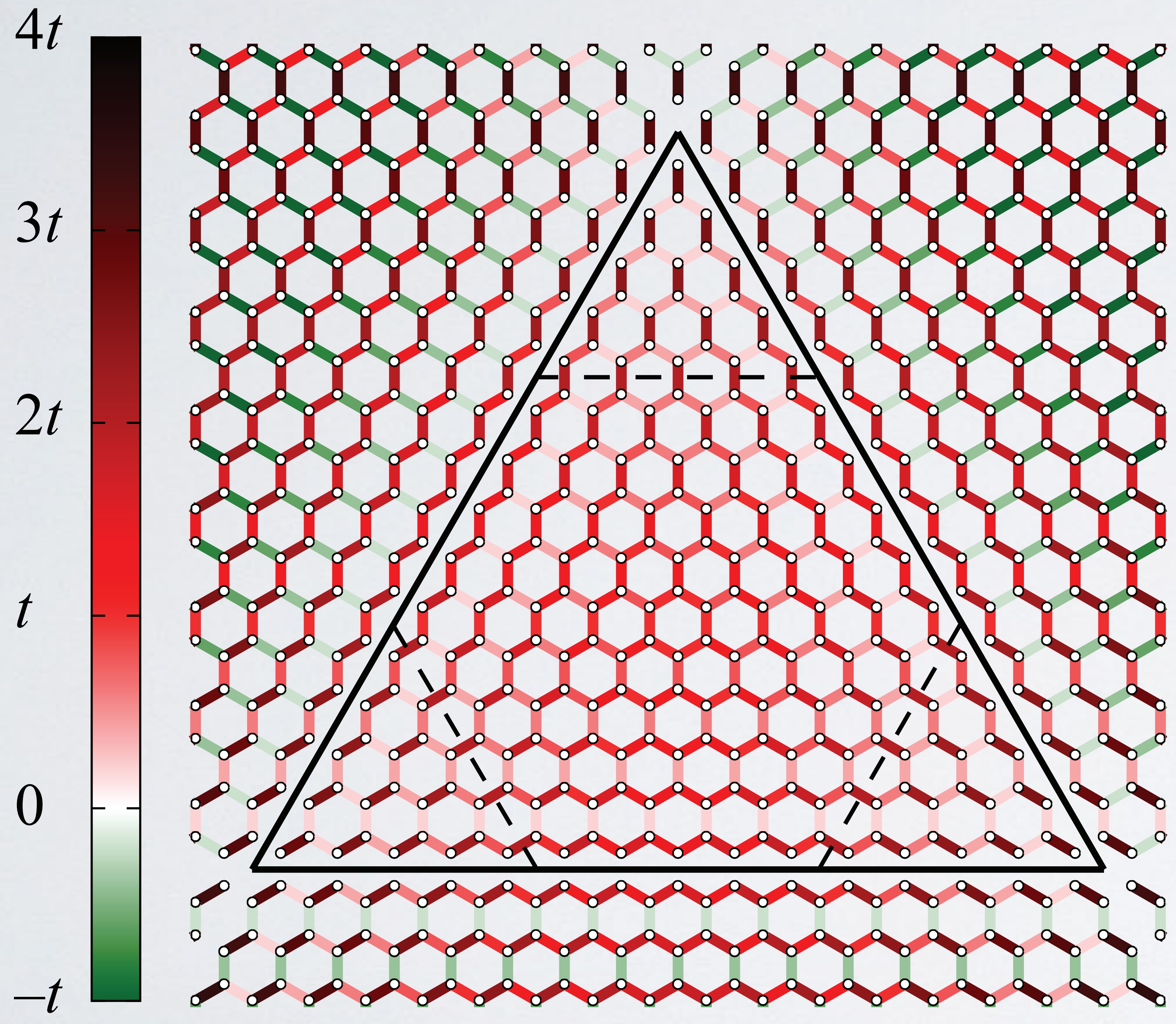

INPHYNI

Finite lattice: optimal geometry

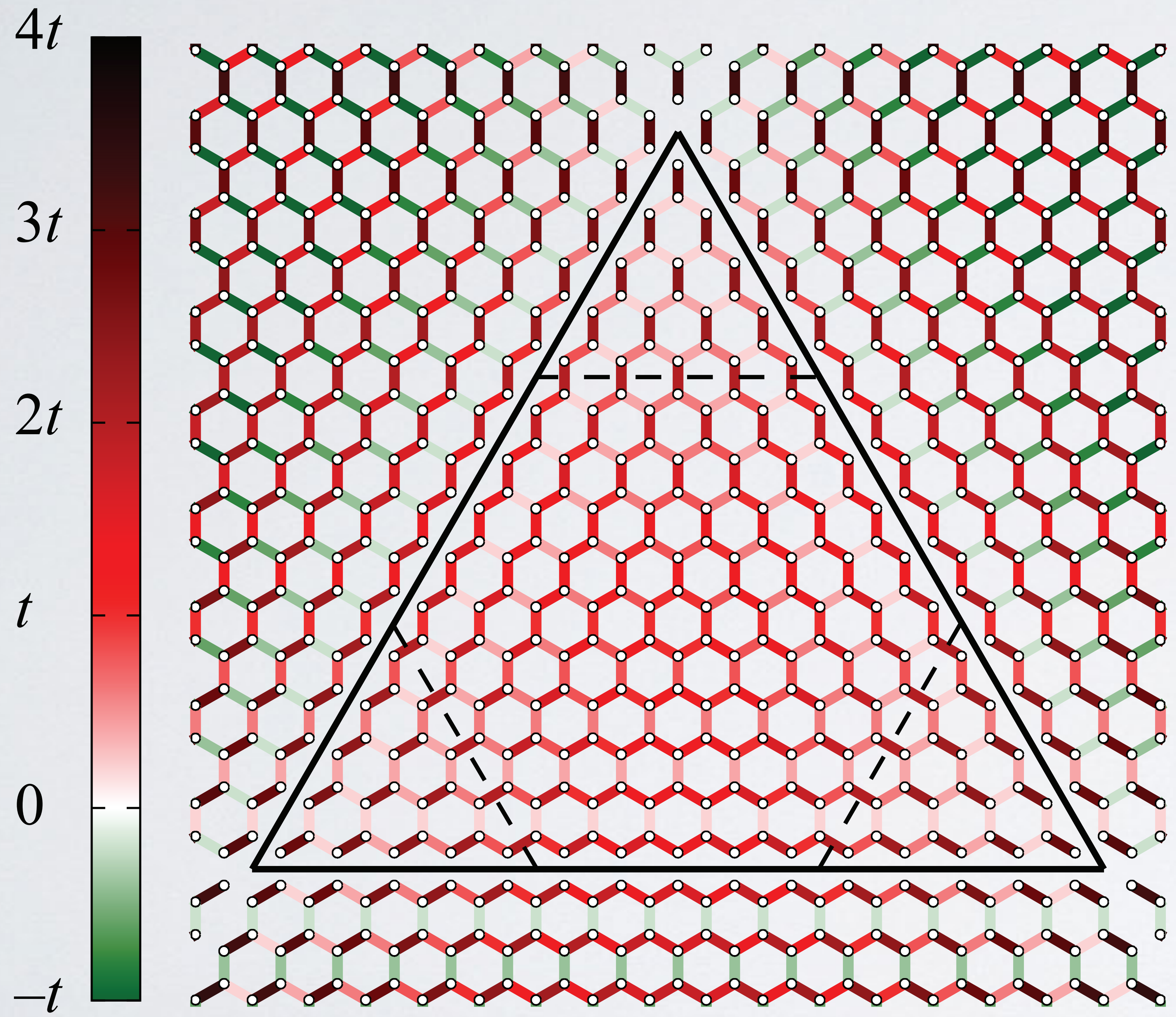

Triangular shape with full zig-zag edges

- uniform pseudo-magnetic field
- L sites on each zig-zag edge
- maximal pseudo-field strength $\beta_m = 4/L$
- coupling drop to zero at the edges for $\beta = \beta_M$
- fully sublattice-polarized edge states/0th Landau levels for $0 \leq \beta \leq \beta_M$

Finite lattice: optimal geometry

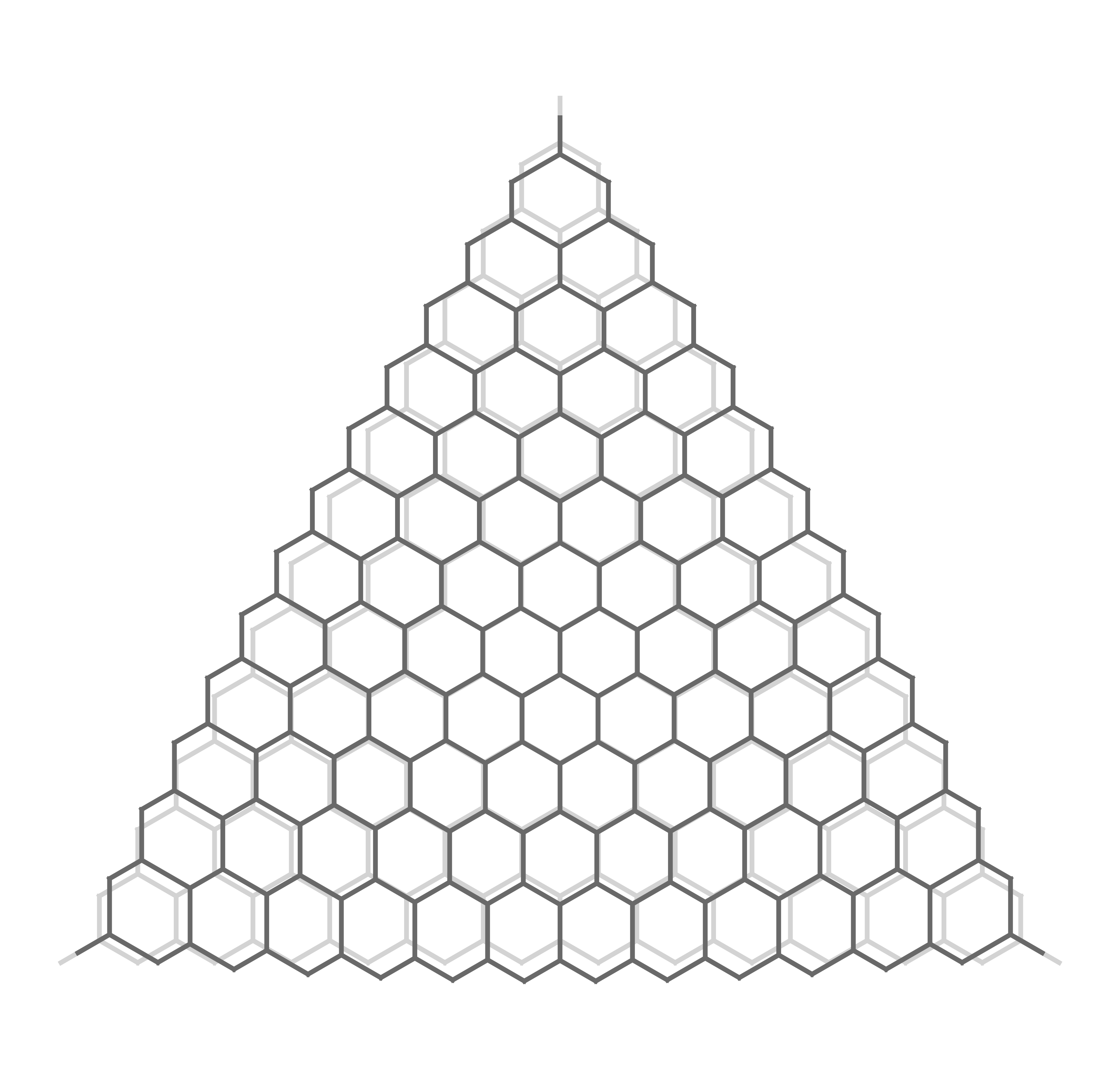

Triangular shape with full zig-zag edges

- uniform pseudo-magnetic field
- L sites on each zig-zag edge
- maximal pseudo-field strength $\beta_m = 4/L$
- coupling drop to zero at the edges for $\beta = \beta_M$
- fully sublattice-polarized edge states/0th Landau levels for $0 \leq \beta \leq \beta_M$

INPHYNI

Finite lattice: optimal geometry

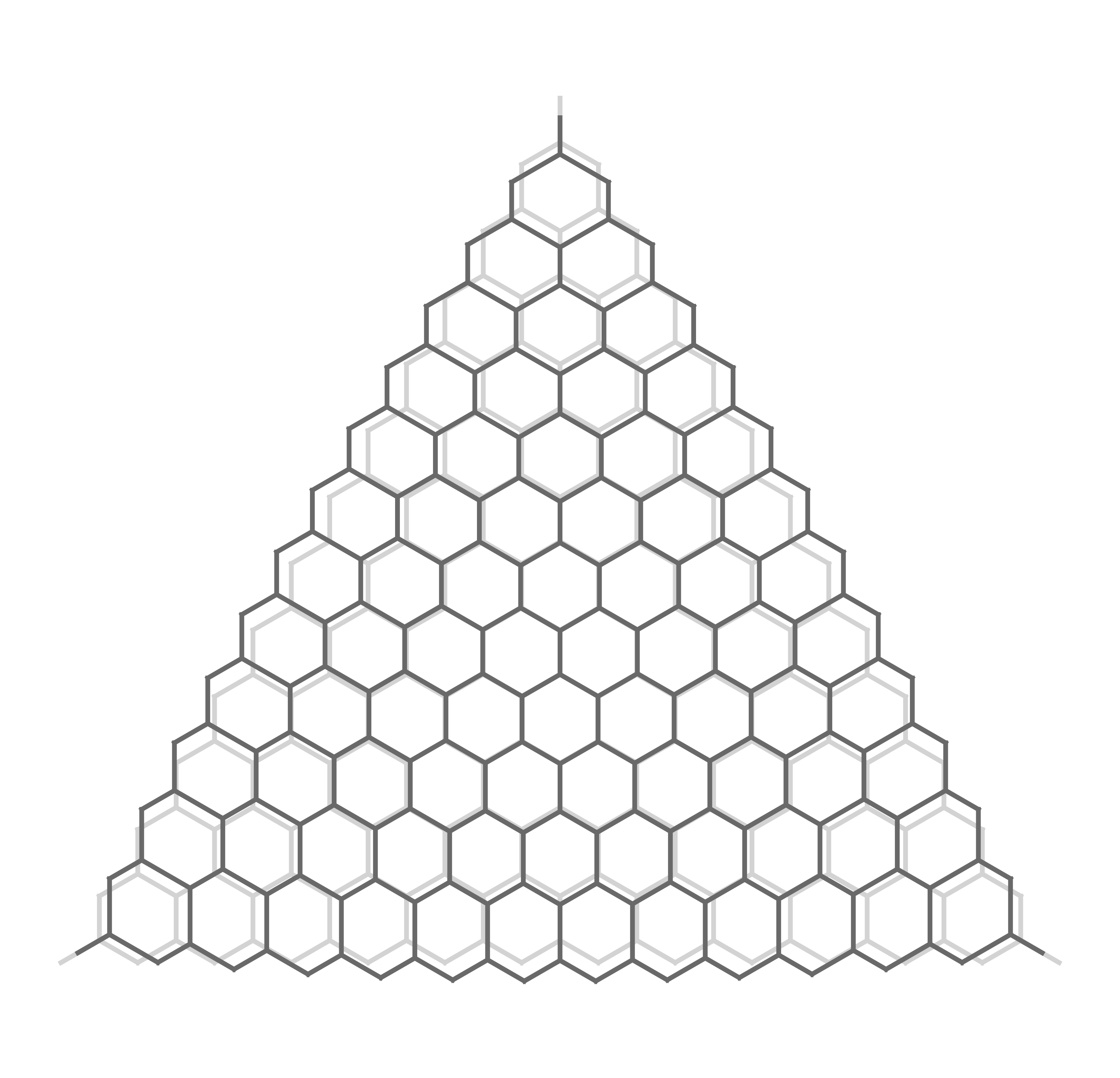

Triangular shape with full … zag edges

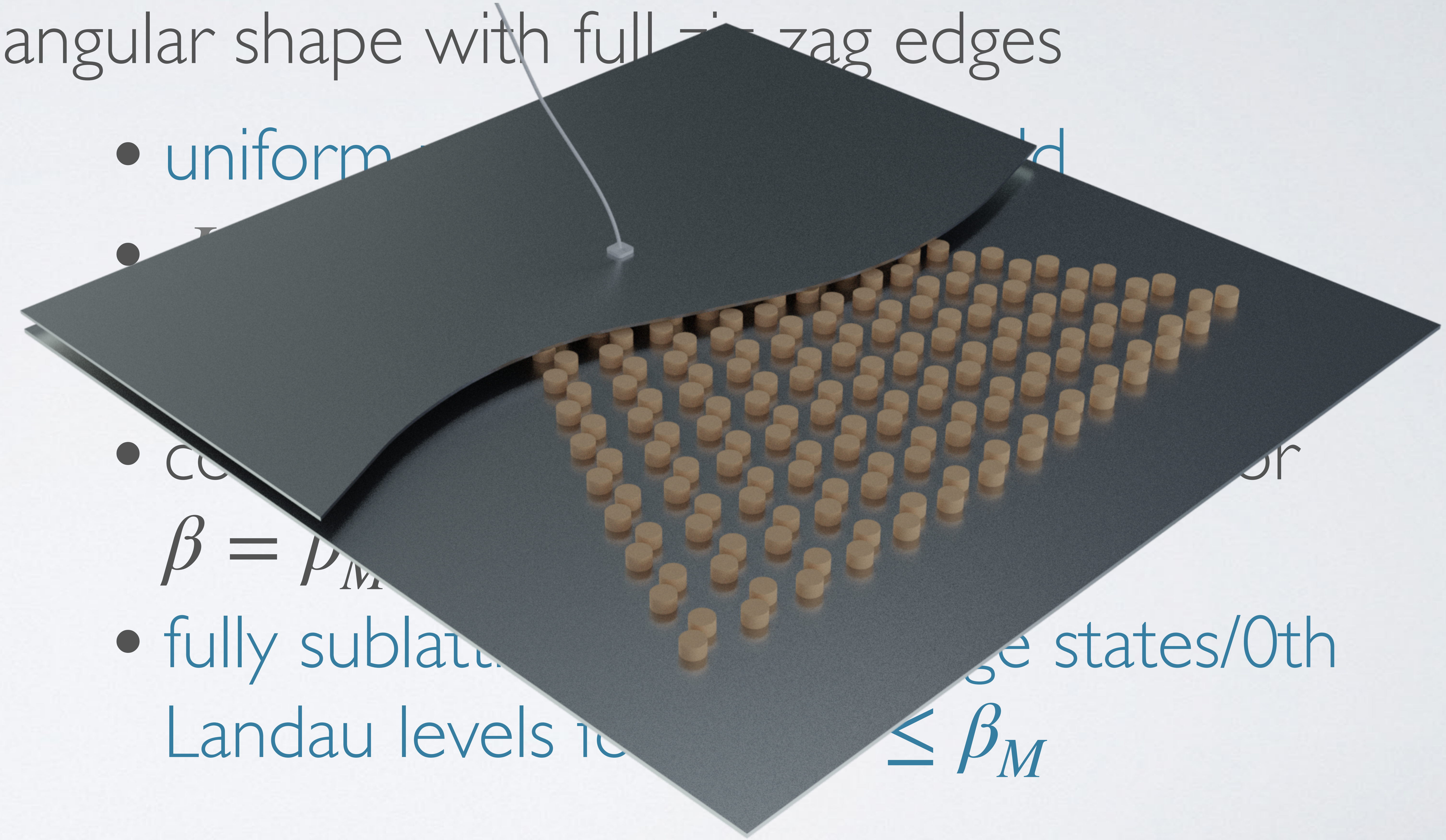

- uniform … d
- co … or
  $\beta = \beta_M$ …
- fully sublatt… e states/0th
  Landau levels fo… $\leq \beta_M$

Finite lattice: optimal geometry

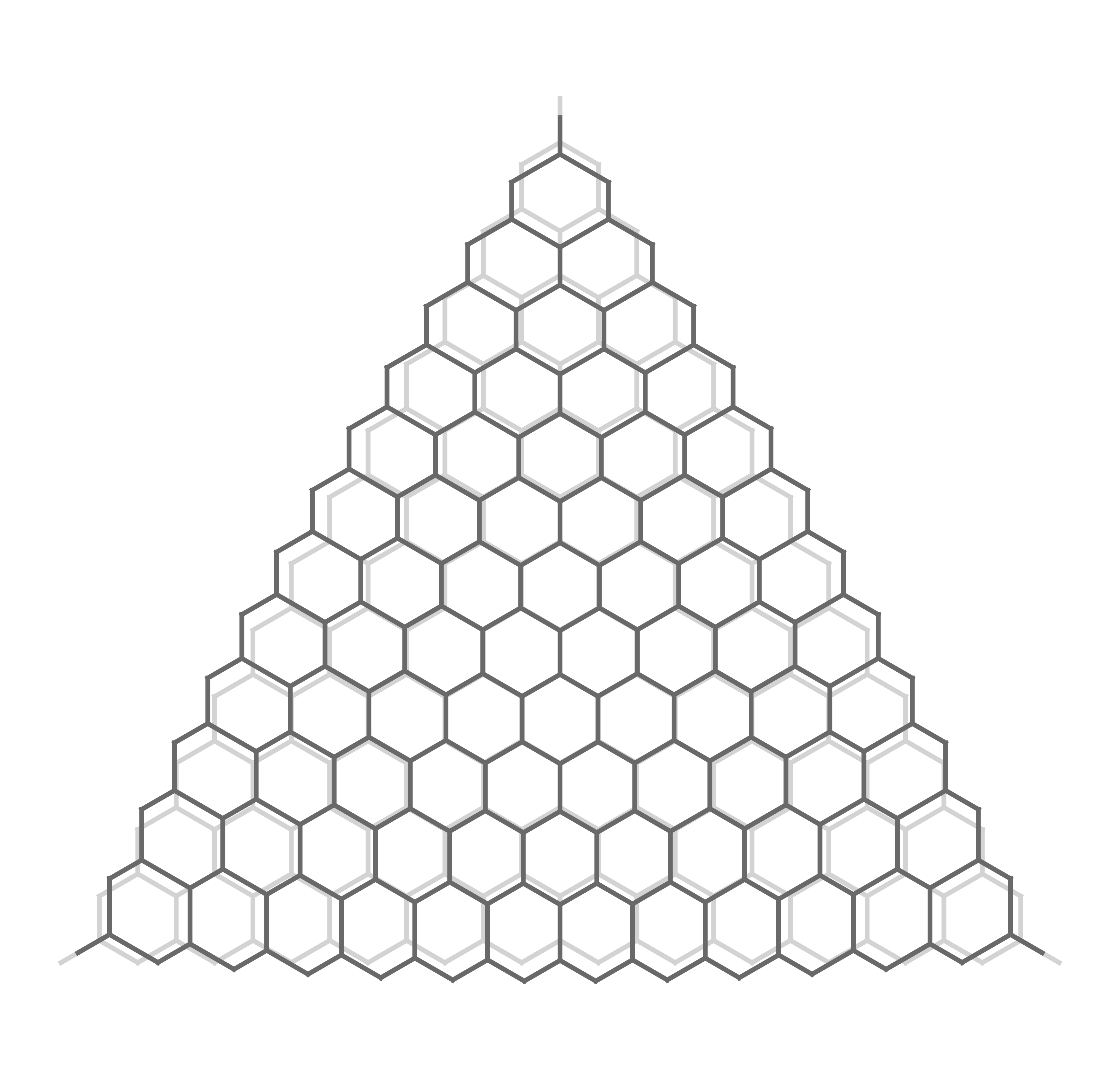

Triangular shape with full zi zag edges

- uniform … d
- …
- co … or $\beta = \beta_M$ …
- fully sublatt … e states/0th Landau levels fo … $\leq \beta_M$

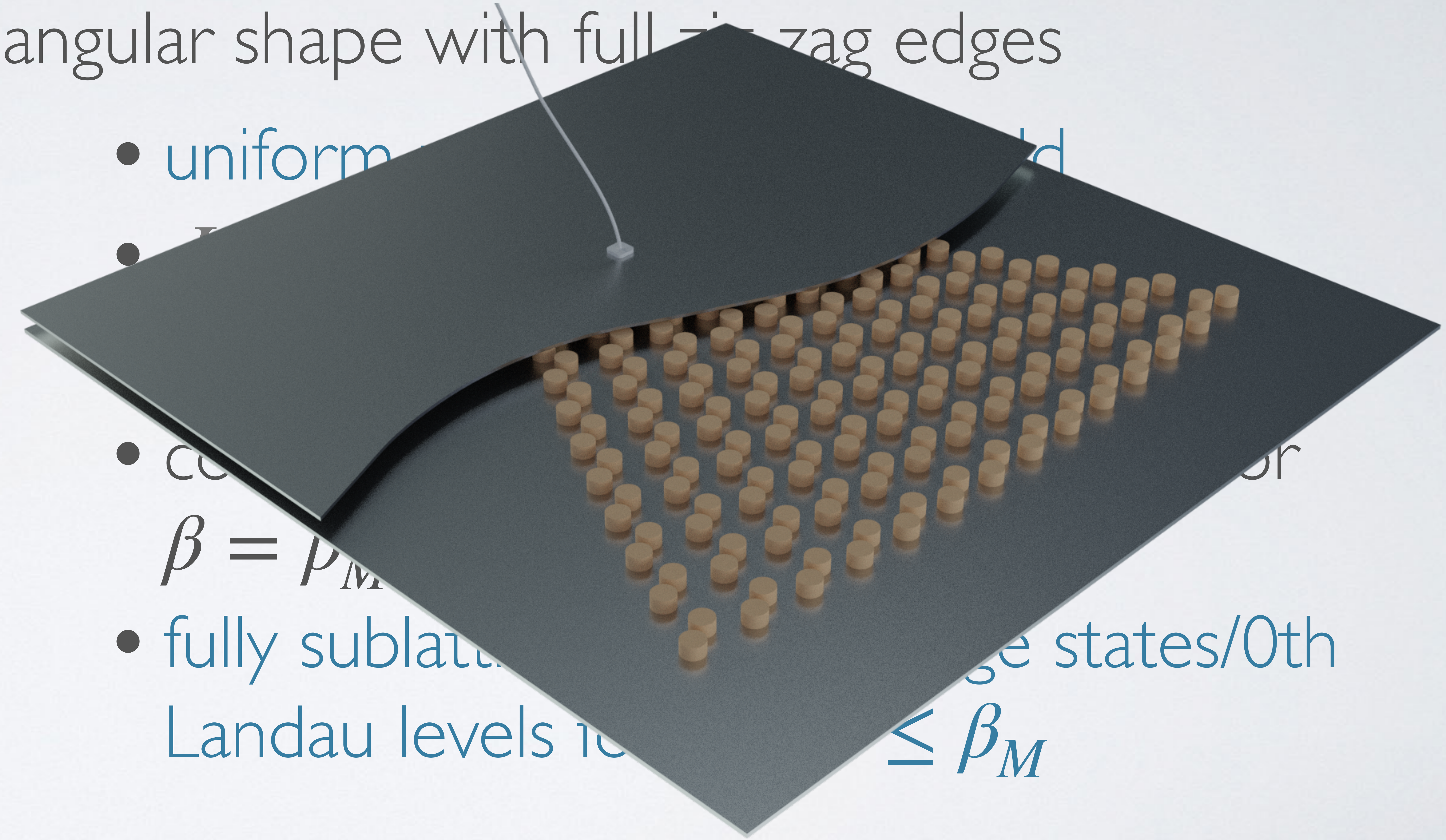

pLL degeneracy driven by the perimeter (not the surface): $L - |n|$

INPHYNI

And the pseudo-Landau levels were!

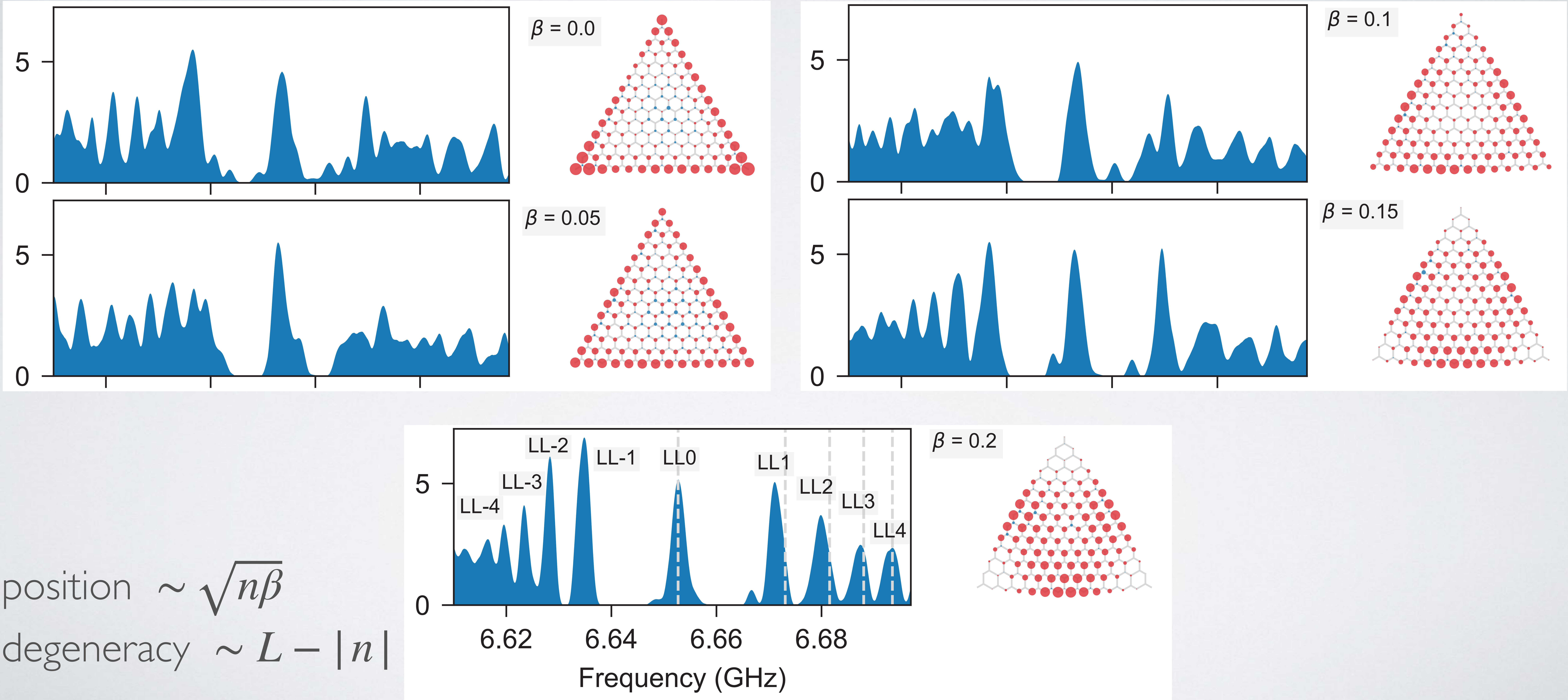

position $\sim \sqrt{n\beta}$

degeneracy $\sim L - |n|$

Light: Science & Applications **9**, 146 (2020)

Supersymmetric node structure

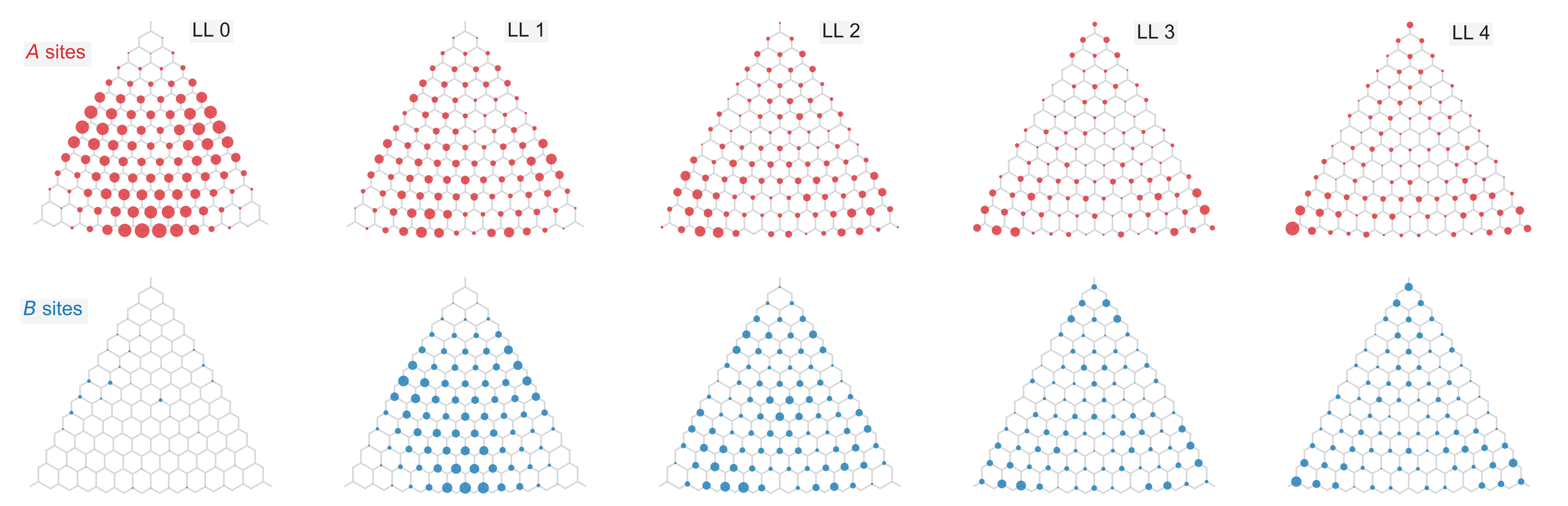

Light: Science & Applications **9**, 146 (2020)

Supersymmetric node structure

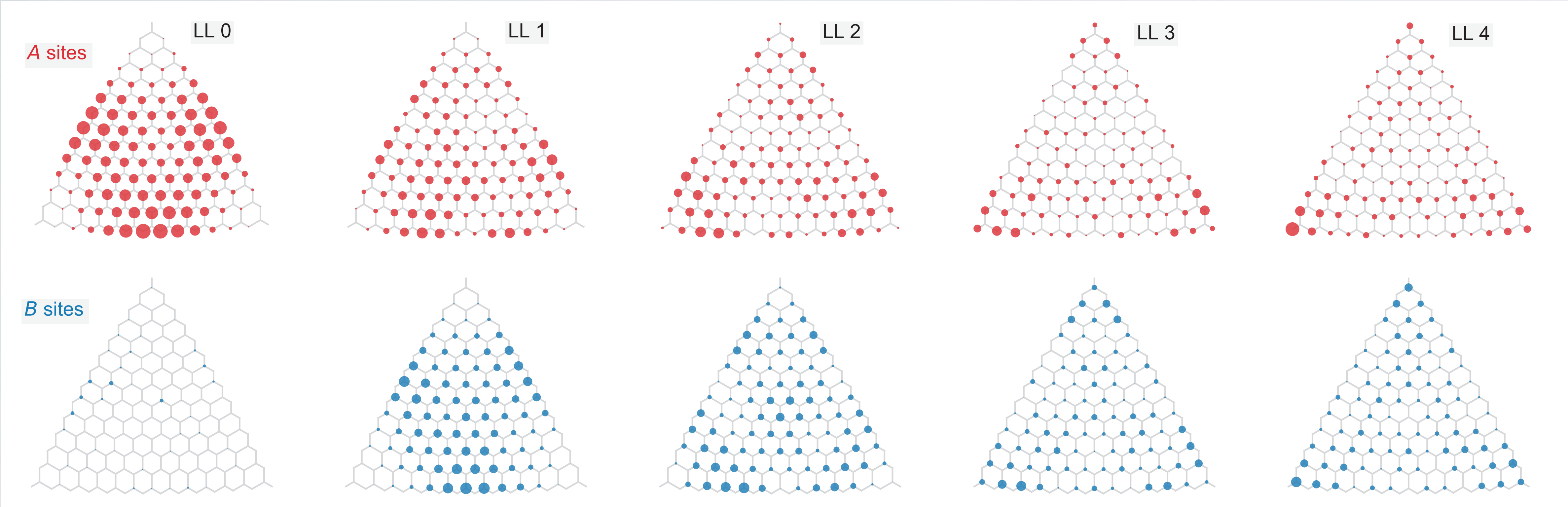

'n' mode index sequence

'$n-1$' mode index sequence

Light: Science & Applications **9**, 146 (2020)

Supersymmetric node structure

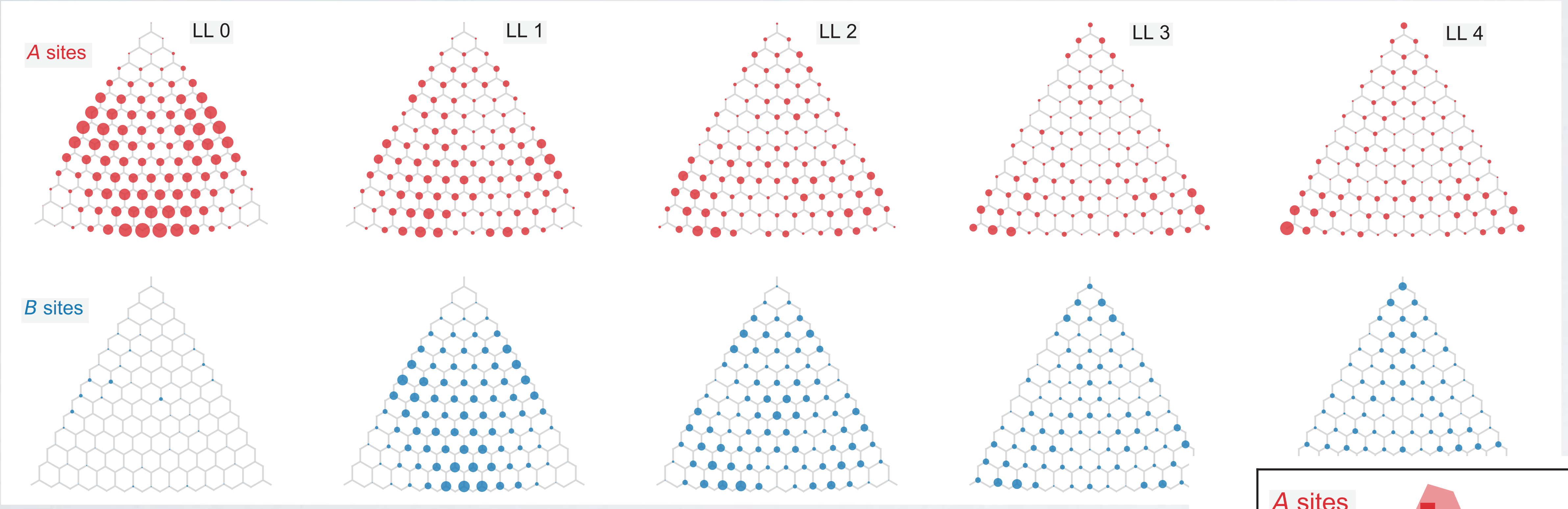

'n' mode index sequence

'$n-1$' mode index sequence

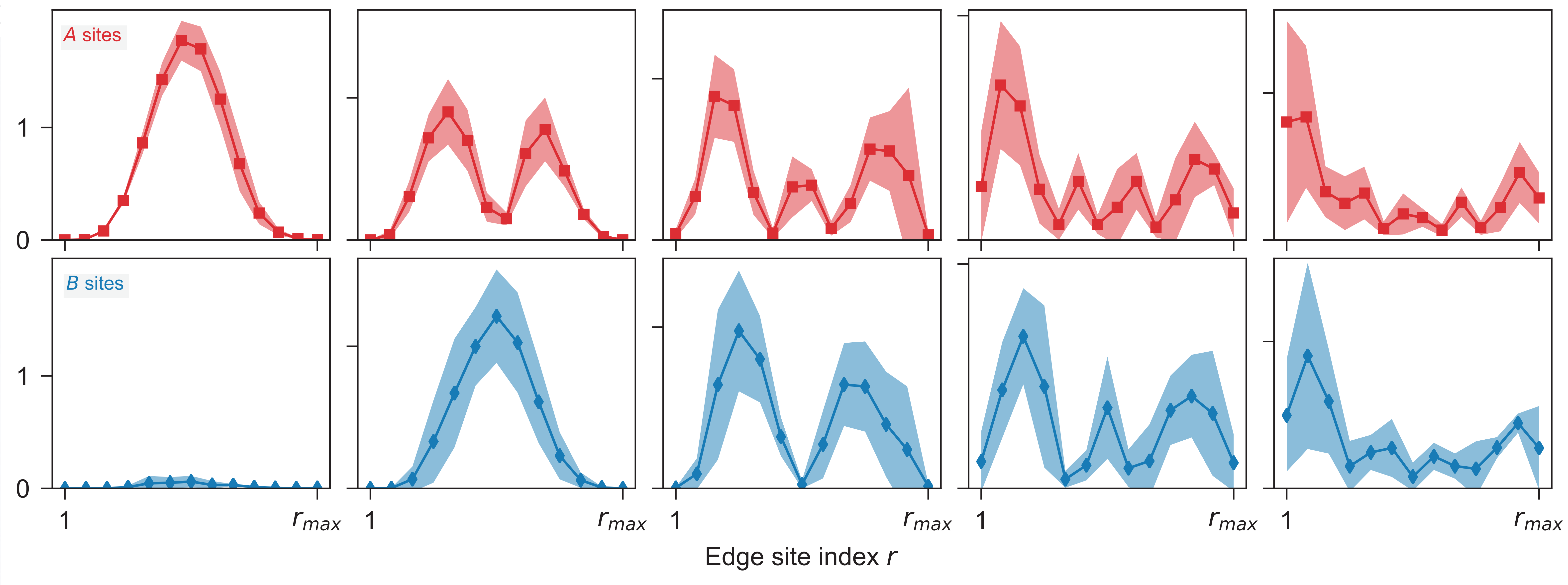

Light: Science & Applications **9**, 146 (2020)

Supersymmetric node structure

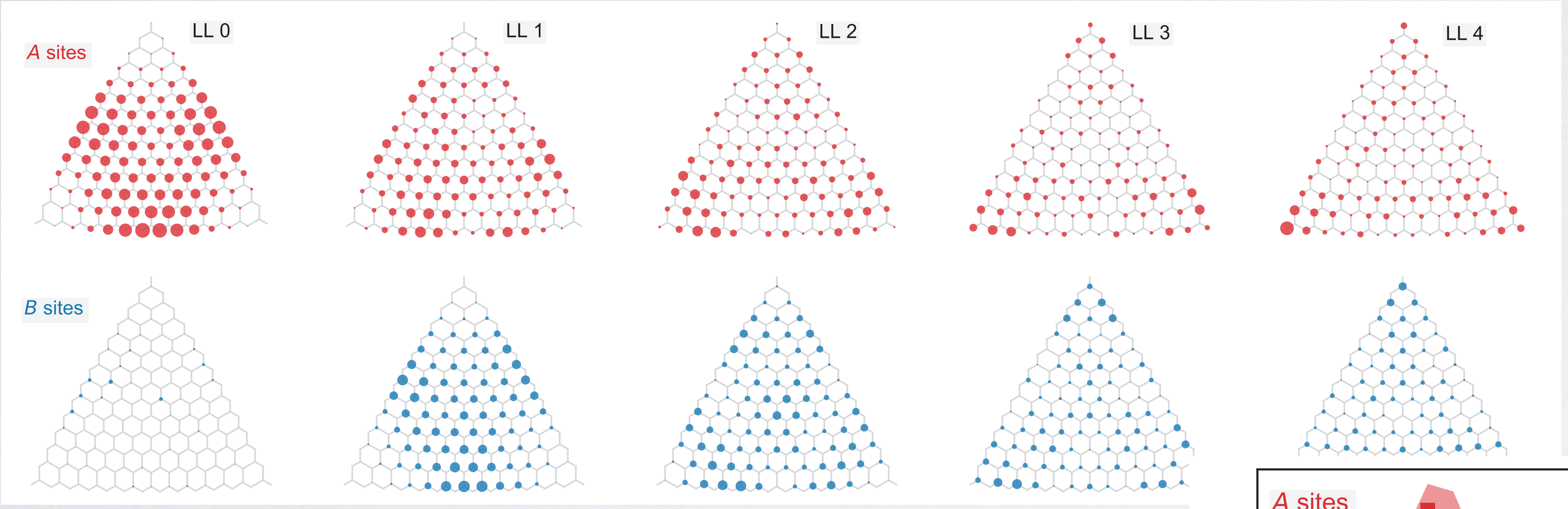

'n' mode index sequence

'$n - 1$' mode index sequence

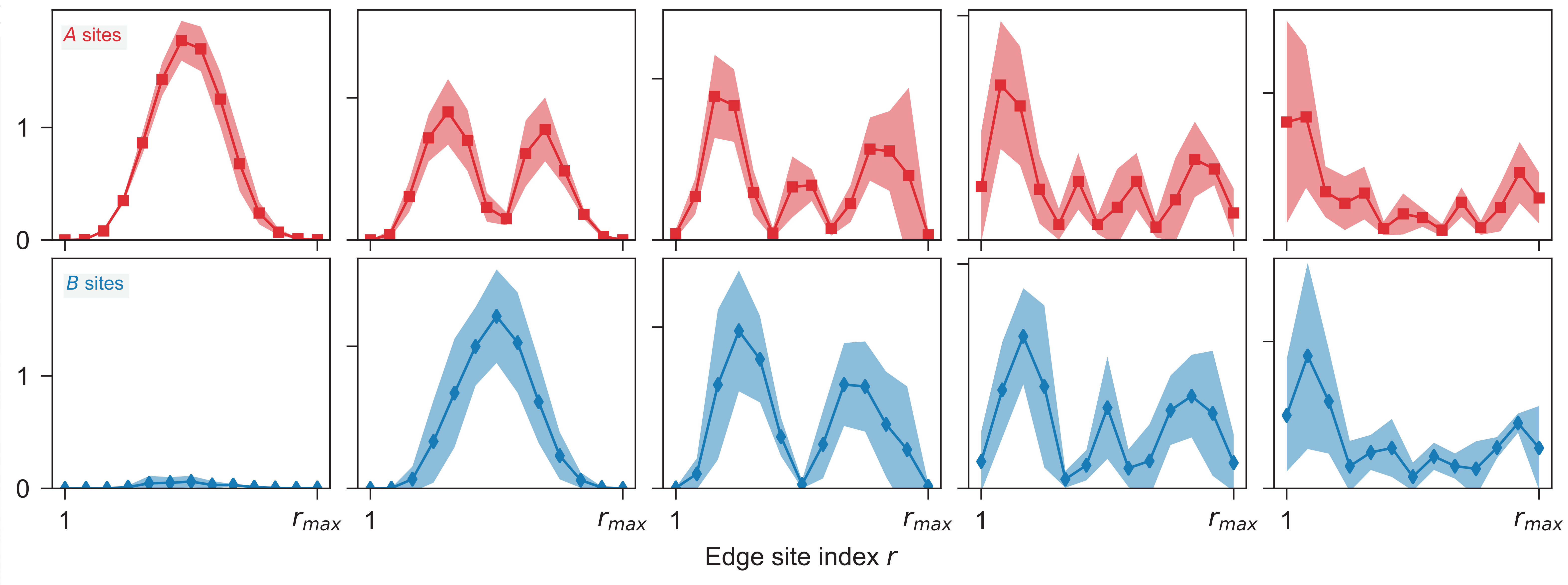

$$\psi_r^{(A,\,\mathrm{edge})} \propto \sin[(|n|+1)\pi r/(L+1)]$$

$$\psi_r^{(B,\,\mathrm{edge})} \propto \sin(|n|\pi r/L)$$

INPHYNI

Light: Science & Applications **9**, 146 (2020)

Supersymmetric node structure

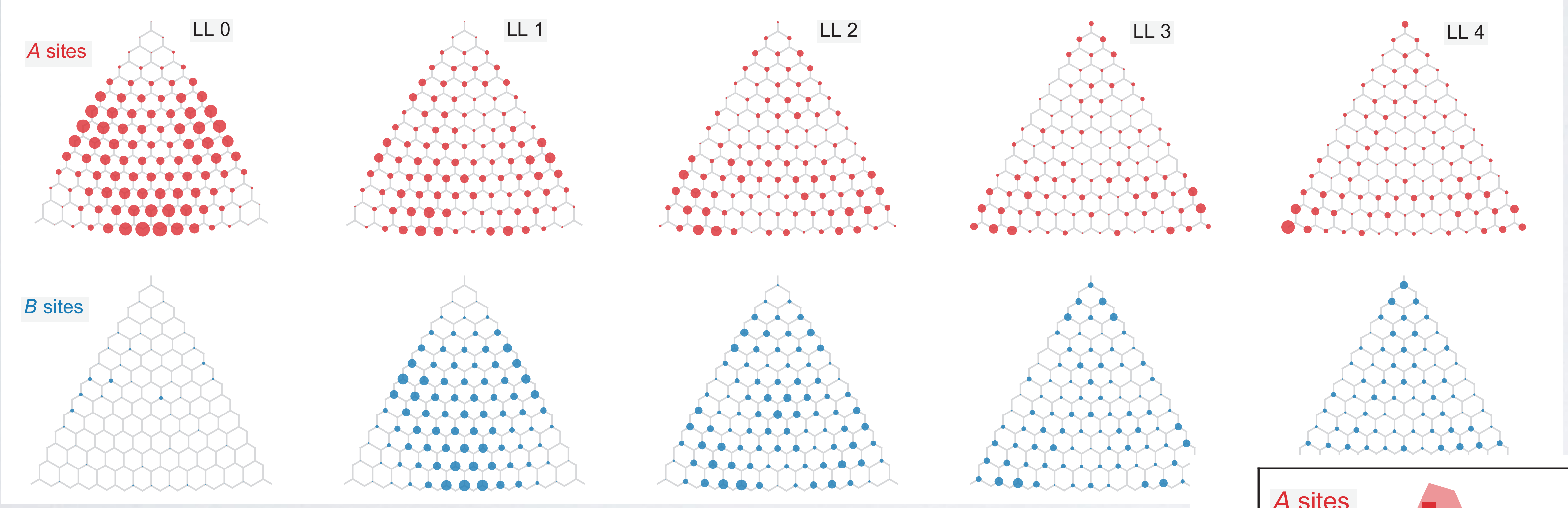

'n' mode index sequence

'$n-1$' mode index sequence

$$\psi_r^{(A,\,\mathrm{edge})} \propto \sin[(|n|+1)\pi r/(L+1)]$$

$$\psi_r^{(B,\,\mathrm{edge})} \propto \sin(|n|\pi r/L)$$

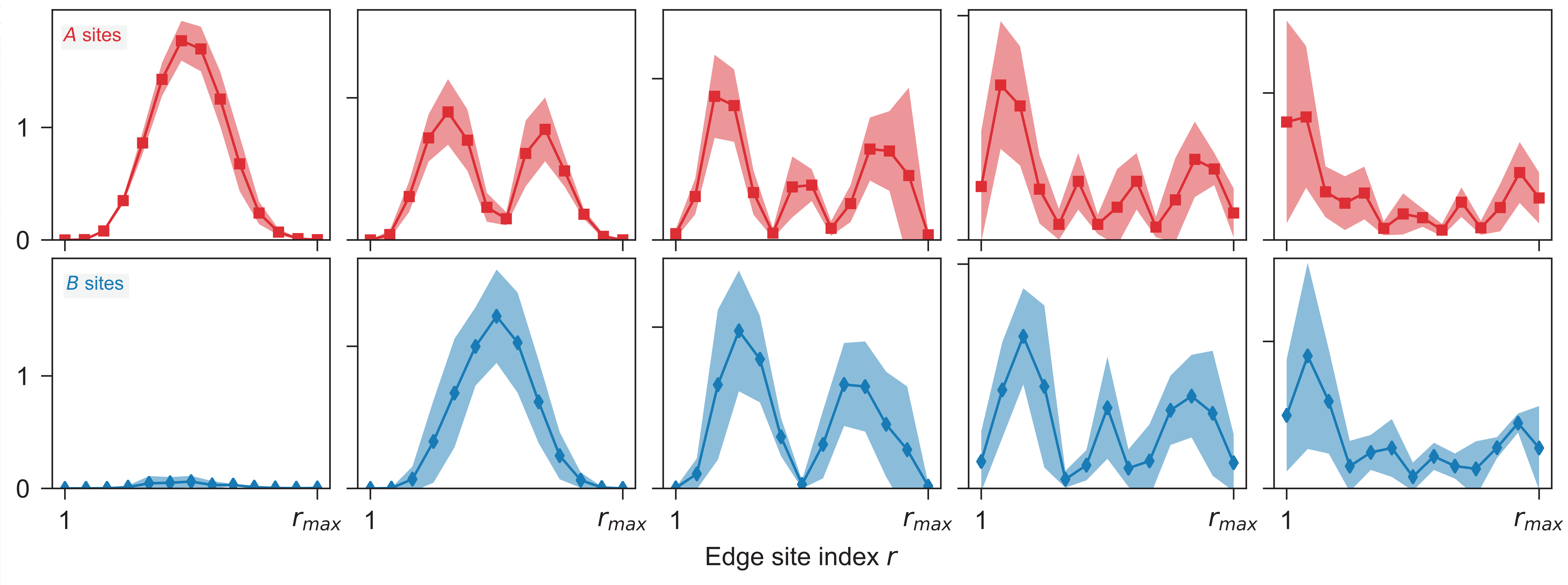

Offsets of the level sequence and nodal patterns both arise from an effective 'supersymmetric' harmonic oscillator Hamiltonian.

Merci Gilles !